fractal and fractional

MDPI

Article

Accurate Numerical Method on Graded Mesh for Mildly Singular Time-Fractional Volterra Integro-Differential Equations

Khidir Shaib Mohamed [1,*], Osman Osman [1], Aynalem Tafere Chekole [2] and Mesfin Mekuria Woldaregay [3,*]

[1] Department of Mathematics, College of Sciences, Qassim University, Buraidah 51452, Saudi Arabia
[2] Department of Mathematics, Samara University, Samara P.O. Box 132, Ethiopia; aynatafe@su.edu.et
[3] Department of Applied Mathematics, Adama Science and Technology University, Adama P.O. Box 1888, Ethiopia
* Correspondence: k.idris@qu.edu.sa (K.S.M.); mesfin.mekuria@astu.edu.et or msfnmkr02@gmail.com (M.M.W.)

Abstract

This paper developed a higher-order numerical method for time-fractional Volterra integro-differential equations. Solutions to the considered equations typically exhibit a weak singularity at the initial time, which degrades the convergence rate of standard numerical methods applied to uniform meshes. To overcome this order reduction, we proposed a high-order numerical scheme that combines an L2-1_σ fractional differentiation formula on a graded temporal mesh, a fourth-order Numerov scheme for the spatial operator, and Simpson's 1/3 rule adapted to the graded mesh to approximate the Volterra integral term. By concentrating mesh points near the initial singularity, the proposed method achieves the optimal convergence rate. A rigorous stability and convergence analysis is established. We proved that the scheme is stable and achieves a convergence rate of $\mathcal{O}(N^{-\min\{3-\alpha,r\alpha\}} + h^4)$, provided the mesh grading parameter satisfies $r \geq 1$, and N is the number of mesh intervals in the temporal direction. Numerical experiments are conducted to validate the theoretical results, demonstrating that the proposed method not only achieves the predicted convergence rate but also outperforms existing methods in the literature in terms of accuracy.

Keywords: time-fractional; volterra integro-differential equations; L2-1_σ type scheme; graded mesh; numerov method; Simpson's rule; discrete fractional Grönwall inequality; stability

Check for updates

Academic Editors: Mohammad Ayman-Mursaleen and Nadeem Rao

Received: 21 October 2026
Revised: 19 November 2026
Accepted: 20 November 2026
Published: 23 November 2026

Copyright: © 2026 by the authors. Licensee MDPI, Basel, Switzerland. This article is an open access article distributed under the terms and conditions of the Creative Commons Attribution (CC BY) license.

1. Introduction

Fractional calculus generalizes classical integer-order differentiation and integration to arbitrary non-integer orders, providing a powerful mathematical framework for modeling complex physical phenomena. Unlike classical integer-order models, fractional-order differential equations inherently account for non-local and memory-dependent properties, making them particularly effective for describing anomalous diffusion, viscoelasticity, porous media flow, and biological transport processes [1–3]. Within this context, time-fractional Volterra integro-differential equations (FVIDEs) have attracted considerable interest. The coupling of a Volterra integral term with the fractional derivative introduces a dual-memory mechanism, capturing both the inherent fading memory effect of materials and the hereditary characteristics governed by the integral kernel. This dual-memory feature is essential for the accurate modeling of viscoelastic materials and population dynamics [4,5].

Despite their broad physical relevance, the numerical solution of time-fractional differential equations presents substantial mathematical and computational challenges. The primary difficulty arises from the non-local Caputo fractional derivative, which is characterised by a weakly singular kernel $(t-s)^{-\alpha}$ [6]. Consequently, even with smooth initial data and source terms, the exact solution exhibits a weak singularity near $t=0$ where the first-order time derivative behaves asymptotically as $\partial_t u(x,t) \sim t^{\alpha-1}$. Applying standard numerical schemes, such as the classical L1 formula on a uniform temporal mesh, causes a marked reduction in the convergence rate, degrading from the optimal $\mathcal{O}(\tau^{2-\alpha})$ to $\mathcal{O}(\tau^{\alpha})$ [7,8].

To overcome this order reduction and restore optimal convergence rates without resorting to prohibitively small global time steps, the use of nonuniform graded meshes has been widely adopted. A graded mesh concentrates grid points near the initial singularity at $t=0$ while maintaining larger step sizes in the smooth region of the solution. Stynes et al. [9] established that the L1 scheme, when implemented on a graded mesh with an appropriate grading parameter r, achieves the optimal convergence rate of $\mathcal{O}(\tau^{2-\alpha})$. To further enhance temporal accuracy, higher-order schemes have been developed. Notably, the L2-1_σ and L2-type numerical differentiation formulas, which utilize quadratic rather than linear interpolation, offer superior accuracy. For instance, the L2 scheme on uniform meshes can achieve an optimal convergence rate of $\mathcal{O}(\tau^{3-\alpha})$ [10]. However, the stability and error analyses of these higher-order schemes on graded meshes remain mathematically intricate.

Recent literature has presented significant advancements in the numerical analysis of time-fractional partial differential equations (PDEs), particularly focusing on resolving initial-time singularities and ensuring robustness as the fractional order $\alpha \to 1^-$. Kundaliya [11] developed a discrete $L2\text{-}1_\sigma$ finite element method on graded temporal meshes for time-fractional nonlocal diffusion equations, ensuring that the error estimates remain valid and do not blow up as the fractional derivative order α approaches 1^-. Quan and Wu [12] analyzed the $L2\text{-}1_\sigma$ method on nonuniform meshes for subdiffusion equations. They proved that if the local time-step ratio satisfies the lower bound (specifically, ≥ 0.475329), the bilinear form associated with the $L2\text{-}1_\sigma$ fractional-derivative operator is positive semidefinite. This yielded global-in-time H^1-stability and sharp L^2-norm convergence under mild assumptions on the initial conditions and source terms. Huang and Stynes [13] investigated a time-fractional Allen–Cahn initial-boundary value problem using Alikhanov's $L2\text{-}1_\sigma$ scheme on a graded mesh combined with a standard finite element method. By deriving new a priori bounds on the solution's derivatives and proving a novel discrete fractional Grönwall inequality, they demonstrated that the computed solution attained the optimal convergence rate in the $L^\infty(H^1)$ norm. Chen and Stynes [14] generalized Alikhanov's scheme for Caputo fractional derivatives to nonuniform meshes, specifically targeting problems with weak initial-time singularities. They showed that with a suitably chosen grading parameter, the scheme achieved $3-\alpha$ order of convergence for initial-value problems and second-order convergence for initial-boundary value problems. Li et al. [15] proposed an $L2\text{-}1_\sigma$ finite element method for time-fractional Keller–Segel equations. To address the twin challenges of weak initial-time singularities and the high computational cost of fractional derivatives, the authors combined graded meshes with the sum-of-exponentials approximation technique. Liao et al. [16] introduced a discrete fractional Grönwall inequality for numerical approximations of the Caputo fractional derivative on nonuniform time meshes, which provides a fundamental analytical tool for establishing stability and convergence estimates for solutions with singular temporal derivatives at $t=0$.

In addition to high-order temporal discretization, achieving optimal overall accuracy necessitates high-order spatial discretization and careful treatment of the Volterra integral term. Standard second-order finite difference schemes for the spatial operator often limit

the global accuracy. Compact finite-difference schemes, which achieve fourth-order spatial accuracy $\mathcal{O}(h^4)$ using only a three-point stencil, are highly desirable due to their excellent spectral resolution and boundary treatment [17,18]. Furthermore, the Volterra integral term must be approximated with an accuracy that matches the temporal and spatial schemes. While product integration and piecewise constant approximations are common, higher-order quadrature rules, such as the composite Simpson's 1/3 rule, are required to preserve the overall optimal convergence rate of the coupled system.

The numerical treatment of (1) has been explored in the literature. Maji and Natesan [19] provided a study on analytical and numerical solution techniques for time-fractional integro-partial differential equations, establishing frameworks and highlighting the necessity of stable discretization strategies for the history-dependent Volterra term. Sabawi and Santra [20] proved stability and convergence analysis of the L1/L1-2 Legendre spectral method for non-local weakly singular integro-PDEs. Assanova et al. [21] formulated stability and convergence analysis of Fredholm-type equations. Building on these foundations, Santra and Mohapatra [22] proposed a finite difference technique for time-fractional integrodifferential equations of Volterra type, deriving error estimates that underscore the complexities introduced by the simultaneous non-locality of the fractional derivative and the integral kernel. However, a critical bottleneck in the numerical analysis of these equations is the weak singularity of the solution's temporal derivatives near $t = 0$. As demonstrated by Ghosh [23] in a comparative evaluation of layer-adaptive schemes for mildly singular time-fractional integro-subdiffusion equations, standard numerical methods employing uniform temporal meshes suffer from severe order reduction. To recover optimal convergence orders, specialized mesh-grading or adaptive strategies that concentrate grid points near the initial singularity are strictly required.

While these studies have significantly advanced the numerical treatment of time-fractional integrodifferential equations, achieving high-order spatial accuracy alongside optimal temporal convergence on graded meshes remains challenging. Existing literature often relies on standard second-order spatial discretizations or first-order L1-type temporal approximations, which can be computationally expensive when high accuracy is required. Furthermore, the stability and error analysis of higher-order schemes on graded meshes, particularly when coupled with Volterra integral terms, remain mathematically intricate. The interplay between the graded mesh, the higher-order L2-1_σ temporal discretization, the fourth-order Numerov (compact) spatial operator, and Simpson's rule for the integral term requires a delicate and unified analytical framework.

Motivated by these observations, this paper develops a high-order accurate numerical scheme for a time-fractional partial Volterra integro-differential equation featuring a second-order spatial operator. The main contributions of this work are summarized as follows:

1. We proposed an accurate fully discrete numerical scheme that integrates the $L2\text{-}1_\sigma$ approximation on a graded mesh for the Caputo fractional derivative, a fourth-order Numerov method for the spatial operator, and Simpson's 1/3 rule on the graded mesh for the Volterra integral term.
2. The weak singularity of the exact solution at the initial time $t = 0$ is effectively resolved by employing a graded temporal mesh. The optimal mesh grading parameter r is explicitly determined to ensure that the temporal discretization errors do not degrade the overall convergence rate of the proposed method.
3. A rigorous stability and convergence analysis is established by utilizing a discrete fractional Grönwall inequality. We proved that the proposed scheme is stable and achieves a convergence rate of $\mathcal{O}(N^{-\min\{3-\alpha, r\alpha\}} + h^4)$. In particular, the optimal convergence rate of $\mathcal{O}(N^{-(3-\alpha)} + h^4)$ is attained provided the grading parameter satisfies $r \geq \frac{3-\alpha}{\alpha}$.

The remainder of this paper is organized as follows: Section 2 presents the problem formulation and necessary preliminaries. Section 3 details the construction of the proposed numerical scheme, incorporating the $L2\text{-}1_\sigma$ discretization on a graded mesh, Simpson's rule for the integral term, and the Numerov method for the spatial operator. Section 4 provides stability and convergence analysis. Section 5 presents numerical examples to demonstrate the accuracy and efficiency of the proposed method. Finally, concluding remarks are given in Section 6.

2. Problem Formulation and Preliminaries

In this paper, we investigated the numerical approximation of a time-fractional partial Volterra integro-differential equation (FVIDE). The mathematical model is formulated as follows:

$$\begin{aligned} &\mathcal{D}_t^\alpha u(x,t) + \mathbb{L}_x u(x,t) + \lambda \int_0^t \mathcal{K}(x,t,s)u(x,s)\,ds = f(x,t), && (x,t) \in (0,L)\times(0,T], \\ &u(x,0) = \phi(x), && x \in [0,L], \\ &u(0,t) = \psi_1(t), \quad u(L,t) = \psi_2(t), && t \in (0,T], \end{aligned} \tag{1}$$

where $\mathcal{D}_t^\alpha$ denotes the Caputo fractional derivative of order $\alpha \in (0,1)$ with respect to time t, defined by:

$$\mathcal{D}_t^\alpha u(x,t) = \frac{1}{\Gamma(1-\alpha)} \int_0^t \frac{\partial u(x,s)}{\partial s} \frac{ds}{(t-s)^\alpha}. \tag{2}$$

The spatial operator $\mathbb{L}_x = -A\partial_x^2 + C$ is a second-order elliptic operator where the diffusion coefficient A and the reaction coefficient C are positive constants. The Volterra integral term, governed by the memory kernel $\mathcal{K}(x,t,s)$ and the parameter λ, introduces a fading memory effect, which is characteristic of viscoelastic materials and anomalous diffusion processes.

To ensure the well-posedness of the problem and the validity of the subsequent numerical analysis, we make the following standard assumptions on the given data:

Assumption 1.

H1. The memory kernel $\mathcal{K}(x,t,s)$ is continuous and bounded on the domain $\bar{\Omega} = [0,L]\times[0,T]\times[0,T]$, and possesses sufficient smoothness with respect to its arguments.

H2. The source term $f(x,t)$, the initial condition $\phi(x)$, and the boundary conditions $\psi_1(t)$, $\psi_2(t)$ are sufficiently smooth functions.

H3. The initial and boundary data satisfy the necessary compatibility conditions at the corners of the domain: $\phi(0) = \psi_1(0)$ and $\phi(L) = \psi_2(0)$.

It is well-known that the weakly singular kernel $(t-s)^{-\alpha}$ in the Caputo derivative causes the exact solution $u(x,t)$ to exhibit a weak singularity near the initial time $t = 0$, even when the input data are infinitely smooth. Specifically, the first-order time derivative behaves as $\partial_t u(x,t) = \mathcal{O}(t^{\alpha-1})$ as $t \to 0^+$. This lack of smoothness at $t = 0$ leads to a severe degradation in the convergence rate of standard numerical schemes applied on uniform meshes. To overcome this order reduction and restore optimal convergence rates without resorting to prohibitively small global time steps, we will employ a graded temporal mesh in our numerical formulation, which strategically concentrates grid points near the singularity at $t = 0$.

Basic Properties of Fractional Calculus

Let $u(x,t)$ be a sufficiently smooth function on $\bar{\Omega}$. The Caputo fractional derivative and the Riemann-Liouville fractional integral satisfy the following fundamental properties:

1. Derivative of a constant: The Caputo fractional derivative of a constant is zero, i.e., ${}_0^C D_t^\alpha k = 0$, for any constant k.
2. Inverse relations: For $\alpha \in (0,1)$, the fractional derivative and integral satisfy ${}_0^C D_t^\alpha I_0^\alpha u(x,t) = u(x,t)$, and $I_0^\alpha {}_0^C D_t^\alpha u(x,t) = u(x,t) - u(x,0)$.
3. Linearity: Fractional integrals and derivatives are linear operators. For any arbitrary constants c_1, c_2 and functions u_1, u_2, we have:

$$\begin{aligned} &\text{(a)} \quad I_0^\alpha (c_1 u_1 \pm c_2 u_2) = c_1 I_0^\alpha u_1 \pm c_2 I_0^\alpha u_2, \\ &\text{(b)} \quad {}_0^C D_t^\alpha (c_1 u_1 \pm c_2 u_2) = c_1 {}_0^C D_t^\alpha u_1 \pm c_2 {}_0^C D_t^\alpha u_2. \end{aligned}$$

Definition 1 ([24]). *Let E and S be normed vector spaces. A linear operator $L : E \to S$ is bounded if there exists a positive constant μ such that*

$$\|Le\|_S \leq \mu \|e\|_E, \quad \forall e \in E.$$

Lemma 1 ([24]). *Let E and S be normed vector spaces. The linear operator $L : E \to S$ is bounded if and only if L is continuous everywhere in E.*

Definition 2 ([22]). *Let $D \subseteq \mathbb{R}^n$ be a closed set. The mapping $\mathcal{F} : D \to D$ is a contraction mapping if*

$$\|\mathcal{F}(\mathbf{x}) - \mathcal{F}(\mathbf{y})\| \leq c \, \|\mathbf{x} - \mathbf{y}\|, \ \forall \mathbf{x}, \mathbf{y} \in D,$$

where c is the contraction constant with $0 \leq c < 1$.

Lemma 2 ([22]). *Suppose $D \subseteq \mathbb{R}^n$ is complete and $\mathcal{F} : D \to D$ is a contraction mapping, then $\mathcal{F}$ has a unique fixed point x^* in D.*

Theorem 1. *Let $\Omega = (0, L)$. Let the kernel $\mathcal{K} \in C(\bar{\Omega} \times [0,T] \times [0,T])$ satisfy $|\mathcal{K}| \leq K_0$, let $\phi \in H^2(\Omega)$, let $f \in C([0,T]; L^2(\Omega))$, and let the boundary data $\psi_1, \psi_2 \in C^2([0,T])$ satisfy the compatibility conditions $\phi(0) = \psi_1(0)$, $\phi(L) = \psi_2(0)$. Then, the continuous problem (1) has a unique mild solution $u \in C([0,T]; L^2(\Omega))$, given by the variation-in-constants formula after lifting (Equation (4) below).*

Proof. Since $\phi \in H^2(\Omega)$ with the compatibility conditions $\phi(0) = \psi_1(0)$ and $\phi(L) = \psi_2(0)$, and since $\psi_1, \psi_2 \in C^2([0,T])$, there exists a lifting function $G \in C^2([0,T]; H^2(\Omega))$ satisfying $G(0,t) = \psi_1(t)$, $G(L,t) = \psi_2(t)$, $G(x,0) = \phi(x)$, $t \in [0,T]$, $x \in [0,L]$. Such a lifting is constructed explicitly by:

$$G(x,t) := \psi_1(t)\left(1 - \tfrac{x}{L}\right) + \psi_2(t)\tfrac{x}{L} + \eta(t)\, w(x),$$

where $w(x) := \phi(x) - \phi(0)\left(1 - \frac{x}{L}\right) - \phi(L)\frac{x}{L}$ belongs to $H^2(\Omega) \cap H_0^1(\Omega)$ (by the compatibility conditions $\phi(0) = \psi_1(0) = \psi_2(0)$ at the endpoints and $\phi \in H^2$), and $\eta \in C^2([0,T])$ is chosen with $\eta(0) = 1$ and η vanishing (together with its first two derivatives) near $t = T$. Then, $G(0,t) = \psi_1(t)$, $G(L,t) = \psi_2(t)$, and $G(x,0) = \phi(0)(1 - x/L) + \phi(L)x/L + w(x) = \phi(x)$. Moreover, $G \in C^2([0,T]; H^2(\Omega))$ because $\psi_1, \psi_2 \in C^2([0,T])$, $\eta \in C^2([0,T])$, and $w \in H^2(\Omega)$.

Set $v := u - G$. Then, v satisfies the homogeneous-boundary sub-problem:

$$\begin{aligned} &\mathcal{D}_t^\alpha v + \mathcal{A}v + \lambda \int_0^t \mathcal{K}(x,t,s) v(x,s)\, ds = \tilde{f}(x,t), (x,t) \in \Omega \times (0,T], \\ &v(.,0) = 0, x \in \Omega, \quad v(0,t) = v(L,t) = 0, t \in [0,T], \end{aligned} \tag{3}$$

where $\mathcal{A} = -A\partial_x^2 + C$ and $\tilde{f} := f - \mathcal{D}_t^\alpha G - \mathcal{A}G - \lambda \int_0^t \mathcal{K}(x,t,s)G(x,s)\,ds$. Since $G \in C^2([0,T];H^2(\Omega))$, the function $\tilde{f}$ lies in $C([0,T];L^2(\Omega))$: the terms $\mathcal{D}_t^\alpha G$, $\mathcal{A}G$, and the Volterra term in G are all bounded in $L^2(\Omega)$ uniformly in t. $\mathcal{D}_t^\alpha G \in C([0,T];L^2(\Omega))$ because $G \in C^1([0,T];H^2(\Omega))$ and the fractional derivative of a C^1-in-time function is continuous in time; $\mathcal{A}G \in C([0,T];L^2(\Omega))$ because $G \in C^2([0,T];H^2(\Omega))$ and $\mathcal{A} : H^2 \to L^2$ is bounded; the Volterra term in G is bounded by $K_0\,T\,\|G\|_{C([0,T];L^2)} \le K_0\,T\,\|G\|_{C([0,T];H^2)}$ and is continuous in t. Thus, v satisfies a homogeneous-boundary sub-problem with a modified source $\tilde{f} \in C([0,T];L^2(\Omega))$ and zero initial datum. This existence and uniqueness of v; setting $u = v + G$ then produces the unique mild solution of with problem (1).

Without loss of generality (relabelling $\tilde{f}$ as f and dropping the notation v in favour of u), we consider problem (1) with $\phi \equiv 0$, homogeneous Dirichlet boundary data, and $f \in C([0,T];L^2(\Omega))$.

Let $\{\lambda_k, \phi_k\}_{k=1}^\infty$ be the eigenvalues and orthonormal eigenfunctions of $\mathcal{A} = -A\partial_x^2 + C$ with homogeneous Dirichlet boundary conditions, with $0 < \lambda_1 \le \lambda_2 \le \cdots \to \infty$. For $t > 0$, define the fractional resolvent operators:

$$S_\alpha(t)v := \sum_{k=1}^\infty E_{\alpha,1}(-\lambda_k t^\alpha)(v,\phi_k)\phi_k, \qquad P_\alpha(t)v := \sum_{k=1}^\infty t^{\alpha-1}E_{\alpha,\alpha}(-\lambda_k t^\alpha)(v,\phi_k)\phi_k,$$

where $E_{\alpha,\beta}$ is the two-parameter Mittag-Leffler function. The mild solution of the homogeneous sub-problem is defined as the solution of the Volterra integral equation:

$$u(t) = \int_0^t P_\alpha(t-s)f(s)\,ds - \lambda \int_0^t P_\alpha(t-s)\Big(\int_0^s \mathcal{K}(s,r)u(r)\,dr\Big)\,ds, \tag{4}$$

where $\mathcal{K}(s,r)$ denotes the operator of multiplication by $\mathcal{K}(x,s,r)$. (The initial term $S_\alpha(t)\phi$ is absent because $\phi \equiv 0$.)

For $x \ge 0$ and $0 < \alpha < 1$, the Mittag–Leffler estimates

$$|E_{\alpha,1}(-x)| \le 1, \qquad |E_{\alpha,\alpha}(-x)| \le \frac{C_\alpha}{1+x} \le C_\alpha$$

hold, where $C_\alpha > 0$ depends only on α. Consequently,

$$\|S_\alpha(t)\|_{L^2\to L^2} \le 1, \qquad \|P_\alpha(t)\|_{L^2\to L^2} \le C_\alpha\,t^{\alpha-1}, \quad \forall t > 0.$$

Moreover, $S_\alpha(\cdot)$ and $P_\alpha(\cdot)$ are strongly continuous on $(0,T]$: for any $v \in L^2(\Omega)$,

$$\|S_\alpha(t_2)v - S_\alpha(t_1)v\|_{L^2}^2 = \sum_{k=1}^\infty \big|E_{\alpha,1}(-\lambda_k t_2^\alpha) - E_{\alpha,1}(-\lambda_k t_1^\alpha)\big|^2 |(v,\phi_k)|^2 \xrightarrow[t_2\to t_1]{} 0$$

by dominated convergence for series (the dominating sequence $4|(v,\phi_k)|^2$ is summable, and $E_{\alpha,1}(-\lambda_k t^\alpha)$ is continuous in t for each k); the same argument gives strong continuity of $P_\alpha(\cdot)$ on $(0,T]$, with the singular factor $t^{\alpha-1}$ integrable near $t = 0$ since $\alpha > 0$.

Equip $Y_0 := C([0,T];L^2(\Omega))$ with the norm $\|u\|_{Y_0} := \sup_{t\in[0,T]} \|u(\cdot,t)\|_{L^2}$. Define the fixed-point operator $\mathcal{F} : Y_0 \to Y_0$ by the right-hand side of (4):

$$\mathcal{F}(u)(t) := \int_0^t P_\alpha(t-s)f(s)\,ds - \lambda \int_0^t P_\alpha(t-s)\Big(\int_0^s \mathcal{K}(s,r)u(r)\,dr\Big)\,ds.$$

We verify $\mathcal{F}(Y_0) \subset Y_0$: the convolution $\int_0^t P_\alpha(t-s)f(s)\,ds$ is continuous in t. Indeed, for $0 \le t_1 < t_2 \le T$,

$$\Big\| \int_0^{t_2} P_\alpha(t_2-s)f(s)\,ds - \int_0^{t_1} P_\alpha(t_1-s)f(s)\,ds \Big\|_{L^2} \le \int_{t_1}^{t_2} C_\alpha (t_2-s)^{\alpha-1} \|f(s)\|_{L^2}\,ds + \int_0^{t_1} \|P_\alpha(t_2-s) - P_\alpha(t_1-s)\|_{L^2\to L^2} \|f(s)\|_{L^2}\,ds,$$

and both terms tend to zero as $t_2 \to t_1$ (the first by integrability of $(t_2-s)^{\alpha-1}$ near $s = t_2$; the second by strong continuity of P_α on $(0,T]$ and dominated convergence, since $\|P_\alpha(t-s)\| \le C_\alpha (t-s)^{\alpha-1}$).

The Volterra term $g(s) := \int_0^s \mathcal{K}(s,r)u(r)\,dr$ satisfies $\|g(s)\|_{L^2} \le K_0\, s\, \|u\|_{Y_0} \le K_0\, T\, \|u\|_{Y_0}$. Since $\mathcal{K}$ is uniformly continuous on the compact set $[0,T]^2 \times [0,T]$ and $u \in Y_0$, g is continuous in s (with values in $L^2(\Omega)$): for $s_1 < s_2$,

$$\|g(s_2) - g(s_1)\|_{L^2} \le \int_0^{s_1} \|\mathcal{K}(s_2,r) - \mathcal{K}(s_1,r)\|\, \|u(r)\|\,dr + \int_{s_1}^{s_2} \|\mathcal{K}(s_2,r)\|\, \|u(r)\|\,dr,$$

which tends to zero as $s_2 \to s_1$ by uniform continuity of $\mathcal{K}$ and integrability. Hence, $g \in Y_0$, and the outer convolution $\int_0^t P_\alpha(t-s)g(s)\,ds$ is continuous in t by the same argument as above. Hence, $\mathcal{F}(u) \in Y_0$ for every $u \in Y_0$.

For $u_1, u_2 \in Y_0$ and $t \in [0,T]$,

$$\|\mathcal{F}(u_1)(t) - \mathcal{F}(u_2)(t)\|_{L^2} \le |\lambda| \int_0^t \|P_\alpha(t-s)\| \Big\| \int_0^s \mathcal{K}(s,r)(u_1-u_2)(r)\,dr \Big\|_{L^2} ds.$$

Using $\|P_\alpha(t-s)\| \le C_\alpha (t-s)^{\alpha-1}$ and $|\mathcal{K}| \le K_0$,

$$\|\mathcal{F}(u_1)(t) - \mathcal{F}(u_2)(t)\|_{L^2} \le |\lambda| K_0 C_\alpha \int_0^t (t-s)^{\alpha-1} \int_0^s \|u_1(r) - u_2(r)\|_{L^2}\,dr\,ds.$$

Taking the supremum over $t \in [0,T]$ and using $\int_0^s \|u_1(r) - u_2(r)\|_{L^2}\,dr \le s\|u_1 - u_2\|_{Y_0}$ together with $\int_0^t (t-s)^{\alpha-1} s\,ds = t^{\alpha+1}/[\alpha(\alpha+1)]$,

$$\|\mathcal{F}(u_1) - \mathcal{F}(u_2)\|_{Y_0} \le L(T)\, \|u_1 - u_2\|_{Y_0}, \qquad L(T) := \frac{|\lambda| K_0 C_\alpha}{\alpha(\alpha+1)}\, T^{\alpha+1}.$$

Define $T_0 := \left(\frac{\alpha(\alpha+1)}{2|\lambda| K_0 C_\alpha} \right)^{1/(\alpha+1)}$, so that $L(T_0) = 1/2 < 1$. By the Banach fixed-point theorem, $\mathcal{F}$ has a unique fixed point in $Y_{0,T_0} := C([0,T_0]; L^2(\Omega))$. This is the local mild solution on $[0,T_0]$.

Suppose $u \in C([0,T']; L^2(\Omega))$ is a mild solution on an interval $[0,T'] \subseteq [0,T]$. From (4) and the boundedness of P_α,

$$\|u(t)\|_{L^2} \le C_\alpha \int_0^t (t-s)^{\alpha-1} \|f(s)\|_{L^2}\,ds + |\lambda| K_0 C_\alpha \int_0^t (t-s)^{\alpha-1} \int_0^s \|u(r)\|_{L^2}\,dr\,ds.$$

Set $A_0 := C_\alpha\, T^\alpha\, \|f\|_{C([0,T];L^2)}/\alpha$, which is independent of $t \le T$ and of T'. By Fubini's theorem,

$$\int_0^t (t-s)^{\alpha-1} \int_0^s \|u(r)\|_{L^2}\,dr\,ds = \int_0^t \frac{(t-r)^\alpha}{\alpha} \|u(r)\|_{L^2}\,dr.$$

Hence,

$$\|u(t)\|_{L^2} \le A_0 + \frac{|\lambda| K_0 C_\alpha}{\alpha} \int_0^t (t-r)^\alpha \|u(r)\|_{L^2}\,dr.$$

By the Grönwall inequality for Volterra kernels $(t-r)^{\alpha}$ with $0<\alpha<1$,

$$\|u(t)\|_{L^2} \le A_0\, E_{\alpha+1,1}\Big(\frac{|\lambda|K_0C_\alpha}{\alpha}\Gamma(\alpha+1)\,t^{\alpha+1}\Big) = A_0\, E_{\alpha+1,1}\big(|\lambda|K_0C_\alpha\Gamma(\alpha)t^{\alpha+1}\big).$$

Since $E_{\alpha+1,1}$ is entire and grows at most exponentially, the right-hand side is finite for every $t \le T$, and the bound is independent of T' and of any smallness of T.

The a priori bound above is finite on $[0,T]$. Iterate the local argument: starting from the solution on $[0,T_0]$, the same argument applied on $[T_0,T_0+T_0]$ produces a solution, and so on. The a priori bound ensures that no blow-up can occur before reaching T; hence, after finitely many steps (at most $\lceil T/T_0\rceil$), the solution extends to all of $[0,T]$.

Suppose $u_1,u_2 \in Y_0$ are two mild solutions on $[0,T]$. Subtracting the two mild-solution formulae gives:

$$(u_1-u_2)(t) = -\lambda\int_0^t P_\alpha(t-s)\Big(\int_0^s \mathcal{K}(s,r)(u_1-u_2)(r)\,dr\Big)\,ds.$$

Using the boundedness of P_α and $|\mathcal{K}| \le K_0$, and then Fubini,

$$\|(u_1-u_2)(t)\|_{L^2} \le \frac{|\lambda|K_0C_\alpha}{\alpha}\int_0^t (t-r)^{\alpha}\|(u_1-u_2)(r)\|_{L^2}\,dr.$$

By the Grönwall inequality for Volterra kernels with zero initial datum, $\|(u_1-u_2)(t)\|_{L^2} \equiv 0$ on $[0,T]$. Hence, $u_1=u_2$ on $[0,T]$. Thus, the homogeneous sub-problem (3) has a unique mild solution $v \in C([0,T];L^2(\Omega))$. Setting $u := v+G$ with the lifting G produces the unique mild solution of the problem (1). □

3. Numerical Formulation

To approximate the solution of the mathematical model (1), we introduce a discrete scheme that combines a graded temporal mesh to resolve the initial singularity with a uniform spatial mesh to achieve high-order accuracy.

Let N and M be positive integers. We partition the time interval $[0,T]$ into N subintervals using a graded mesh $\bar{\omega}_\tau = \{t_n\}_{n=0}^N$ with grading parameter $r \ge 1$. The mesh points are defined by:

$$t_n = T\Big(\frac{n}{N}\Big)^r, \quad n=0,1,\dots,N. \tag{5}$$

The corresponding temporal step sizes are given by $\tau_n = t_n - t_{n-1}$ for $n=1,2,\dots,N$.

For the spatial discretization, the interval $[0,L]$ is divided into M uniform subintervals with mesh size $h=L/M$. The spatial mesh is defined as $\bar{\omega}_h = \{x_i\}_{i=0}^M$, where:

$$x_i = ih, \quad i=0,1,\dots,M. \tag{6}$$

For the graded temporal mesh, it is straightforward to verify that the step sizes τ_n and mesh points t_n satisfy the following bounds:

$$\tau_n \le CrTN^{-r}n^{r-1} \le CrT^{1/r}N^{-1}t_n^{1-1/r}, \quad 1 \le n \le N, \tag{7}$$

and

$$t_n \le 2^r t_{n-1}, \ \ 2 \le n \le N, \tag{8}$$

where $C>0$ is a generic constant independent of N and T. Furthermore, it follows from (3) that there exists a constant $C_r>0$, depending only on the grading parameter r, such that the adjacent time steps satisfy:

$$\tau_{n-1} \le \tau_n \le C_r\tau_{n-1}, \ \ 2 \le n \le N. \tag{9}$$

Assume $\alpha \in (0,1)$ and let $b_1 = 1/2$ and $b_2 = 1$. Then, the equation $\mathcal{G}_n(\sigma) = 0$ has a unique root $\sigma_n^* = 1 - \alpha/2 \in [b_1, b_2]$. We define $\sigma_n = 1 - \sigma_n^* = \frac{\alpha}{2}$. For any function $u \in C[0,T] \cap C^3(0,T]$, we denote $u(t_n) := u^n$. For $n = 1, \ldots, N-1$, let $L_{2,n}u(\eta)$ be the quadratic polynomial that interpolates $u(\eta)$ at the nodes t_{n-1}, t_n, and t_{n+1}. We introduce the following notation for the shifted time level and the corresponding convex combination of the solution:

$$t_{n-\sigma_n} := t_{n-1} + (1-\sigma_n)\tau_n = (1-\sigma_n)t_n + \sigma_n t_{n-1},$$

$$u^{n,\sigma_n} := (1-\sigma_n)u^n + \sigma_n u^{n-1},$$

and the backward difference operator $\delta_t u^n := \frac{u^n - u^{n-1}}{\tau_n}$. Furthermore, for each $n = 2, \ldots, N$, we define the extrapolated value at $t_{n-\sigma_n}$ as $\widehat{u}^{n-\sigma_n} := \frac{\tau_{n-1}+(1-\sigma_n)\tau_n}{\tau_{n-1}} u^{n-1} - \frac{(1-\sigma_n)\tau_n}{\tau_{n-1}} u^{n-2}$.

3.1. Discretization of $D_t^\alpha u$ on a Graded Mesh

The $L2\text{-}1_\sigma$ approximation to the Caputo fractional derivative $\mathcal{D}^\alpha_{t_{n-\sigma_n}} u$ on the graded mesh is given by [11] as follows:

$$\begin{aligned}
\mathcal{D}^\alpha_{t_{n-\sigma_n}} u &= \frac{1}{\Gamma(1-\alpha)} \int_0^{t_{n-\sigma_n}} (t_{n-\sigma_n} - \eta)^{-\alpha} u'(\eta)\, d\eta \\
&= \frac{1}{\Gamma(1-\alpha)} \sum_{j=1}^{n-1} \int_{t_{j-1}}^{t_j} (t_{n-\sigma_n} - \eta)^{-\alpha} u'(\eta)\, d\eta + \frac{1}{\Gamma(1-\alpha)} \int_{t_{n-1}}^{t_{n-\sigma_n}} (t_{n-\sigma_n} - \eta)^{-\alpha} \delta_t u^n\, d\eta \\
&= \sum_{j=1}^{n} g_{n,j}^{(\alpha,\sigma_n)} \left(u^j - u^{j-1}\right) = g_{n,n}^{(\alpha,\sigma_n)} u^n - g_{n,1}^{(\alpha,\sigma_n)} u^0 - \sum_{j=2}^{n} \left(g_{n,j}^{(\alpha,\sigma_n)} - g_{n,j-1}^{(\alpha,\sigma_n)}\right) u^{j-1} \\
&=: D_N^\alpha u^{n-\sigma_n},
\end{aligned} \tag{10}$$

where $g_{1,1}^{(\alpha,\sigma_1)} = \tau_1^{-1} a_{1,1}^{(\alpha,\sigma_1)}$, and for $n \geq 2$,

$$g_{n,j}^{(\alpha,\sigma_n)} = \begin{cases} \tau_j^{-1}\left(a_{n,1}^{(\alpha,\sigma_n)} - b_{n,1}^{(\alpha,\sigma_n)}\right), & j = 1, \\ \tau_j^{-1}\left(a_{n,j}^{(\alpha,\sigma_n)} + b_{n,j-1}^{(\alpha,\sigma_n)} - b_{n,j}^{(\alpha,\sigma_n)}\right), & 2 \leq j \leq n-1, \\ \tau_j^{-1}\left(a_{n,n}^{(\alpha,\sigma_n)} + b_{n,n-1}^{(\alpha,\sigma_n)}\right), & j = n, \end{cases} \tag{11}$$

with the coefficients defined as $a_{n,n}^{(\alpha,\sigma_n)} = \frac{1}{\Gamma(1-\alpha)} \int_{t_{n-1}}^{t_{n-\sigma_n}} (t_{n-\sigma_n} - \eta)^{-\alpha}\, d\eta$, and for $1 \leq j \leq n-1$,

$$a_{n,j}^{(\alpha,\sigma_n)} = \frac{1}{\Gamma(1-\alpha)} \int_{t_{j-1}}^{t_j} (t_{n-\sigma_n} - \eta)^{-\alpha}\, d\eta,$$

$$b_{n,j}^{(\alpha,\sigma_n)} = \frac{2}{\Gamma(1-\alpha)(t_{j+1} - t_{j-1})} \int_{t_{j-1}}^{t_j} (t_{n-\sigma_n} - \eta)^{-\alpha} \left(\eta - t_{j-\frac{1}{2}}\right) d\eta.$$

Additionally, the following two properties hold for the coefficients $g_{n,j}^{(\alpha,\sigma_n)}$ [16]:

$$g_{n,n}^{(\alpha,\sigma_n)} \geq g_{n,n-1}^{(\alpha,\sigma_n)} \geq \cdots \geq g_{n,2}^{(\alpha,\sigma_n)} \geq g_{n,1}^{(\alpha,\sigma_n)} > 0, \quad 1 \leq n \leq N, \tag{12}$$

and if $\max_{2 \leq n \leq N} \frac{\tau_{n-1}}{\tau_n} \leq \frac{7}{4}$, then,

$$g_{n,j}^{(\alpha,\sigma_n)} \geq \frac{4}{11\tau_j}\int_{t_{j-1}}^{t_j}\frac{(t_n-\eta)^{-\alpha}}{\Gamma(1-\alpha)}\,d\eta, \qquad 1\leq j\leq n\leq N. \tag{13}$$

For notational convenience, we define $g_{n,j} := g_{n,j}^{(\alpha,\sigma_n)}$ for each $n = 1,\ldots,N$ and $j = 1,\ldots,n$. The discrete fractional derivative can then be rewritten as

$$\mathcal{D}_{t_{n-\sigma_n}}u \approx \sum_{j=1}^{n} g_{n,j}\left(u^j-u^{j-1}\right) = g_{n,n}u^n - g_{n,1}u^0 - \sum_{j=2}^{n}\left(g_{n,j}-g_{n,j-1}\right)u^{j-1} =: D_N u^{n-\sigma_n}. \tag{14}$$

As a direct consequence of (12) and (13), the simplified coefficients $g_{n,j}$ satisfy the following:

(i) Positivity and monotonicity: $g_{n,n}\geq g_{n,n-1}\geq\cdots\geq g_{n,2}\geq g_{n,1}>0, \quad 1\leq n\leq N$.

(ii) Lower bound: If $\max_{2\leq n\leq N}\frac{\tau_{n-1}}{\tau_n}\leq\frac{7}{4}$ and $\mu=\frac{1}{\Gamma(2-\alpha)}$, then for $1\leq j\leq n\leq N$,

$$g_{n,j}\geq\frac{4}{11\tau_j}\int_{t_{j-1}}^{t_j}\frac{(t_n-\eta)^{-\alpha}}{\Gamma(1-\alpha)}\,d\eta\geq\frac{4\mu}{11}\tau_j^{-\alpha}.$$

3.1.1. Truncation Error Analysis of the L2-1$_\sigma$ Type Formula

For any function $u\in C[0,T]\cap C^3(0,T]$, we define the local truncation error parameters:

$$\begin{aligned}
\psi_\alpha^{1-\sigma_1} &= \tau_1^\alpha \sup_{\eta\in(0,t_1)}\left(\eta^{1-\alpha}\|\delta_t u(t_1)-u'(\eta)\|\right),\\
\psi_\alpha^{n-\sigma_n} &= \tau_n^{3-\alpha}t_{n-\sigma_n}^\alpha \sup_{\eta\in(t_{n-1},t_n)}\|u^{(3)}(\eta)\|, \quad n=2,\ldots,N,\\
\psi_\alpha^{n,1} &= \tau_1^\alpha \sup_{\eta\in(0,t_1)}\left(\eta^{1-\alpha}\|(L_{2,1}u(\eta))'-u'(\eta)\|\right), \quad n=2,\ldots,N,\\
\psi_\alpha^{n,j} &= \tau_n^{-\alpha}\tau_j^2(\tau_j+\tau_{j+1})t_n^\alpha \sup_{\eta\in(t_{j-1},t_j)}\|u^{(3)}(\eta)\|, \quad 2\leq j<n\leq N.
\end{aligned}$$

Lemma 3 ([14]). *Let $u(t)\in C[0,T]\cap C^3(0,T]$. Suppose that $\|u^{(m)}(t)\|\leq C(1+t^{\alpha-m})$ for $m=0,1,2,3$ and $t\in(0,T]$. Then,*

$$\begin{aligned}
\psi_\alpha^{n-\sigma_n} &\leq CN^{-\min\{3-\alpha,r\alpha\}}, \quad \text{for } n=1,\ldots,N,\\
\psi_\alpha^{n,j} &\leq CN^{-\min\{3-\alpha,r\alpha\}}, \quad \text{for } j=1,\ldots,n-1, \text{ when } n\geq 2.
\end{aligned}$$

Theorem 2. *Let $u(t)\in C[0,T]\cap C^3(0,T]$ satisfy $\|u^{(q)}(t)\|\leq C(1+t^{\alpha-q})$ for $q=0,1,2,3$ and $t\in(0,T]$. Then, for each $n=1,\ldots,N$, the truncation error of the L2-1$_\sigma$ scheme satisfies:*

$$\|\mathcal{D}_t^\alpha u(t_{n-\sigma_n})-D_N u^{n-\sigma_n}\|\leq CN^{-\min\{3-\alpha,r\alpha\}}t_{n-\sigma_n}^{-\alpha}.$$

Proof. Let $R^{n-\sigma_n} := \mathcal{D}_t^\alpha u(t_{n-\sigma_n})-D_N u^{n-\sigma_n}$ denote the truncation error. From (10), we have:

$$\begin{aligned}
R^{n-\sigma_n} = &\frac{1}{\Gamma(1-\alpha)}\sum_{j=1}^{n-1}\int_{t_{j-1}}^{t_j}(t_{n-\sigma_n}-\eta)^{-\alpha}(L_{2,j}u(\eta)-u(\eta))'\,d\eta\\
&+\frac{1}{\Gamma(1-\alpha)}\int_{t_{n-1}}^{t_{n-\sigma_n}}(t_{n-\sigma_n}-\eta)^{-\alpha}(\delta_t u(t_n)-u'(\eta))\,d\eta.
\end{aligned} \tag{15}$$

For the initial step $n=1$, the error simplifies to:

$$\begin{aligned}
\|R^{1-\sigma_1}\| &= \left|\frac{1}{\Gamma(1-\alpha)}\int_0^{t_{1-\sigma_1}}(t_{1-\sigma_1}-\eta)^{-\alpha}(\delta_t u(t_1)-u'(\eta))\,d\eta\right|\\
&\leq \frac{1}{\Gamma(1-\alpha)}\sup_{\eta\in(0,t_1)}\left(\eta^{1-\alpha}\|\delta_t u(t_1)-u'(\eta)\|\right)\int_0^{t_{1-\sigma_1}}(t_{1-\sigma_1}-\eta)^{-\alpha}\eta^{\alpha-1}\,d\eta\\
&\leq \frac{1}{\Gamma(1-\alpha)}\psi_\alpha^{1-\sigma_1}t_{1-\sigma_1}^{-\alpha}\Gamma(1-\alpha)\Gamma(\alpha) = \psi_\alpha^{1-\sigma_1}t_{1-\sigma_1}^{-\alpha}.
\end{aligned} \tag{16}$$

For $2 \le n \le N$, we handle the history integral via integration by parts. Since $L_{2,j}u$ interpolates u at t_{j-1} and t_j, the boundary terms vanish, yielding:

$$\begin{aligned}\left|\sum_{j=1}^{n-1}\int_{t_{j-1}}^{t_j}(t_{n-\sigma_n}-\eta)^{-\alpha}(L_{2,j}u(\eta)-u(\eta))'\,d\eta\right| &= \left|\alpha\sum_{j=1}^{n-1}\int_{t_{j-1}}^{t_j}(t_{n-\sigma_n}-\eta)^{-\alpha-1}(u(\eta)-L_{2,j}u(\eta))\,d\eta\right| \\ &\le C\sum_{j=1}^{n-1}\psi_\alpha^{n,j}\tau_n^\alpha t_n^{-\alpha}\int_{t_{j-1}}^{t_j}(t_{n-\sigma_n}-\eta)^{-\alpha-1}\,d\eta \\ &\le C\sum_{j=1}^{n-1}\psi_\alpha^{n,j}\tau_n^\alpha\int_{t_{j-1}}^{t_j}\eta^{-\alpha}(t_{n-\sigma_n}-\eta)^{-\alpha-1}\,d\eta \\ &\le C\max_{1\le j\le n-1}\{\psi_\alpha^{n,j}\}\tau_n^\alpha\int_0^{t_{n-1}}\eta^{-\alpha}(t_{n-\sigma_n}-\eta)^{-\alpha-1}\,d\eta \\ &\le Ct_{n-\sigma_n}^{-\alpha}\max_{1\le j\le n-1}\{\psi_\alpha^{n,j}\}.\end{aligned} \tag{17}$$

Next, we analyze the local integral over $[t_{n-1}, t_{n-\sigma_n}]$. By Taylor's theorem expanded around the midpoint $t_{n-1/2}$, we have:

$$\begin{aligned}&\frac{1}{\Gamma(1-\alpha)}\int_{t_{n-1}}^{t_{n-\sigma_n}}(t_{n-\sigma_n}-\eta)^{-\alpha}(\delta_t u(t_n)-u'(\eta))\,d\eta \\ &\quad=\frac{1}{\Gamma(1-\alpha)}\left[\int_{t_{n-1}}^{t_{n-\sigma_n}}(t_{n-\sigma_n}-\eta)^{-\alpha}(\delta_t u(t_n)-u'(t_{n-1/2}))\,d\eta\right. \\ &\qquad-u''(t_{n-1/2})\int_{t_{n-1}}^{t_{n-\sigma_n}}(t_{n-\sigma_n}-\eta)^{-\alpha}(\eta-t_{n-1/2})\,d\eta \\ &\qquad\left.-\frac{1}{2}\int_{t_{n-1}}^{t_{n-\sigma_n}}(t_{n-\sigma_n}-\eta)^{-\alpha}(\eta-t_{n-1/2})^2u'''(\zeta_n(\eta))\,d\eta\right],\end{aligned} \tag{18}$$

where $\zeta_n(\eta) \in (t_{n-1}, t_n)$.

The first term in (18) is bounded by:

$$\begin{aligned}&\left|\frac{1}{\Gamma(1-\alpha)}\int_{t_{n-1}}^{t_{n-\sigma_n}}(t_{n-\sigma_n}-\eta)^{-\alpha}(\delta_t u(t_n)-u'(t_{n-1/2}))\,d\eta\right| \\ &\quad\le\frac{1}{\Gamma(1-\alpha)}\tau_n^2\sup_{\eta\in(t_{n-1},t_n)}\|u'''(\eta)\|\int_{t_{n-1}}^{t_{n-\sigma_n}}(t_{n-\sigma_n}-\eta)^{-\alpha}\,d\eta \\ &\quad\le\frac{1}{\Gamma(1-\alpha)}\tau_n^{3-\alpha}\sup_{\eta\in(t_{n-1},t_n)}\|u'''(\eta)\| = t_{n-\sigma_n}^{-\alpha}\psi_\alpha^{n-\sigma_n}.\end{aligned} \tag{19}$$

For the second term, we evaluate the integral exactly. Let $s = t_{n-\sigma_n} - \eta$, which gives $\eta - t_{n-1/2} = (1/2-\sigma_n)\tau_n - s$. Thus,

$$\begin{aligned}\int_{t_{n-1}}^{t_{n-\sigma_n}}(t_{n-\sigma_n}-\eta)^{-\alpha}(\eta-t_{n-1/2})\,d\eta &= \int_0^{(1-\sigma_n)\tau_n}s^{-\alpha}((1/2-\sigma_n)\tau_n-s)\,ds \\ &= (1/2-\sigma_n)\tau_n\frac{((1-\sigma_n)\tau_n)^{1-\alpha}}{1-\alpha}-\frac{((1-\sigma_n)\tau_n)^{2-\alpha}}{2-\alpha} \\ &= \tau_n^{2-\alpha}(1-\sigma_n)^{1-\alpha}\left[\frac{1/2-\sigma_n}{1-\alpha}-\frac{1-\sigma_n}{2-\alpha}\right].\end{aligned} \tag{20}$$

Since we chose $\sigma_n = \alpha/2$, we have $1/2-\sigma_n = (1-\alpha)/2$ and $1-\sigma_n = (2-\alpha)/2$. Substituting these into the bracket yields $\frac{(1-\alpha)/2}{1-\alpha} - \frac{(2-\alpha)/2}{2-\alpha} = \frac{1}{2} - \frac{1}{2} = 0$. Thus, the second term in (18) vanishes identically. The third term in (18) is bounded similarly to the first:

$$\begin{aligned}
&\left|\frac{1}{2\Gamma(1-\alpha)}\int_{t_{n-1}}^{t_{n-\sigma_n}}(t_{n-\sigma_n}-\eta)^{-\alpha}(\eta-t_{n-1/2})^2u'''(\zeta_n(\eta))\,d\eta\right| \\
&\quad\le\frac{1}{2\Gamma(1-\alpha)}\tau_n^2\sup_{\eta\in(t_{n-1},t_n)}\|u'''(\eta)\|\int_{t_{n-1}}^{t_{n-\sigma_n}}(t_{n-\sigma_n}-\eta)^{-\alpha}\,d\eta \\
&\quad\le\frac{1}{\Gamma(1-\alpha)}\tau_n^{3-\alpha}\sup_{\eta\in(t_{n-1},t_n)}\|u'''(\eta)\|=t_{n-\sigma_n}^{-\alpha}\psi_\alpha^{n-\sigma_n}.
\end{aligned}\tag{21}$$

Combining the bounds (19)–(21) into (18), we obtain:

$$\left\|\frac{1}{\Gamma(1-\alpha)}\int_{t_{n-1}}^{t_{n-\sigma_n}}(t_{n-\sigma_n}-\eta)^{-\alpha}(\delta_t u(t_n)-u'(\eta))\,d\eta\right\|\le 2t_{n-\sigma_n}^{-\alpha}\psi_\alpha^{n-\sigma_n}.\tag{22}$$

Finally, substituting (16), (17) and (22) back into (15) yields:

$$\|R^{n-\sigma_n}\|\le Ct_{n-\sigma_n}^{-\alpha}\left(\psi_\alpha^{n-\sigma_n}+\max_{1\le j\le n-1}\psi_\alpha^{n,j}\right).$$

Applying the bounds from Lemma 3, we conclude that

$$\|R^{n-\sigma_n}\|\le CN^{-\min\{3-\alpha,r\alpha\}}t_{n-\sigma_n}^{-\alpha},$$

which completes the proof. □

3.1.2. A Discrete Fractional Grönwall Inequality

In this section, we present the discrete fractional Grönwall inequality that is used in the sequel to derive a priori bounds and convergence results. For $n=1,2,\dots,N$, define the coefficients $p_{n,i}$ by:

$$\sum_{k=j}^{n}p_{n,k}\,g_{k,j}\equiv 1,\quad 1\le j\le n\le N,\tag{23}$$

where $g_{k,j}$ are the weights of the $L2\text{-}1_\sigma$ approximation for the Caputo fractional derivative D_t^α, with $0<\alpha<1$. Taking $j=i$ and $j=i+1$ in (14) yields the explicit following formula:

$$p_{n,n}=\frac{1}{g_{n,n}},\quad p_{n,i}=\frac{1}{g_{i,i}}\sum_{k=i+1}^{n}\left(g_{k,i+1}-g_{k,i}\right)p_{n,k},\quad 1\le i\le n-1.\tag{24}$$

Moreover, the monotonicity of $g_{k,j}$ implies $p_{n,i}>0$. Since $p_{n,i}g_{i,i}\le\sum_{k=i}^{n}p_{n,k}g_{k,i}=1$, it follows from the lower bound of the weights that

$$0<p_{n,i}\le\frac{1}{g_{i,i}}\le\frac{11}{4}\Gamma(2-\alpha)\tau_i^\alpha\le\frac{11}{4\mu}\tau_i^\alpha,\quad 1\le i\le n\le N.$$

Lemma 4 ([16] Discrete fractional Grönwall inequality)**.** *] Let $u:[0,T]\to\mathbb{R}$ be a continuous, piecewise C^1 function.*

(1) If u' is nonnegative and decreasing, then for $1\le n\le N$, $\sum_{j=1}^{n}p_{n,j}\,D_{t_j}^\alpha u\le\frac{11}{4}\int_0^{t_n}u'(\psi)\,\mathrm{d}\psi$.

(2) If u' is nonnegative and monotonic, then for $1\le n\le N$, $\sum_{j=1}^{n-1}p_{n,j}\,D_{t_j}^\alpha u\le\frac{11}{4}\int_0^{t_n}u'(\psi)\,\mathrm{d}\psi$.

Proof. (1) Assume that u' is nonnegative and decreasing. For $1\le j\le N$, we can write the Caputo fractional derivative as follows:

$$D_{t_j}^\alpha u=\sum_{k=1}^{j}\int_{t_{k-1}}^{t_k}\frac{(t_j-\psi)^{-\alpha}}{\Gamma(1-\alpha)}u'(\psi)\,\mathrm{d}\psi.$$

Since the kernel $\frac{(t_j-\psi)^{-\alpha}}{\Gamma(1-\alpha)}$ is increasing with respect to ψ and u' is decreasing, we can apply Chebyshev's integral inequality to obtain:

$$\int_{t_{k-1}}^{t_k} \frac{(t_j-\psi)^{-\alpha}}{\Gamma(1-\alpha)}\, u'(\psi)\,\mathrm{d}\psi \;\le\; \Big(\frac{1}{\tau_k}\int_{t_{k-1}}^{t_k} \frac{(t_j-\psi)^{-\alpha}}{\Gamma(1-\alpha)}\,\mathrm{d}\psi\Big)\Big(\int_{t_{k-1}}^{t_k} u'(\psi)\,\mathrm{d}\psi\Big).$$

Summing this inequality over $k = 1, \dots, j$ yields:

$$D^{\alpha}_{t_j} u \;\le\; \sum_{k=1}^{j}\Big(\frac{1}{\tau_k}\int_{t_{k-1}}^{t_k} \frac{(t_j-\psi)^{-\alpha}}{\Gamma(1-\alpha)}\,\mathrm{d}\psi\Big)\Big(\int_{t_{k-1}}^{t_k} u'(\psi)\,\mathrm{d}\psi\Big).$$

By the lower bound for the discrete convolution weights $g_{j,k}$ given in (13), we have:

$$\frac{1}{\tau_k}\int_{t_{k-1}}^{t_k} \frac{(t_j-\psi)^{-\alpha}}{\Gamma(1-\alpha)}\,\mathrm{d}\psi \le \frac{11}{4}\, g_{j,k}.$$

Consequently, $D^{\alpha}_{t_j} u \le \frac{11}{4}\sum_{k=1}^{j} g_{j,k}\int_{t_{k-1}}^{t_k} u'(\psi)\,\mathrm{d}\psi$.

Multiplying by $p_{n,j}$ and summing over $j = 1, \dots, n$ gives:

$$\sum_{j=1}^{n} p_{n,j}\, D^{\alpha}_{t_j} u \le \frac{11}{4}\sum_{j=1}^{n} p_{n,j}\sum_{k=1}^{j} g_{j,k}\int_{t_{k-1}}^{t_k} u'(\psi)\,\mathrm{d}\psi = \frac{11}{4}\sum_{k=1}^{n}\Big(\int_{t_{k-1}}^{t_k} u'(\psi)\,\mathrm{d}\psi\Big)\sum_{j=k}^{n} p_{n,j} g_{j,k}.$$

Using the identity (24), namely $\sum_{j=k}^{n} p_{n,j} g_{j,k} = 1$, we obtain:

$$\sum_{j=1}^{n} p_{n,j}\, D^{\alpha}_{t_j} u \le \frac{11}{4}\sum_{k=1}^{n}\int_{t_{k-1}}^{t_k} u'(\psi)\,\mathrm{d}\psi = \frac{11}{4}\int_{0}^{t_n} u'(\psi)\,\mathrm{d}\psi.$$

(2) Assume that u' is nonnegative and monotonic. If u' is decreasing, the result follows directly from part (1), since $p_{n,j} > 0$ and $D^{\alpha}_{t_j} u \ge 0$. Hence,

$$\sum_{j=1}^{n-1} p_{n,j}\, D^{\alpha}_{t_j} u \le \sum_{j=1}^{n} p_{n,j}\, D^{\alpha}_{t_j} u \le \frac{11}{4}\int_{0}^{t_n} u'(\psi)\,\mathrm{d}\psi.$$

Now, suppose that u' is increasing. Then,

$$\sum_{j=1}^{n-1} p_{n,j}\, D^{\alpha}_{t_j} u = \sum_{j=1}^{n-1} p_{n,j}\sum_{k=1}^{j}\int_{t_{k-1}}^{t_k} \frac{(t_j-\psi)^{-\alpha}}{\Gamma(1-\alpha)}\, u'(\psi)\,\mathrm{d}\psi.$$

Since $u'(\psi) \le u'(t_k)$ for $\psi \in (t_{k-1}, t_k)$, we have:

$$\begin{aligned}\sum_{j=1}^{n-1} p_{n,j}\, D^{\alpha}_{t_j} u &\le \sum_{j=1}^{n-1} p_{n,j}\sum_{k=1}^{j} u'(t_k)\int_{t_{k-1}}^{t_k} \frac{(t_j-\psi)^{-\alpha}}{\Gamma(1-\alpha)}\,\mathrm{d}\psi \\ &\le \frac{11}{4}\sum_{j=1}^{n-1} p_{n,j}\sum_{k=1}^{j} u'(t_k)\, g_{j,k}\,\tau_k = \frac{11}{4}\sum_{k=1}^{n-1} u'(t_k)\,\tau_k \sum_{j=k}^{n-1} p_{n,j} g_{j,k}.\end{aligned}$$

From (23), we know that $\sum_{j=k}^{n-1} p_{n,j} g_{j,k} \le \sum_{j=k}^{n} p_{n,j} g_{j,k} = 1$. Therefore,

$$\sum_{j=1}^{n-1} p_{n,j}\, D^{\alpha}_{t_j} u \le \frac{11}{4}\sum_{k=1}^{n-1} u'(t_k)\,\tau_k.$$

Since the mesh is graded, $\tau_k \le \tau_{k+1}$. Furthermore, because u' is increasing, $u'(t_k)\tau_{k+1} \le \int_{t_k}^{t_{k+1}} u'(\psi)\,\mathrm{d}\psi$. This implies:

$$\sum_{j=1}^{n-1} p_{n,j}\, D_{t_j}^{\alpha} u \le \frac{11}{4}\sum_{k=1}^{n-1} u'(t_k)\,\tau_{k+1} \le \frac{11}{4}\sum_{k=1}^{n-1}\int_{t_k}^{t_{k+1}} u'(\psi)\,\mathrm{d}\psi$$
$$= \frac{11}{4}\int_{t_1}^{t_n} u'(\psi)\,\mathrm{d}\psi \le \frac{11}{4}\int_{0}^{t_n} u'(\psi)\,\mathrm{d}\psi,$$

□

The following hypotheses on the kernel $\mathcal{K}$, the solution u, and the initial datum φ are used in the quadrature error analysis.

Hypothesis 1.

(K1) Regularity of the kernel: *For each $(x,t) \in [0,L]\times(0,T]$, the map $s \mapsto \mathcal{K}(x,t,s)$ belongs to $C^4([0,T])$, and there exists a constant $C_{\mathcal{K}} > 0$ such that $\left|\partial_s^m \mathcal{K}(x,t,s)\right| \le C_{\mathcal{K}}$, $m = 0,1,2,3,4$, uniformly in $(x,t,s) \in [0,L]\times[0,T]\times[0,T]$.*

(K2) Regularity of the solution: *The solution u of the continuous problem (1) satisfies the weak-singularity bounds $\left|\partial_t^m u(x,t)\right| \le C_u\left(1 + t^{\alpha-m}\right)$, $m = 0,1,2,3,4$, uniformly in $x \in [0,L]$ and $t \in (0,T]$, where $C_u > 0$ is a constant independent of x and t.*

(K3) Initial datum and compatibility: *The initial datum satisfies $\varphi \in H^2(\Omega)\cap H_0^1(\Omega)$, so that φ is bounded and continuous on $\bar{\Omega}$, and the compatibility conditions $\varphi(0) = \psi_1(0)$, $\varphi(L) = \psi_2(0)$ hold for the boundary data ψ_1, ψ_2.*

Under (K1)–(K3), the Volterra integrand $g(s) = \mathcal{K}(x,t,s)u(x,s)$ admits the split $g(s) = g(0) + \tilde{g}(s)$ with $g(0) = \mathcal{K}(x,t,0)\varphi(x)$ and $\tilde{g}(s) = g(s) - g(0)$. By Leibniz' rule and the standard expansion $u(x,s) = \varphi(x) + O(s^{\alpha})$ near $s = 0$, the remainder satisfies:

$$|\tilde{g}^{(m)}(s)| \le C\, s^{\alpha-m}, \qquad m = 0,1,2,3,4, \qquad s \in (0,T].$$

Theorem 3 ([13,25]). *Let Λ be a positive constant independent of n, and let $\lambda_i \ge 0$ be constants satisfying $0 < \sum_{i=0}^{n-1}\lambda_i \le \Lambda$ for $n \ge 1$. Suppose the nonnegative sequences $\{\xi_n, \zeta_n : n \ge 1\}$ are bounded and the nonnegative grid function $\{u_n : n \ge 0\}$ satisfies:*

$$\sum_{k=1}^{n} g_{n,k}\,\nabla_\tau(u_k)^2 \;\le\; \sum_{k=1}^{n}\lambda_{n-k}\,(u_{k,\theta_1})^2 + \xi_n\, u_{n,\theta_2} + (\zeta_n)^2, \quad 1 \le n \le N, \tag{25}$$

where $\nabla_\tau(u_k)^2 := (u_k)^2 - (u_{k-1})^2$, and for $i = 1,2$ and each n, $u_{n,\theta_i} := \theta_i\, u_{n-1} + (1-\theta_i)\, u_n$, $\theta_i \in [0,1]$. If the non-uniform graded mesh satisfies the maximum time-step criterion $\tau_N \le \left[\frac{11}{2\mu}\Lambda\right]^{-1/\alpha}$, then

$$u_n \;\le\; 2E_\alpha\Big(\tfrac{11}{2\mu}\,\Lambda\, t_n^{\alpha}\Big)\Big[\,u_0 + \max_{1\le k\le n}\sum_{j=1}^{k} p_{k,j}\,(\xi_j + \zeta_j) + \max_{1\le j\le n}\zeta_j\Big], \quad n = 1,\ldots,N. \tag{26}$$

Proof. Replace the index n in (25) by j, multiply by $p_{n,j} \ge 0$, and sum over $j = 1,\ldots,n$ to obtain:

$$\sum_{j=1}^{n} p_{n,j}\sum_{k=1}^{j} g_{j,k}\nabla_\tau(u_k)^2 \;\le\; \sum_{j=1}^{n} p_{n,j}\Big(\sum_{k=1}^{j}\lambda_{j-k}(u_{k,\theta_1})^2 + \xi_j\, u_{j,\theta_2} + (\zeta_j)^2\Big). \tag{27}$$

By definition of $p_{n,j}$, we have the exact telescoping identity:

$$\sum_{j=1}^{n} p_{n,j} \sum_{k=1}^{j} g_{j,k} \nabla_\tau (u_k)^2 \;=\; (u_n)^2 - (u_0)^2. \tag{28}$$

Substituting (28) into (27) yields:

$$(u_n)^2 \;\le\; (u_0)^2 + \sum_{j=1}^{n} p_{n,j} \Big(\sum_{k=1}^{j} \lambda_{j-k} (u_{k,\theta_1})^2 \Big) + \sum_{j=1}^{n} p_{n,j} \big(\xi_j \, u_{j,\theta_2} + (\zeta_j)^2 \big). \tag{29}$$

For $n = 1, \ldots, N$, set:

$$F_n := 2E_\alpha\Big(\tfrac{11}{2\mu} \Lambda \, t_n^\alpha \Big), \quad G_n := u_0 + \max_{1 \le k \le n} \sum_{j=1}^{k} p_{k,j} (\xi_j + \zeta_j) + \max_{1 \le j \le n} \zeta_j. \tag{30}$$

Then, estimate (26) can be rewritten as $u_n \le F_n \, G_n$. Both F_n and G_n are non-decreasing in n.

If $u_1 \le \zeta_1$, then $u_1 \le G_1 \le F_1 G_1$. Otherwise, $u_1 > \zeta_1 \ge 0$. Then, (30) with $n = 1$ gives:

$$(u_1)^2 \;\le\; (u_0)^2 + p_{1,1} \, \lambda_0 \, (u_{1,\theta_1})^2 + p_{1,1} \big(\xi_1 \, u_{1,\theta_2} + \zeta_1^2 \big). \tag{31}$$

If $u_1 \le u_0$, then $u_1 \le G_1 \le F_1 G_1$. So, assume $u_1 > u_0$. Then $\max\{u_{1,\theta_1}, u_{1,\theta_2}\} \le u_1$, and since $\zeta_1 \le u_1$, we may replace $\zeta_1^2 \le \zeta_1 u_1$ in (31), giving

$$(u_1)^2 \;\le\; u_1 G_1 + (u_1)^2 \, p_{1,1} \, \lambda_0. \tag{32}$$

By the bound $p_{1,1} \le \frac{11}{4\mu} \tau_1^\alpha$ and the time-step criterion, $p_{1,1} \, \lambda_0 \le \frac{11}{4\mu} \, \tau_1^\alpha \, \Lambda \le \frac{1}{2}$. Inserting this into (32) and dividing by $u_1 > 0$, we obtain $u_1 \le 2G_1 \le F_1 G_1$.

Fix $k \in \{2, \ldots, N\}$ and assume (30) holds for $n = 1, \ldots, k-1$. Set $\zeta_k^* := \max_{1 \le j \le k} \zeta_j$. If $u_k \le \zeta_k^*$, the result follows immediately. Otherwise, $u_k > \zeta_k^* \ge 0$. For $n = k$,

$$(u_k)^2 \;\le\; (u_0)^2 + \sum_{j=1}^{k} p_{k,j} \Big(\sum_{s=1}^{j} \lambda_{j-s} (u_{s,\theta_1})^2 \Big) + \sum_{j=1}^{k} p_{k,j} \big(\xi_j \, u_{j,\theta_2} + \zeta_j \, u_k \big). \tag{33}$$

Choose $\tau \in \{0, 1, \ldots, k-1\}$ such that $u_\tau = \max_{0 \le j \le k-1} u_j$. If $u_k \le u_\tau$, then $u_k \le F_k G_k$. So assume $u_k > u_\tau$. Then, $u_{j,\theta_i} \le u_k$. Hence, (33) implies:

$$(u_k)^2 \;\le\; u_k \, u_0 + u_k \sum_{j=1}^{k-1} p_{k,j} \Big(\sum_{s=1}^{j} \lambda_{j-s} \, u_{s,\theta_1} \Big) + (u_k)^2 \, p_{k,k} \sum_{s=1}^{k} \lambda_{k-s} + u_k \sum_{j=1}^{k} p_{k,j} (\xi_j + \zeta_j). \tag{34}$$

By $p_{k,k} \le \frac{11}{4\mu} \tau_k^\alpha$, we have $p_{k,k} \sum_{s=1}^{k} \lambda_{k-s} \le \frac{1}{2}$. Substituting into (34), cancelling $\frac{1}{2}(u_k)^2$, and dividing by $u_k > 0$, we obtain:

$$u_k \;\le\; 2\Big(u_0 + \sum_{j=1}^{k-1} p_{k,j} \sum_{s=1}^{j} \lambda_{j-s} \, u_{s,\theta_1} + \sum_{j=1}^{k} p_{k,j} (\xi_j + \zeta_j) \Big). \tag{35}$$

By the inductive hypothesis, $u_{s,\theta_1} \le F_s G_s$. Since $G_s \le G_k$ and $\sum_{s=1}^{j} \lambda_{j-s} \le \Lambda$:

$$\sum_{j=1}^{k-1} p_{k,j} \sum_{s=1}^{j} \lambda_{j-s} \, u_{s,\theta_1} \le \Lambda \, G_k \sum_{j=1}^{k-1} p_{k,j} \, F_j \;=\; 2\Lambda \, G_k \sum_{j=1}^{k-1} p_{k,j} \, E_\alpha\Big(\tfrac{11}{2\mu} \Lambda \, t_j^\alpha \Big). \tag{36}$$

Applying the discrete convolution inequality for the Mittag-Leffler function [16] with $K = \frac{11}{2\mu}\Lambda$:

$$\sum_{j=1}^{k-1} p_{k,j}\, E_\alpha\Big(\tfrac{11}{2\mu}\Lambda\, t_j^\alpha\Big) \;\le\; \frac{11}{4\mu\big(\frac{11}{2\mu}\Lambda\big)}\Big(E_\alpha\Big(\tfrac{11}{2\mu}\Lambda\, t_k^\alpha\Big)-1\Big) \;=\; \frac{1}{2\Lambda}\Big(E_\alpha\Big(\tfrac{11}{2\mu}\Lambda\, t_k^\alpha\Big)-1\Big). \tag{37}$$

Substituting (37) into (36) yields:

$$\sum_{j=1}^{k-1} p_{k,j} \sum_{s=1}^{j} \lambda_{j-s}\, u_{s,\theta_1} \;\le\; G_k\Big(E_\alpha\Big(\tfrac{11}{2\mu}\Lambda\, t_k^\alpha\Big)-1\Big). \tag{38}$$

Inserting (38) into (35) gives $u_k \;\le\; 2\Big(u_0 + G_k\Big(E_\alpha\Big(\tfrac{11}{2\mu}\Lambda\, t_k^\alpha\Big)-1\Big) + \sum_{j=1}^{k} p_{k,j}(\xi_j+\zeta_j)\Big)$. By definition of G_k, $u_0 + \sum_{j=1}^{k} p_{k,j}(\xi_j+\zeta_j) \le G_k$. Hence, $u_k \;\le\; 2G_k\, E_\alpha\Big(\tfrac{11}{2\mu}\Lambda\, t_k^\alpha\Big) \;=\; F_k\, G_k$, which completes the proof. □

3.2. Simpson's Rule on the Graded Mesh

Let $n \ge 2$ be an even integer. The Volterra integral term evaluated at the fractional time level $t_{n-\sigma_n}$ is given by $\int_0^{t_{n-\sigma_n}} \mathcal{K}(x, t_{n-\sigma_n}, s)u(x,s)\,\mathrm{d}s$, where $t_{n-\sigma_n} = t_{n-1} + (1-\sigma_n)\tau_n$ and $\sigma_n = \alpha/2$. We split the integral into two parts:

$$\int_0^{t_{n-\sigma_n}} g(s)\,\mathrm{d}s = \int_0^{t_{n-2}} g(s)\,\mathrm{d}s + \int_{t_{n-2}}^{t_{n-\sigma_n}} g(s)\,\mathrm{d}s, \qquad g(s) := \mathcal{K}(x, t_{n-\sigma_n}, s)u(x,s). \tag{39}$$

For $n = 2$, the interval $[0, t_0]$ is degenerate, and the integral reduces to $\int_0^{t_{2-\sigma_2}} g(s)\,\mathrm{d}s = \int_{t_0}^{t_{2-\sigma_2}} g(s)\,\mathrm{d}s$. Let $h_1 = \tau_1$, $h_2 = (1-\sigma_2)\tau_2$, and $H = h_1 + h_2$. Using the quadratic interpolant of g through the nodes t_0, t_1, and $t_{2-\sigma_2}$, we obtain the following approximation:

$$\int_{t_0}^{t_{2-\sigma_2}} g(s)\,\mathrm{d}s \approx \tilde{I}_0^{(S),2} g(t_0) + \tilde{I}_1^{(S),2} g(t_1) + \tilde{I}_{2,\sigma_2}^{(S)} g(t_{2-\sigma_2}),$$

where the weights are given by:

$$\begin{aligned}
\tilde{I}_0^{(S),2} &= \frac{H(2h_1 - h_2)}{6h_1} = \frac{\big(\tau_1 + (1-\sigma_2)\tau_2\big)\big(2\tau_1 - (1-\sigma_2)\tau_2\big)}{6\tau_1},\\
\tilde{I}_1^{(S),2} &= \frac{H^3}{6h_1h_2} = \frac{\big(\tau_1 + (1-\sigma_2)\tau_2\big)^3}{6\tau_1(1-\sigma_2)\tau_2},\\
\tilde{I}_{2,\sigma_2}^{(S)} &= \frac{H(2h_2 - h_1)}{6h_2} = \frac{\big(\tau_1 + (1-\sigma_2)\tau_2\big)\big(2(1-\sigma_2)\tau_2 - \tau_1\big)}{6(1-\sigma_2)\tau_2}.
\end{aligned}$$

For $n \ge 4$, we approximate the integral over $[0, t_{n-2}]$ using the composite Simpson's rule on the graded mesh. The corresponding weights are defined as follows:

$$\begin{aligned}
\bar{I}_0^{(S)} &= \frac{(\tau_1+\tau_2)(2\tau_1-\tau_2)}{6\tau_1},\\
\bar{I}_{2j-1}^{(S)} &= \frac{(\tau_{2j-1}+\tau_{2j})^3}{6\tau_{2j-1}\tau_{2j}}, \qquad j = 1,2,\ldots,\frac{n-2}{2},\\
\bar{I}_{2j}^{(S)} &= \frac{(\tau_{2j-1}+\tau_{2j})(2\tau_{2j}-\tau_{2j-1})}{6\tau_{2j}} + \frac{(\tau_{2j+1}+\tau_{2j+2})(2\tau_{2j+1}-\tau_{2j+2})}{6\tau_{2j+1}}, \quad j = 1,2,\ldots,\frac{n-4}{2},\\
\bar{I}_{n-2}^{(S)} &= \frac{(\tau_{n-3}+\tau_{n-2})(2\tau_{n-2}-\tau_{n-3})}{6\tau_{n-2}}.
\end{aligned}$$

This yields $\int_0^{t_{n-2}} g(s)\,\mathrm{d}s \approx \sum_{k=0}^{n-2} \bar{I}_k^{(S)} g(t_k)$.

For the remaining subinterval $[t_{n-2}, t_{n-\sigma_n}]$, we set $h_1 = \tau_{n-1}$, $h_2 = (1-\sigma_n)\tau_n$, $H = h_1 + h_2 = \tau_{n-1} + (1-\sigma_n)\tau_n$. Using the quadratic interpolant of g through t_{n-2}, t_{n-1}, and $t_{n-\sigma_n}$, we obtain:

$$\int_{t_{n-2}}^{t_{n-\sigma_n}} g(s)\,\mathrm{d}s \approx w_{n-2} g(t_{n-2}) + w_{n-1} g(t_{n-1}) + w_{n-\sigma_n} g(t_{n-\sigma_n}),$$

where $w_{n-2} = \frac{H(2h_1 - h_2)}{6h_1}$, $\quad w_{n-1} = \frac{H^3}{6h_1 h_2}$, $\quad w_{n-\sigma_n} = \frac{H(2h_2 - h_1)}{6h_2}$. Combining the quadrature over $[0, t_{n-2}]$ and $[t_{n-2}, t_{n-\sigma_n}]$, and collecting the coefficients of $g(t_k)$, we arrive at:

$$\int_0^{t_{n-\sigma_n}} g(s)\,\mathrm{d}s = \sum_{k=0}^{n-3} \bar{I}_k^{(S)} g(t_k) + \tilde{I}_{n-2}^{(S),n} g(t_{n-2}) + \tilde{I}_{n-1}^{(S),n} g(t_{n-1}) + \tilde{I}_{n,\sigma_n}^{(S)} g(t_{n-\sigma_n}) + R_n^{(S)},$$

where the modified weights at the end of the interval are:

$$\tilde{I}_{n-2}^{(S),n} = \bar{I}_{n-2}^{(S)} + w_{n-2}, \quad \tilde{I}_{n-1}^{(S),n} = w_{n-1}, \quad \tilde{I}_{n,\sigma_n}^{(S)} = w_{n-\sigma_n}.$$

Consequently, the discrete approximation of the Volterra integral term at the spatial node x_i can be written as follows:

$$\mathcal{J}_{n-\sigma_n}^{S} U_i^n := \sum_{k=0}^{n-3} \bar{I}_k^{(S)} K_{i,k} U_i^k + \tilde{I}_{n-2}^{(S),n} K_{i,n-2} U_i^{n-2} + \tilde{I}_{n-1}^{(S),n} K_{i,n-1} U_i^{n-1} + \tilde{I}_{n,\sigma_n}^{(S)} K_{i,n} U_i^{n,\sigma_n},$$

where $K_{i,k} = \mathcal{K}(x_i, t_{n-\sigma_n}, t_k)$, $K_{i,n} = \mathcal{K}(x_i, t_{n-\sigma_n}, t_{n-\sigma_n})$, and $U_i^{n,\sigma_n} = (1-\sigma_n) U_i^n + \sigma_n U_i^{n-1}$.

Substituting the definition of U_i^{n,σ_n} and regrouping the terms at the current and previous time levels, we obtain:

$$\begin{aligned}
\int_0^{t_{n-\sigma_n}} \mathcal{K}(x_i, t_{n-\sigma_n}, s) u(x_i, s)\,\mathrm{d}s \approx & \sum_{k=0}^{n-3} \bar{I}_k^{(S)} K_{i,k} U_i^k + \tilde{I}_{n-2}^{(S),n} K_{i,n-2} U_i^{n-2} \\
& + \tilde{I}_{n-1}^{(S),n} K_{i,n-1} U_i^{n-1} + \tilde{I}_{n,\sigma_n}^{(S)} K_{i,n} \left[(1-\sigma_n) U_i^n + \sigma_n U_i^{n-1} \right] \\
= & \sum_{k=0}^{n-3} \bar{I}_k^{(S)} K_{i,k} U_i^k + \tilde{I}_{n-2}^{(S),n} K_{i,n-2} U_i^{n-2} \\
& + \left[\tilde{I}_{n-1}^{(S),n} K_{i,n-1} + \sigma_n \tilde{I}_{n,\sigma_n}^{(S)} K_{i,n} \right] U_i^{n-1} + (1-\sigma_n) \tilde{I}_{n,\sigma_n}^{(S)} K_{i,n} U_i^n \\
= & \mathcal{J}_{n-\sigma_n}^{S} U_i^n + R_S^{(n)}.
\end{aligned}$$

Theorem 4. *Let $t_k = T(k/N)^r$, $r \geq 1$, and let $g(s) = g(s; x, t) = K(x, t, s) u(x, s)$ with K, u, φ satisfying* (K1)–(K3). *Write $g = g(0) + \tilde{g}$ with $g(0) = K(x, t, 0)\varphi(x)$ and $\tilde{g} = g - g(0)$, so that*

$$|\tilde{g}^{(m)}(s)| \leq C\, s^{\alpha - m}, \ m = 0, 1, 2, 3, 4, \ s \in (0, T],$$

uniformly in $x \in [0, L]$ and $t \in (0, T]$. Let $Q_n(g)$ be the adapted quadrature of $\int_0^{t_{n-\sigma_n}} g(s)\,\mathrm{d}s$

(a) Even n: *composite Simpson on the panels $[t_{2j-2}, t_{2j}]$ for $j = 1, \ldots, n/2 - 1$, plus the final fractional panel $[t_{n-2}, t_{n-\sigma_n}]$;*

(b) Odd n: *composite Simpson on the pure panels $[t_{2j-2}, t_{2j}]$ for $j = 1, \ldots, (n-1)/2$ (which covers $[0, t_{n-1}]$), plus the trapezoidal rule on the final fractional sub-interval $[t_{n-1}, t_{n-\sigma_n}]$.*

Then, with $\beta := r(\alpha + 1)$,

$$\left|R_n^{(S)}\right| = \left|\int_0^{t_{n-\sigma_n}} g(s)\,ds - Q_n(g)\right| \le C\begin{cases} N^{-\beta}, & \beta < 3, \\ N^{-3}\log N, & \beta = 3, \\ N^{-3}, & \beta > 3, \end{cases}$$

uniformly in $n = 1, \dots, N$ *and in* x. *Consequently,*

$$\left|R_n^{(S)}\right| \le C\,N^{-\min\{3,\,r(\alpha+1)\}}(\log N)^{\delta_{r(\alpha+1),3}} \le C\,N^{-\min\{3-\alpha,\,r\alpha\}},$$

and C *depends only on* α, r, T, C_K, C_u*—not on* N, n *or* h.

Proof. Throughout, C denotes a generic constant with the above dependence (so, in particular, it may depend on T and on the grading parameter r), and $\rho_r := 2^r - 1$ is the maximal forward mesh ratio, so that on every panel

$$1 \le h_2/h_1 \le \rho_r, \qquad H = h_1 + h_2 \le (1+\rho_r)h_1. \tag{40}$$

Because the quadrature is interpolatory, its weights sum to the length of the integration interval; hence, constants are integrated exactly and $R_n^{(S)}(g) = R_n^{(S)}(\tilde{g})$. The bounds on $\tilde{g}^{(m)}$ follow from Leibniz' rule: for $m \ge 1$,

$$\tilde{g}^{(m)}(s) = \sum_{j=0}^{m} \binom{m}{j} \partial_s^j K(x,t,s)\,\partial_s^{m-j} u(x,s),$$

and by (K1)–(K2) each term is bounded by $C\big(1 + s^{\alpha-(m-j)}\big) \le Cs^{\alpha-m}$ for $s \in (0,T]$ (using $s \le T$ and $\alpha - m < 0$). For $m = 0$, $\tilde{g}(s) = K(x,t,s)\big(u(x,s) - \varphi(x)\big) + \big(K(x,t,s) - K(x,t,0)\big)\varphi(x)$, whose two terms are $O(s^\alpha)$ and $O(s) \le CT^{1-\alpha}s^\alpha$ respectively. In particular $\tilde{g}(0) = 0$ and $\tilde{g}' \in L^1(0,T)$, whereas $\tilde{g}'', \tilde{g}''' \notin L^1$ near 0.

On a panel $[x_0, x_2]$ with nodes x_0, $x_1 = x_0 + h_1$, $x_2 = x_0 + H$, the quadratic-interpolatory weights are:

$$w_0 = \frac{H(2h_1 - h_2)}{6h_1}, \qquad w_1 = \frac{H^3}{6h_1h_2}, \qquad w_2 = \frac{H(2h_2 - h_1)}{6h_2}. \tag{41}$$

They are obtained by integrating the three Lagrange basis polynomials, so the rule is exact on $\mathbb{P}_2$ and $w_0 + w_1 + w_2 = H$. By (40),

$$|w_0| \le \tfrac{2+\rho_r}{6}H, \qquad 0 < w_1 \le \tfrac{(1+\rho_r)^3}{6}H, \qquad |w_2| \le \tfrac{1}{2}H, \tag{42}$$

so all weights are $O(H)$ uniformly over panels.

Eexplicit Peano kernel: Let $E(\phi) := \int_{x_0}^{x_2}\phi - \sum_{i=0}^{2} w_i\phi(x_i)$. Since $E|_{\mathbb{P}_2} = 0$, Peano's theorem gives, for $\phi \in W^{3,1}(x_0, x_2)$,

$$E(\phi) = \tfrac{1}{2}\int_{x_0}^{x_2} K_3(s)\,\phi'''(s)\,ds, \qquad K_3(s) := E_\tau\big[(\tau - s)_+^2\big]. \tag{43}$$

Writing $\sigma = s - x_0 \in [0, H]$ and using $(x_0 - s)_+ = 0$,

$$K_3(\sigma) = \frac{(H-\sigma)^3}{3} - w_1(h_1 - \sigma)_+^2 - w_2(H-\sigma)^2. \tag{44}$$

From (41)–(44), we obtain by direct computation:

$$K_3(0) = \frac{H^3}{3} - w_1 h_1^2 - w_2 H^2 = 0, \tag{45}$$

$$K_3'(0) = -H^2 + 2w_1 h_1 + 2w_2 H = 0, \tag{46}$$

$$K_3''(0^+) = 2H - 2w_1 - 2w_2 = 2w_0, \tag{47}$$

$$K_3(H) = 0, \qquad K_3'(H) = 0. \tag{48}$$

These four identities are exact for arbitrary h_1, h_2, not only for $h_1 = h_2$.

Kernel bounds: from (44) and (42), for all $\sigma \in [0, H]$:

$$|K_3(\sigma)| \le \frac{H^3}{3} + w_1 h_1^2 + |w_2| H^2 \le \left(\tfrac{1}{3} + \tfrac{1}{6} + \tfrac{1}{2}\right) H^3 = H^3. \tag{49}$$

Moreover, on the first subinterval $\sigma \in [0, h_1]$ we have $K_3''(\sigma) = 2(H - \sigma) - 2w_1 - 2w_2$; hence, $|K_3''| \le C_{\rho_r} H$ there by (42); combining with (45) and (46) and Taylor's theorem,

$$|K_3(\sigma)| \le \tfrac{1}{2} C_{\rho_r} H \sigma^2, \qquad 0 \le \sigma \le h_1. \tag{50}$$

The singular first panel $[t_0, t_2]$: Here $h_1 = \tau_1$, $H \le C\tau_2 \le C h_1$, and $\tilde{g}'''$ is not integrable, so (43) cannot be invoked directly. For $0 < \varepsilon < h_1$, $\tilde{g} \in C^3[\varepsilon, H]$ and two integrations by parts give:

$$\tfrac{1}{2} \int_\varepsilon^H K_3 \tilde{g}''' = \tfrac{1}{2} \left[K_3 \tilde{g}''\right]_\varepsilon^H - \tfrac{1}{2} \left[K_3' \tilde{g}'\right]_\varepsilon^H + \tfrac{1}{2} \int_\varepsilon^H K_3'' \tilde{g}'.$$

By (48), the contributions at H vanish. At $\varepsilon \to 0^+$, (45)–(50) give $|K_3(\varepsilon)\tilde{g}''(\varepsilon)| \le CH\varepsilon^2 \varepsilon^{\alpha-2} = CH\varepsilon^\alpha \to 0$ and $|K_3'(\varepsilon)\tilde{g}'(\varepsilon)| \le CH\varepsilon \cdot \varepsilon^{\alpha-1} = CH\varepsilon^\alpha \to 0$. Since K_3'' is bounded and piecewise continuous and $\tilde{g}' \in L^1$, the limit exists and

$$E_1(\tilde{g}) = \tfrac{1}{2} \int_0^H K_3''(s)\, \tilde{g}'(s)\, ds, \qquad |E_1(\tilde{g})| \le CH \int_0^H s^{\alpha-1} ds \le CH^{\alpha+1} \le CN^{-r(\alpha+1)}. \tag{51}$$

This holds for every $r \ge 1$; the exceptional value $r = \log_2 3$ plays no role.

Regular panels $[t_{2j-2}, t_{2j}]$, $j \ge 2$: Here $t_{2j-2} > 0$, $\tilde{g} \in C^3$ up to the endpoints, and (43)–(49) give the following classical bound:

$$|E_j| \le \tfrac{1}{2} H_j^4 \max_{[t_{2j-2}, t_{2j}]} |\tilde{g}'''|.$$

On the graded mesh, $H_j \le C\tau_{2j} \le CN^{-r} j^{r-1}$ and $t_{2j-2} \ge cN^{-r} j^r$ for $j \ge 2$, whence,

$$|E_j| \le C\left(N^{-r} j^{r-1}\right)^4 \left(N^{-r} j^r\right)^{\alpha-3} = C\, N^{-r(\alpha+1)}\, j^{r(\alpha+1)-4} = C\, N^{-\beta} j^{\beta-4}. \tag{52}$$

Case I n even: final fractional panel. For even $n \ge 4$ the last panel $[t_{n-2}, t_{n-\sigma_n}]$ has length $H_f \le 2\tau_n \le CN^{-r} n^{r-1}$ and left endpoint $t_{n-2} \ge cN^{-r} n^r$; estimate (52) applies verbatim with $j \asymp n/2$, so it is absorbed into the sum of summation and the exact dominance conditions.

Case II n odd: trapezoidal rule on the final fractional sub-interval. For odd $n \ge 3$, the composite Simpson rule covers $[0, t_{n-1}]$ with $(n-1)/2$ macro-panels. The error from these regular Simpson panels is bounded exactly as in Regular panels $[t_{2j-2}, t_{2j}]$, $j \ge 2$, and their sum over j is handled in summation and the exact dominance conditions. The only additional term is the trapezoidal rule on the final sub-interval $[t_{n-1}, t_{n-\sigma_n}]$ of length $h_4 = (1 - \sigma_n)\tau_n \le \tau_n$. Since $t_{n-1} > 0$, $\tilde{g}''$ is bounded on this sub-interval. The standard trapezoidal error formula gives

$$\left|E_n^{\mathrm{tr}}\right| \le \frac{h_4^3}{12} \max_{[t_{n-1}, t_{n-\sigma_n}]} |\tilde{g}''| \le C\, \tau_n^3\, t_{n-1}^{\alpha-2} \le C\, N^{-\beta}\, n^{\beta-3}.$$

The maximum over $n \geq 3$ is attained at $n = O(1)$ if $\beta < 3$ and at $n = N$ if $\beta > 3$, yielding the uniform bound $|E_n^{\mathrm{tr}}| \leq CN^{-\min\{3,\beta\}}$. For $n = 1$, the interval is $[0, t_{1-\sigma_1}]$, and the pointwise formula fails because $\max|\tilde{g}''| = \infty$. Instead, we use the Peano kernel for the trapezoidal rule, $K_{\mathrm{tr}}(s) = \frac{1}{2}s(h_4 - s)$ for $s \in [0, h_4]$. Since $|K_{\mathrm{tr}}(s)| \leq \frac{1}{2}h_4 s$ and $|\tilde{g}''(s)| \leq Cs^{\alpha-2}$,

$$|E_1^{\mathrm{tr}}| \leq \int_0^{h_4} |K_{\mathrm{tr}}(s)|\,|\tilde{g}''(s)|\,ds \leq Ch_4 \int_0^{h_4} s^{\alpha-1}\,ds = Ch_4 \cdot \frac{h_4^{\alpha}}{\alpha} = Ch_4^{\alpha+1} \leq CN^{-\beta},$$

using $h_4 \leq \tau_1 \leq CN^{-r}$. Thus, for all odd $n \geq 1$, the trapezoidal error is uniformly bounded by $CN^{-\min\{3,\beta\}}$. Since there is only one trapezoidal sub-interval for each odd n, there is no accumulation sum; its contribution is added once to the global bound at each level.

Summation and the exact dominance conditions: At the level n under consideration, the total quadrature error decomposes as follows:

$$\left|R_n^{(S)}\right| \;\leq\; S_{\mathrm{S}}(n) + S_1 + |E_n^{\mathrm{tr}}|\,\mathbf{1}_{n\ \mathrm{odd}},$$

where $S_{\mathrm{S}}(n)$ is the accumulated Simpson-panel error over the regular panels, S_1 is the singular first-panel error, and $|E_n^{\mathrm{tr}}|$ is the single trapezoidal sub-interval at level n (there is no sum over odd levels, because each level's quadrature is a separate quantity). Summing (52) over $j = 2, \ldots, \lfloor n/2 \rfloor \leq N/2$ and comparing with $\sum_{j \leq N/2} j^{\beta-4}$:

$$S_{\mathrm{S}}(n) \leq CN^{-\beta} \sum_{j=1}^{N/2} j^{\beta-4} \leq C \begin{cases} N^{-\beta}, & \beta < 3 \quad \text{(series converges)}, \\ N^{-3}\log N, & \beta = 3 \quad \text{(harmonic series)}, \\ N^{-3}, & \beta > 3 \quad \text{(power series)}. \end{cases}$$

Singular first panel. $S_1 \leq CN^{-\beta}$ by (51), which is of the same order as $S_{\mathrm{S}}(n)$ in the regime $\beta < 3$ and strictly smaller than $S_{\mathrm{S}}(n)$ in the regime $\beta > 3$.

Trapezoidal contribution: $|E_n^{\mathrm{tr}}| \leq CN^{-\min\{3,\beta\}}$ uniformly in n. We distinguish the two regimes:

- If $\beta \leq 3$, then $\min\{3, \beta\} = \beta$, so $|E_n^{\mathrm{tr}}| \leq CN^{-\beta}$. This is of the same order as $S_{\mathrm{S}}(n)$ (which is also $O(N^{-\beta})$ for $\beta \leq 3$), so the total is $O(N^{-\beta})$.
- If $\beta > 3$, then $\min\{3, \beta\} = 3$, so $|E_n^{\mathrm{tr}}| \leq CN^{-3}$. This is of the same order as $S_{\mathrm{S}}(n) = O(N^{-3})$, so the total is $O(N^{-3})$ (the two contributions add to $O(N^{-3})$ with a constant factor).

In neither regime is the trapezoidal contribution larger than the Simpson-panel accumulation; it is at most of the same order. Therefore, the trapezoidal replacement does not change the total order, and

$$\left|R_n^{(S)}\right| \leq C \begin{cases} N^{-\beta}, & \beta < 3, \\ N^{-3}\log N, & \beta = 3, \\ N^{-3}, & \beta > 3, \end{cases}$$

which is the claimed bound. The singular endpoint governs the rate when $\beta < 3$; the accumulation of regular panels governs it when $\beta > 3$; the transition $\beta = 3$ produces exactly one logarithm.

$$|R_n^{(S)}| \leq C\left(N^{-\beta} + N^{-\min\{3,\beta\}}(\log N)^{\delta_{\beta,3}}\right) \leq CN^{-\min\{3,\beta\}}(\log N)^{\delta_{\beta,3}}.$$

Since $3 > 3-\alpha$ and $\beta = r(\alpha+1) > r\alpha$, we have $\min\{3,\beta\} \geq \min\{3-\alpha, r\alpha\}$. The only case in which the logarithm survives is $\beta = 3$, i.e., $r = 3/(\alpha+1)$; then,

$$r\alpha = \frac{3\alpha}{1+\alpha} < 3-\alpha \quad \Longleftrightarrow \quad \alpha^2+\alpha < 3,$$

which holds for every $\alpha \in (0,1)$. Hence $\min\{3-\alpha, r\alpha\} = r\alpha < 3$ and $N^{-3}\log N / N^{-r\alpha} = N^{r\alpha-3}\log N \to 0$, so the logarithmic term is strictly dominated by $N^{-r\alpha}$. In all cases,

$$|R_n^{(S)}| \leq C\, N^{-\min\{3-\alpha,\, r\alpha\}},$$

uniformly in n and x □

Remark 1. *If n is odd, we apply the composite Simpson's rule on the subintervals up to* $[0, t_{n-1}]$*, and employ the trapezoidal rule on the final fractional subinterval* $[t_{n-1}, t_{n-\sigma_n}]$ *to maintain the overall accuracy of the scheme.*

For odd $n \geq 1$, the quadrature nodes on $[0, t_{n-\sigma_n}]$ are:

$$t_0, t_1, \ldots, t_{n-1},\ t_{n-\sigma_n}, \qquad t_{n-\sigma_n} := (1-\sigma_n)t_n + \sigma_n t_{n-1} = t_{n-1} + (1-\sigma_n)\tau_n,$$

with $\sigma_n = \alpha/2 \in (0, 1/2)$. For $n = 1$, the nodes are simply t_0 and $t_{1-\sigma_1}$; for $n \geq 3$, the last node $t_{n-\sigma_n}$ is the fractional endpoint inside the interval $[t_{n-1}, t_n]$. On each regular Simpson macro-panel $[t_{2j-2}, t_{2j}]$, $j = 1, \ldots, (n-1)/2$, the three quadratic weights are

$$\omega_{2j-2}^{(j)} = \frac{H_j(2\tau_{2j-1} - \tau_{2j})}{6\tau_{2j-1}}, \qquad \omega_{2j-1}^{(j)} = \frac{H_j^3}{6\tau_{2j-1}\tau_{2j}}, \qquad \omega_{2j}^{(j)} = \frac{H_j(2\tau_{2j} - \tau_{2j-1})}{6\tau_{2j}},$$

with $H_j := \tau_{2j-1} + \tau_{2j}$. On the last subinterval $[t_{n-1}, t_{n-\sigma_n}]$ of length $h_3 := (1-\sigma_n)\tau_n$, the trapezoidal rule has the two non-negative weights:

$$\omega_{n-1}^{(t)} = \omega_{n,\sigma_n}^{(t)} = \frac{h_3}{2}.$$

The trapezoidal rule gives:

$$\int_{t_{n-1}}^{t_{n-\sigma_n}} g(s)\, ds \approx \frac{h_3}{2}\, g(t_{n-1}) + \frac{h_3}{2}\, g(t_{n-\sigma_n}),$$

and the fractional endpoint value $U^{n,\sigma_n} = (1-\sigma_n)U^n + \sigma_n U^{n-1}$ is split accordingly. Consequently, the discrete Volterra term for odd n is:

$$\mathcal{J}_{n-\sigma_n}^{SN} U^n = \sum_{k=0}^{n-1} \omega_{n,k}^S\, K_{n,k} U^k + \omega_{n,n-1}\, K_{n,n-1} U^{n-1} + \omega_{n,n}\, K_{n,n} U^n,$$

where

- $\omega_{n,k}^S = \omega_k^{(j)}$ for $k = 2j-2, 2j-1, 2j$ on each Simpson macro-panel, with $\omega_{n,n-1}^S$ denoting the last Simpson weight on the panel $[t_{n-3}, t_{n-1}]$ (contributing at the node t_{n-1});
- The total coefficient at level $n-1$ is:

$$\omega_{n,n-1} := \omega_{n,n-1}^S + \frac{h_3}{2} + \sigma_n \frac{h_3}{2} = \omega_{n,n-1}^S + \frac{(1-\sigma_n)(1+\sigma_n)}{2}\tau_n;$$

- The current-level coefficient is:

$$\omega_{n,n} = (1-\sigma_n)\frac{h_3}{2} = \frac{(1-\sigma_n)^2\tau_n}{2}.$$

Both $\omega_{n,n-1}$ and $\omega_{n,n}$ are well defined and $\omega_{n,n} > 0$.

Polynomial exactness for odd n: The composite Simpson rule on each macro-panel $[t_{2j-2}, t_{2j}]$ is exact for quadratic polynomials. The trapezoidal rule on $[t_{n-1}, t_{n-\sigma_n}]$ is exact for linear polynomials:

$$\int_{t_{n-1}}^{t_{n-\sigma_n}} p(s)\,ds = \frac{h_3}{2}\big(p(t_{n-1}) + p(t_{n-\sigma_n})\big) \qquad \forall p \in \mathcal{P}_1.$$

Consequently, the overall quadrature for odd n has degree of exactness 2 on the regular Simpson macro-panels and 1 on the single trapezoidal subinterval. In particular, the constant part of the Volterra integrand is integrated exactly, so $R_n^{(S)}(g) = R_n^{(S)}(\tilde{g})$ holds for odd n as well.

Local truncation error for the trapezoidal subinterval: For $g \in C^2$ on $[t_{n-1}, t_{n-\sigma_n}]$, the trapezoidal remainder is:

$$\int_{t_{n-1}}^{t_{n-\sigma_n}} g(s)\,ds - \frac{h_3}{2}\big(g(t_{n-1}) + g(t_{n-\sigma_n})\big) = -\frac{h_3^3}{12}\,g''(\xi_n), \qquad \xi_n \in (t_{n-1}, t_{n-\sigma_n}), \tag{53}$$

so, the local error on this subinterval satisfies:

$$\big|E_n^{\mathrm{trap}}\big| \le \frac{h_3^3}{12} \max_{[t_{n-1},t_{n-\sigma_n}]} |g''| \le C\,h_3^3\,t_{n-1}^{\alpha-2} \le C\,(N^{-r}n^{r-1})^3\,(N^{-r}n^r)^{\alpha-2} = C\,N^{-r(\alpha+1)}n^{r(\alpha+1)-3}.$$

For odd $n \ge 3$, $t_{n-1} > 0$ and this bound is valid. The maximum over $n \ge 3$ is attained either at $n = O(1)$ (giving $O(N^{-r(\alpha+1)})$) or at $n = N$ (giving $O(N^{-3})$ for $r(\alpha+1) > 3$), so in all cases

$$\big|E_n^{\mathrm{trap}}\big| \le C\,N^{-\min\{3,r(\alpha+1)\}} \qquad \forall\, n \text{ odd},\ n \ge 3.$$

For $n = 1$, the trapezoidal subinterval is $[t_0, t_{1-\sigma_1}]$ with $t_0 = 0$, and the pointwise formula $-h_3^3/12\,g''(\xi)$ is not applicable because $\max_{[0,h_3]}|g''| = +\infty$. Instead, we use the Peano kernel for the trapezoidal rule: on $[0, h_3]$,

$$\big|E_1^{\mathrm{trap}}\big| = \left|\int_0^{h_3} K^{\mathrm{trap}}(s)\,g''(s)\,ds\right|, \qquad \big|K^{\mathrm{trap}}(s)\big| = \frac{s(h_3-s)}{2} \le C\,s\,h_3.$$

Using $|g''(s)| \le Cs^{\alpha-2}$ and the extra factor s from the Peano kernel near $s = 0$,

$$\big|E_1^{\mathrm{trap}}\big| \le C\int_0^{h_3} s\,h_3 \cdot s^{\alpha-2}\,ds = C\,h_3\int_0^{h_3} s^{\alpha-1}\,ds = C\,h_3^{\alpha+1} \le C\,N^{-r(\alpha+1)}.$$

Hence, the bound $\big|E_n^{\mathrm{trap}}\big| \le CN^{-\min\{3,r(\alpha+1)\}}$ holds for all odd $n \ge 1$. In particular, the trapezoidal step does not degrade the rate established for the composite Simpson part on $[0, t_{n-1}]$, because both terms share the same size $N^{-\min\{3,r(\alpha+1)\}}$. The composite Simpson rule on $[0, t_{n-1}]$ covers the $(n-1)/2$ regular macro-panels $[t_{2j-2}, t_{2j}]$, $j = 1, \ldots, (n-1)/2$, and no fractional endpoint appears (the last panel $[t_{n-3}, t_{n-1}]$ ends at the grid node t_{n-1}). The Peano-kernel analysis is therefore a simpler version of the even-n analysis in Theorem 4, with no fractional endpoint to handle: the singular first panel $[t_0, t_2]$ contributes $O(N^{-r\alpha})$, and the regular panels together with the last macro-panel $[t_{n-3}, t_{n-1}]$ contribute $O(N^{-\min\{3,r(\alpha+1)\}}(\log N)^{\delta_{r(\alpha+1),3}})$. Hence, the composite Simpson part on $[0, t_{n-1}]$ satisfies

$$\left|\int_0^{t_{n-1}} g\,ds - \mathcal{Q}_n^S(g)\right| \le C\,N^{-\min\{r\alpha,3\}}. \tag{54}$$

Combining (53) and (54), the local error per odd step is $\|R_n^{(S)}\|_{\mathcal{H}} \le C\,N^{-\min\{r\alpha,3\}}$ uniformly in $n \ge 1$.

The discrete fractional Grönwall inequality (Theorem 3) is applied under the step-size restriction $\tau_N \le \tau_{\text{crit}}$. The convolution coefficients $\lambda_{n-k} = \lambda C_K|\omega_{n,k}|$ satisfy $\sum_{k=1}^{n}\lambda_{n-k} \le \lambda C_K C_w T$ by the total-variation bound, so the Grönwall hypothesis is met. Consequently, the accumulated error from the quadrature is bounded by:

$$\|R^{\text{acc}}\|_{\mathcal{H}} \le C\sum_{k=1}^{n} p_{n,k}\|R_k^{(S)}\|_{\mathcal{H}} \le C\,N^{-\min\{r\alpha,3\}},$$

with no logarithmic factor in the final rate. For even n, gives the sharper bound $|R_n^{(S)}| \le C\,N^{-\min\{r\alpha,4\}}$, For odd n, give $|R_n^{(S)}| \le C\,N^{-\min\{r\alpha,3\}}$. Therefore, for all $n \ge 1$, $|R_n^{(S)}| \le C\,N^{-\min\{r\alpha,3\}}$

3.3. Numerov Scheme for the Spatial Operator $\mathbb{L}_x$

To achieve high-order spatial accuracy, we discretize the spatial domain $[0, L]$ using a uniform mesh. For a given positive integer M, let $x_i = ih$ for $i = 0, 1, \ldots, M$, where $h = L/M$ is the spatial step size. The foundation of the classical Numerov scheme is the fourth-order compact difference operator $\mathcal{H}$, defined by its action on a grid function U_i as follows:

$$\mathcal{H}U_i = \begin{cases} \dfrac{1}{12}U_{i+1} + \dfrac{10}{12}U_i + \dfrac{1}{12}U_{i-1} = \left(1 + \dfrac{h^2}{12}\delta_x^2\right)U_i, & \text{if } i = 1, 2, \ldots, M-1, \\ U_i, & \text{if } i = 0, M, \end{cases} \tag{55}$$

where $\delta_x^2 U_i = \frac{1}{h^2}(U_{i+1} - 2U_i + U_{i-1})$ is the standard second-order central difference operator.

The key property of the compact operator $\mathcal{H}$ is its ability to approximate the second derivative with fourth-order accuracy, which is the defining feature of the Numerov method. The following lemma, established in [17], provides the theoretical foundation for the Numerov approximation:

Lemma 5 ([17]). *Let $\mathcal{H}$ be the compact operator defined in (40). Suppose $u(x) \in C^6[0, L]$. Then, at the interior grid points x_i ($i = 1, 2, \ldots, M-1$), the following Numerov approximation holds:*

$$\mathcal{H}u_{xx}(x_i) = \delta_x^2 u(x_i) + \mathcal{O}(h^4). \tag{56}$$

Since $\mathcal{H}$ is invertible on the space of grid functions satisfying homogeneous boundary conditions, we can write $\mathcal{H}^{-1} = \left(1 + \frac{h^2}{12}\delta_x^2\right)^{-1}$. Applying $\mathcal{H}^{-1}$ to (56) yields the standard Numerov spatial discretization:

$$u_{xx}(x_i) = \mathcal{H}^{-1}\delta_x^2 u(x_i) + \mathcal{O}(h^4). \tag{57}$$

Throughout, we set $K_{i,n} := K(x_i, t_{n-\sigma_n}, t_{n-\sigma_n})$, $\quad K_{i,k} := K(x_i, t_{n-\sigma_n}, t_k)$.

For even $n \ge 2$, define the discrete Volterra operator:

$$\mathcal{J}_{n-\sigma_n}^{SN} U_i^n := \sum_{k=0}^{n-3} \bar{I}_k^{(S)} K_{i,k} U_i^k + \tilde{I}_{n-2}^{(S),n} K_{i,n-2} U_i^{n-2} + \tilde{I}_{n-1}^{(S),n} K_{i,n-1} U_i^{n-1} + \tilde{I}_{n,\sigma_n}^{(S)} K_{i,n} U_i^{n,\sigma_n},$$

where $U_i^{n,\sigma_n} = (1-\sigma_n)U_i^n + \sigma_n U_i^{n-1}$, $\;K_{i,k} = \mathcal{K}(x_i, t_{n-\sigma_n}, t_k)$, $\;K_{i,n} = \mathcal{K}(x_i, t_{n-\sigma_n}, t_{n-\sigma_n})$.

For $n = 2$, the sum $\sum_{k=0}^{n-3}$ is empty and the weights $\tilde{I}_0^{(S),2}$, $\tilde{I}_1^{(S),2}$, $\tilde{I}_{2,\sigma_2}^{(S)}$ are used. The fully discrete equation at $t_{n-\sigma_n}$ is:

$$D_N^{\alpha} U_i^{n-\sigma_n} - A\mathcal{H}^{-1}\delta_x^2 U_i^{n,\sigma_n} + CU_i^{n,\sigma_n} + \lambda \mathcal{J}_{n-\sigma_n}^{SN} U_i^n = f_i^{n-\sigma_n} + R_i^{n-\sigma_n}, \quad i = 1, \dots, M-1,$$

where $D_N^{\alpha} U_i^{n-\sigma_n} = g_{n,n} U_i^n - g_{n,1} U_i^0 - \sum_{j=2}^{n} (g_{n,j} - g_{n,j-1}) U_i^{j-1}$. Substituting this expression and expanding $\mathcal{J}_{n-\sigma_n}^{SN} U_i^n$ gives:

$$\begin{aligned}
&\left[g_{n,n} + (1-\sigma_n)C + \lambda(1-\sigma_n)\tilde{I}_{n,\sigma_n}^{(S)} K_{i,n}\right] U_i^n - (1-\sigma_n) A\mathcal{H}^{-1}\delta_x^2 U_i^n \\
&\quad = f_i^{n-\sigma_n} + R_i^{n-\sigma_n} + g_{n,1} U_i^0 + \sum_{j=2}^{n} (g_{n,j} - g_{n,j-1}) U_i^{j-1} - \sigma_n C U_i^{n-1} + \sigma_n A\mathcal{H}^{-1}\delta_x^2 U_i^{n-1} \\
&\qquad - \lambda \mathcal{B}_i^n - \lambda \sigma_n \tilde{I}_{n,\sigma_n}^{(S)} K_{i,n} U_i^{n-1},
\end{aligned} \tag{58}$$

where $\mathcal{B}_i^n := \sum_{k=0}^{n-3} \tilde{I}_k^{(S)} K_{i,k} U_i^k + \tilde{I}_{n-2}^{(S),n} K_{i,n-2} U_i^{n-2} + \tilde{I}_{n-1}^{(S),n} K_{i,n-1} U_i^{n-1}$.

Applying the compact operator $\mathcal{H}$ to both sides of (58), and using

$$\mathcal{H}[A\mathcal{H}^{-1}\delta_x^2 U] = A\delta_x^2 U, \qquad \mathcal{H}[CU] = C\mathcal{H}[U],$$

we obtain:

$$\begin{aligned}
&\mathcal{H}\left[\left(g_{n,n} + (1-\sigma_n)C + \lambda(1-\sigma_n)\tilde{I}_{n,\sigma_n}^{(S)} K_{i,n}\right) U_i^n\right] - (1-\sigma_n) A\delta_x^2 U_i^n \\
&\quad = \mathcal{H} f_i^{n-\sigma_n} + \mathcal{H} R_i^{n-\sigma_n} + g_{n,1}\mathcal{H}[U^0]_i + \sum_{j=2}^{n} (g_{n,j} - g_{n,j-1})\mathcal{H}[U^{j-1}]_i \\
&\qquad - \sigma_n C\mathcal{H}[U^{n-1}]_i + \sigma_n A\delta_x^2 U_i^{n-1} - \lambda\mathcal{H}[\mathcal{B}_i^n] - \lambda\sigma_n \tilde{I}_{n,\sigma_n}^{(S)}\left[K_{i,n}\mathcal{H}[U^{n-1}]_i + \mathcal{C}_{i,n}^{-} U_{i-1}^{n-1} + \mathcal{C}_{i,n}^{+} U_{i+1}^{n-1}\right].
\end{aligned} \tag{59}$$

Here, $\mathcal{H}[\mathcal{B}_i^n] = \sum_{k=0}^{n-3} \tilde{I}_k^{(S)} \mathcal{H}[K_{i,k} U_i^k] + \tilde{I}_{n-2}^{(S),n} \mathcal{H}[K_{i,n-2} U_i^{n-2}] + \tilde{I}_{n-1}^{(S),n} \mathcal{H}[K_{i,n-1} U_i^{n-1}]$.

For any grid function U and coefficient K, the exact algebraic identity

$$\mathcal{H}[K_i U_i] = K_i \mathcal{H}[U]_i + \frac{K_{i-1} - K_i}{12} U_{i-1} + \frac{K_{i+1} - K_i}{12} U_{i+1}$$

holds. Equivalently,

$$\mathcal{H}[K_i U_i] = K_i \mathcal{H}[U]_i + \mathcal{C}_i^{-} U_{i-1} + \mathcal{C}_i^{0} U_i + \mathcal{C}_i^{+} U_{i+1},$$

with $\mathcal{C}_i^{-} = \frac{K_{i-1} - K_i}{12}$, $\mathcal{C}_i^{0} = 0$, $\mathcal{C}_i^{+} = \frac{K_{i+1} - K_i}{12}$. Substituting these expressions, along with

$$\mathcal{H}[U^k]_i = \frac{1}{12} U_{i-1}^k + \frac{10}{12} U_i^k + \frac{1}{12} U_{i+1}^k, \quad \delta_x^2 U_i^k = \frac{U_{i+1}^k - 2U_i^k + U_{i-1}^k}{h^2},$$

yields the tridiagonal system

$$A_i^{+} U_{i+1}^n + B_i U_i^n + A_i^{-} U_{i-1}^n = \mathcal{F}_i^{n-\sigma_n}, \qquad i = 1, \dots, M-1, \tag{60}$$

where

$$\begin{aligned}
A_i^{+} &= \frac{1}{12}\left[g_{n,n} + (1-\sigma_n)C + \lambda(1-\sigma_n)\tilde{I}_{n,\sigma_n}^{(S)} K_{i,n}\right] - \frac{(1-\sigma_n)A}{h^2} + \lambda(1-\sigma_n)\tilde{I}_{n,\sigma_n}^{(S)} \mathcal{C}_{i,n}^{+}, \\
B_i &= \frac{10}{12}\left[g_{n,n} + (1-\sigma_n)C + \lambda(1-\sigma_n)\tilde{I}_{n,\sigma_n}^{(S)} K_{i,n}\right] + \frac{2(1-\sigma_n)A}{h^2}, \\
A_i^{-} &= \frac{1}{12}\left[g_{n,n} + (1-\sigma_n)C + \lambda(1-\sigma_n)\tilde{I}_{n,\sigma_n}^{(S)} K_{i,n}\right] - \frac{(1-\sigma_n)A}{h^2} + \lambda(1-\sigma_n)\tilde{I}_{n,\sigma_n}^{(S)} \mathcal{C}_{i,n}^{-},
\end{aligned}$$

and

$$\begin{aligned}\mathcal{F}_i^{n-\sigma_n} =& \mathcal{H}f_i^{n-\sigma_n} + g_{n,1}\mathcal{H}[U^0]_i + \sum_{j=2}^{n}(g_{n,j} - g_{n,j-1})\mathcal{H}[U^{j-1}]_i + \sigma_n A\delta_x^2 U_i^{n-1} - \sigma_n C\mathcal{H}[U^{n-1}]_i \\ & - \lambda\sigma_n \tilde{I}_{n,\sigma_n}^{(S)}\left[K_{i,n}\mathcal{H}[U^{n-1}]_i + \mathcal{C}_{i,n}^{-}U_{i-1}^{n-1} + \mathcal{C}_{i,n}^{+}U_{i+1}^{n-1}\right] - \lambda\left[\sum_{k=0}^{n-3}\bar{I}_k^{(S)}\left(K_{i,k}\mathcal{H}[U^k]_i + \mathcal{C}_{i,k}^{-}U_{i-1}^{k} + \mathcal{C}_{i,k}^{+}U_{i+1}^{k}\right)\right. \\ & + \tilde{I}_{n-2}^{(S),n}\left(K_{i,n-2}\mathcal{H}[U^{n-2}]_i + \mathcal{C}_{i,n-2}^{-}U_{i-1}^{n-2} + \mathcal{C}_{i,n-2}^{+}U_{i+1}^{n-2}\right) \\ & \left. + \tilde{I}_{n-1}^{(S),n}\left(K_{i,n-1}\mathcal{H}[U^{n-1}]_i + \mathcal{C}_{i,n-1}^{-}U_{i-1}^{n-1} + \mathcal{C}_{i,n-1}^{+}U_{i+1}^{n-1}\right)\right] + \mathcal{H}R_i^{n-\sigma_n}.\end{aligned}$$

Remark 2. *Equation (60) is a tridiagonal system at each time level n, which can be efficiently solved using the Thomas algorithm in $\mathcal{O}(M)$ operations. The compact operator $\mathcal{H}$ is applied to all terms, ensuring that the fourth-order spatial accuracy is maintained throughout the scheme. The Volterra integral terms are treated explicitly using previously computed values U^k for $k < n$, preserving the marching-in-time structure of the numerical method.*

Theorem 5 (Spatial Truncation Error of the Numerov Scheme)**.** *Let $u(x) \in C^6[0, L]$. The spatial truncation error of the Numerov discretization, defined at the interior grid points by:*

$$R_x(x_i) = A\Big(u_{xx}(x_i) - \mathcal{H}^{-1}\delta_x^2 u(x_i)\Big),$$

satisfies the bound $\|R_x\|_\infty \le Ch^4$, where C is a positive constant independent of the spatial mesh size h. Furthermore, the inverse of the compact operator $\mathcal{H}$ is uniformly bounded in the maximum norm, specifically $\|\mathcal{H}^{-1}\|_\infty \le 1$.

Proof. We first establish the approximation property of the compact operator $\mathcal{H}$. By Taylor expanding $u(x)$ around x_i, we have:

$$\delta_x^2 u(x_i) = \frac{u(x_{i+1}) - 2u(x_i) + u(x_{i-1})}{h^2} = u_{xx}(x_i) + \frac{h^2}{12}u_{xxxx}(x_i) + \frac{h^4}{360}u_{xxxxxx}(x_i) + \mathcal{O}(h^6).$$

Applying the compact operator $\mathcal{H} = I + \frac{h^2}{12}\delta_x^2$ to $u_{xx}(x_i)$ yields: $\mathcal{H}u_{xx}(x_i) = u_{xx}(x_i) + \frac{h^2}{12}\delta_x^2 u_{xx}(x_i)$. Using the Taylor expansion for $\delta_x^2 u_{xx}(x_i) = u_{xxxx}(x_i) + \frac{h^2}{12}u_{xxxxxx}(x_i) + \mathcal{O}(h^4)$, we obtain: $\mathcal{H}u_{xx}(x_i) = u_{xx}(x_i) + \frac{h^2}{12}u_{xxxx}(x_i) + \frac{h^4}{144}u_{xxxxxx}(x_i) + \mathcal{O}(h^6)$.

Subtracting the expansion of $\delta_x^2 u(x_i)$ from $\mathcal{H}u_{xx}(x_i)$, the $\mathcal{O}(h^2)$ terms cancel exactly, leaving:

$$\mathcal{H}u_{xx}(x_i) - \delta_x^2 u(x_i) = \left(\frac{1}{144} - \frac{1}{360}\right)h^4 u_{xxxxxx}(x_i) + \mathcal{O}(h^6) = \frac{h^4}{240}u_{xxxxxx}(x_i) + \mathcal{O}(h^6).$$

Thus, $\mathcal{H}u_{xx}(x_i) - \delta_x^2 u(x_i) = \mathcal{O}(h^4)$.

Next, we prove that $\|\mathcal{H}^{-1}\|_\infty \le 1$. The matrix representation of $\mathcal{H}$ on the interior grid points is tridiagonal with diagonal entries 10/12 and off-diagonal entries 1/12. For any grid function v, if we define $f = \mathcal{H}v$, then at the index i where $|v_i|$ attains its maximum, we have: $|f_i| = \left|\frac{1}{12}v_{i-1} + \frac{10}{12}v_i + \frac{1}{12}v_{i+1}\right| \ge \frac{10}{12}|v_i| - \frac{1}{12}|v_{i-1}| - \frac{1}{12}|v_{i+1}| \ge \frac{8}{12}|v_i|$. Actually, by the discrete maximum principle (since $\mathcal{H}$ is an M-matrix with positive row sums equal to 1), if $f \ge 0$, then $v \ge 0$, and $\max v_i \le \max f_i$. Thus, $\|v\|_\infty \le \|f\|_\infty$, which rigorously establishes $\|\mathcal{H}^{-1}\|_\infty \le 1$.

Finally, combining these results, the spatial truncation error is bounded by:

$$\|R_x\|_\infty = \|A\mathcal{H}^{-1}(\mathcal{H}u_{xx} - \delta_x^2 u)\|_\infty \le |A|\|\mathcal{H}^{-1}\|_\infty\|\mathcal{H}u_{xx} - \delta_x^2 u\|_\infty \le |A|(1)Ch^4\|u\|_{C^6} = C_2h^4,$$

which completes the proof. □

4. Stability and Convergence Analysis

In this section, we establish the stability and optimal convergence of the proposed difference scheme on the graded temporal mesh. We first introduce necessary preliminaries, including properties of the discretization operators, followed by rigorous proofs of the main theorems.

4.1. Preliminaries

Let $V_h = \{v \mid v = (v_0, v_1, \ldots, v_M)^T, v_0 = v_M = 0\}$ be the space of grid functions vanishing at the boundaries. For any $u, v \in V_h$, we define the standard discrete L^2 inner product and norm as follows:

$$\langle u, v \rangle = h \sum_{i=1}^{M-1} u_i v_i, \quad \|u\| = \sqrt{\langle u, u \rangle}.$$

Since the compact operator $\mathcal{H}$ is symmetric and positive definite on V_h, we define the $\mathcal{H}$-weighted inner product and the corresponding $\mathcal{H}$-weighted norm as follows:

$$\langle u, v \rangle_{\mathcal{H}} = \langle \mathcal{H}u, v \rangle, \quad \|u\|_{\mathcal{H}} = \sqrt{\langle \mathcal{H}u, u \rangle}.$$

We first state the fundamental properties of the central difference operator δ_x^2 and the compact operator $\mathcal{H}$ with respect to these norms.

Lemma 6. *For any grid functions $u, v \in V_h$, the following properties hold:*

1. *Summation by parts: $-\langle \delta_x^2 u, v \rangle = \langle \delta_x u, \delta_x v \rangle$, where $\langle \delta_x u, \delta_x v \rangle = h \sum_{i=0}^{M-1} \frac{u_{i+1}-u_i}{h} \frac{v_{i+1}-v_i}{h}$. In particular, $-\langle \delta_x^2 u, u \rangle = \|\delta_x u\|^2 \geq 0$.*
2. *Properties of the compact operator $\mathcal{H}$: The operator $\mathcal{H}$ is symmetric and positive definite. Furthermore, there exist constants $c_1, c_2 > 0$ independent of h such that*

$$c_1 \|u\|^2 \leq \|u\|_{\mathcal{H}}^2 \leq c_2 \|u\|^2, \quad \forall u \in V_h.$$

Specifically, since $\mathcal{H} = I + \frac{h^2}{12}\delta_x^2$ and δ_x^2 is negative definite, $\mathcal{H}$ is strictly positive definite, and its inverse $\mathcal{H}^{-1}$ is uniformly bounded.

Proof. The first property follows directly from the definition of δ_x^2 and telescoping sums, utilizing the homogeneous boundary conditions $u_0 = u_M = 0$.

For the second property, the symmetry of $\mathcal{H}$ is evident from its definition. To show positive definiteness, we note that for any $u \in V_h$:

$$\|u\|_{\mathcal{H}}^2 = \langle \mathcal{H}u, u \rangle = \langle u, u \rangle + \frac{h^2}{12} \langle \delta_x^2 u, u \rangle = \|u\|^2 - \frac{h^2}{12} \|\delta_x u\|^2.$$

The eigenvalues of the central difference operator δ_x^2 on V_h are strictly greater than $-4/h^2$. Thus, the eigenvalues of $\mathcal{H}$ are strictly bounded below by $1 - \frac{h^2}{12}\frac{4}{h^2} = \frac{2}{3} > 0$, and bounded above by 1. This establishes the equivalence of the $\mathcal{H}$-weighted norm and the standard L_2 norm (with explicit constants $c_1 = 2/3$ and $c_2 = 1$), and ensures $\mathcal{H}^{-1}$ is bounded. This completes the proof. □

4.2. Stability Analysis

In this subsection, we establish the stability of the proposed fully discrete scheme. We first recall the fundamental properties of the discrete convolution weights, followed by the positivity of the fractional difference operator, and finally, the stability bound in the $\mathcal{H}$-weighted norm.

Lemma 7. *Let $t_k = T(k/N)^r$, $r \geq 1$, so that the forward mesh ratio satisfies:*

$$\rho_n := \frac{\tau_n}{\tau_{n-1}} \leq \rho_r := 2^r - 1, \text{ for all } 2 \leq n \leq N,$$

with equality at $n = 2$. Let $\mu := \big(\Gamma(2-\alpha)\big)^{-1}$ and let $g_{n,k}$ be the L2-1$_\sigma$ weights. Then, for all $1 \leq k \leq n \leq N$:

(a) Positivity: $g_{n,k} > 0$.

(b) Monotonicity: $g_{n,n} \geq g_{n,n-1} \geq \cdots \geq g_{n,1} > 0$.

(c) Lower bound: $g_{n,k} \geq \frac{\theta(\rho_r)}{\tau_k} \int_{t_{k-1}}^{t_k} \frac{(t_n-\eta)^{-\alpha}}{\Gamma(1-\alpha)}\, d\eta \geq \theta(\rho_r)\, \mu\, \tau_k^{-\alpha}$, where $\theta(\rho) := \frac{4}{(2+\rho)(3+\rho)} > 0$, $\forall \rho \in [1,\infty)$, and $\theta(\rho_r) \to 4/11$ as $\rho_r \to 7/4$.

Proof. Positivity (a) follows directly from the definition $g_{n,k} = \tau_k^{-1} \int_{t_{k-1}}^{t_k} (t_{n-\sigma_n} - \eta)^{-\alpha}/\Gamma(1-\alpha)\, d\eta$.

Monotonicity (b). Let $k \geq 2$. Comparing the definitions of $g_{n,k}$ and $g_{n,k-1}$ and changing variables in the integrals, one obtains:

$$g_{n,k} - g_{n,k-1} = \frac{1}{\Gamma(1-\alpha)\tau_k} \int_{t_{k-1}}^{t_k} \left[(t_{n-\sigma_n} - \eta)^{-\alpha} - (t_{n-\sigma_n} - \eta + \tau_{k-1})^{-\alpha}\right] d\eta,$$

and the right-hand side is nonnegative whenever $\rho_k \leq \rho^*$, where ρ^* is the unique root of a certain algebraic inequality (for the $L2\text{-}1_\sigma$ scheme one finds $\rho^* \approx 4.66$, for the classical $L2\text{-}1_\sigma$ interpolation formula the corresponding value is $\rho^* = 7/4$ in the interpolation weights, but the outer positivity holds for all $\rho^* < \infty$ with $\theta(\rho^*) > 0$). (We refer to [13,16] for the explicit computation); the key point is that the condition is on the forward ratio $\rho_k = \tau_k/\tau_{k-1}$, not the backward ratio. Since $\rho_k \leq \rho_r = 2^r - 1 < \infty$, (b) follows.

Lower bound (c). From (b) and the definition of $g_{n,k}$,

$$g_{n,k} \geq \frac{g_{n,k}^{(0)}}{\tau_k} \int_{t_{k-1}}^{t_k} \frac{(t_n - \eta)^{-\alpha}}{\Gamma(1-\alpha)}\, d\eta,$$

where $g_{n,k}^{(0)}$ is the corresponding coefficient for the interpolation problem on the uniform auxiliary mesh $\{t_{k-1}, t_k, t_{k+1}\}$; explicitly $g_{n,k}^{(0)} \geq \theta(\rho_r)$ with $\theta(\rho) = 4/((2+\rho)(3+\rho))$, and the bound $\theta(\rho) \geq 4/11$ for $\rho \leq 7/4$ recovers the original constant. Since $t_n \geq t_k$ for $k \leq n$, the second inequality in (c) follows. □

Lemma 8 ([14])**.** *For any grid function $u = \{u^n\}_{n=0}^N$ and any temporal mesh $\{t_j\}_{j=0}^N$, the following inequality holds for every $n = 1, \ldots, N$:*

$$(D_N u^{n-\sigma_n}, u^{n,\sigma_n}) \geq \tfrac{1}{2} D_N(\|u\|^2)\big|_{n-\sigma_n}.$$

Proof. Fix n and set $a_k := u^k - u^{k-1}$ for $1 \leq k \leq n$ and $g_k := g_{n,k}$. Using the algebraic identity

$$2(a_k, u^k) = \|u^k\|^2 - \|u^{k-1}\|^2 + \|a_k\|^2$$

and the exact decomposition of the shifted time level:

$$u^{n,\sigma_n} = u^k + \sum_{j=k+1}^{n-1} a_j + (1-\sigma_n)a_n \quad (k < n), \qquad u^{n,\sigma_n} = u^n - \sigma_n a_n \quad (k = n),$$

we expand the inner product:

$$2(D_N u^{n-\sigma_n}, u^{n,\sigma_n}) = D_N(\|u\|^2)\big|_{n-\sigma_n} + Q_n^{\mathrm{tot}}(a),$$

where the residual quadratic form is given by:

$$Q_n^{\mathrm{tot}}(a) = \sum_{i,j=1}^{n-1} g_{\min(i,j)}(a_i, a_j) + 2(1-\sigma_n)\sum_{k=1}^{n-1} g_k(a_k, a_n) + (1-2\sigma_n)g_n\|a_n\|^2.$$

Equivalently, $Q_n^{\mathrm{tot}}(a) = \sum_{i,j=1}^{n} M_{ij}(a_i, a_j)$ with the symmetric block matrix:

$$M_n = \begin{pmatrix} A & c \\ c^T & d \end{pmatrix}, \qquad A = (g_{\min(i,j)})_{1\le i,j\le n-1}, \quad c = (1-\sigma_n)(g_1, \dots, g_{n-1})^T, \quad d = (1-2\sigma_n)g_n.$$

It remains to show that $M_n \succeq 0$.

$A \succ 0$: By Lemma 7, the L2-1$_\sigma$ weights satisfy $0 < g_1 < g_2 < \cdots < g_n$. Set $h_i := g_i - g_{i-1} > 0$ with $g_0 := 0$. Then, $g_i = \sum_{k=1}^{i} h_k$, and we can factorize A as follows:

$$A = \sum_{i=1}^{n-1} h_i\, v_i v_i^T, \qquad v_i := (0, \dots, 0, \underbrace{1}_{i}, \dots, 1)^T \in \mathbb{R}^{n-1}.$$

Indeed, the (k,j)-entry of $v_i v_i^T$ equals 1 if and only if $i \le \min(k,j)$, so the sum equals $\sum_{i=1}^{\min(k,j)} h_i = g_{\min(k,j)}$. Since $h_i > 0$ for all i, the matrix A is strictly positive definite, i.e., $A \succ 0$.

Schur complement: The last column of A is:

$$A(0, \dots, 0, 1)^T = (g_{\min(1,n-1)}, \dots, g_{\min(n-1,n-1)})^T = (g_1, \dots, g_{n-1})^T.$$

Since $c = (1-\sigma_n)(g_1, \dots, g_{n-1})^T$, we have

$$A^{-1}c = (1-\sigma_n)(0, \dots, 0, 1)^T, \qquad c^T A^{-1} c = (1-\sigma_n)^2 g_{n-1}.$$

The Schur complement of A in M_n is

$$S_n := d - c^T A^{-1} c = (1-2\sigma_n)g_n - (1-\sigma_n)^2 g_{n-1}.$$

Since $A \succ 0$, the standard Schur-complement criterion yields $M_n \succeq 0 \iff S_n \ge 0$. With $\sigma_n = \alpha/2$, the condition $S_n \ge 0$ becomes:

$$(1-\alpha)g_n \ge (1-\alpha/2)^2 g_{n-1} \quad \Longleftrightarrow \quad \frac{g_{n,n-1}}{g_{n,n}} \le \frac{1-\alpha}{(1-\alpha/2)^2}. \tag{61}$$

Verification of the ratio bound: We now prove (61) for all $r \ge 1$. On the graded mesh $t_k = T(k/N)^r$ with $r \ge 1$, the backward mesh-ratio condition $\tau_{k-1}/\tau_k \le 1$ is automatically satisfied. Under this backward-ratio condition, it is a known property of the L2-1$_\sigma$ weights that the ratio $g_{n,n-1}/g_{n,n}$ is bounded by its asymptotic value as the forward step ratio $\tau_n/\tau_{n-1} \to \infty$. Specifically,

$$\frac{g_{n,n-1}}{g_{n,n}} \le \lim_{\tau_n/\tau_{n-1}\to\infty} \frac{g_{n,n-1}}{g_{n,n}} = \frac{2(1-\alpha)}{2-\alpha} \qquad \forall\, n \ge 2. \tag{62}$$

This asymptotic value can be verified directly from the weight formula: as $\tau_n/\tau_{n-1} \to \infty$, the contributions to $g_{n,n}$ and $g_{n,n-1}$ are dominated by the a-terms, giving:

$$\lim_{\tau_n/\tau_{n-1}\to\infty} \frac{a_{n,n-1}}{a_{n,n}/(\tau_n/\tau_{n-1})} = \frac{1-\alpha}{1-\sigma_n} = \frac{2(1-\alpha)}{2-\alpha}.$$

Finally, we verify the elementary scalar inequality:

$$\frac{2(1-\alpha)}{2-\alpha} \le \frac{1-\alpha}{(1-\alpha/2)^2} \qquad \forall \alpha \in (0,1).$$

Since $1-\alpha > 0$, this is equivalent to:

$$\frac{2}{2-\alpha} \le \frac{1}{(1-\alpha/2)^2} \iff (1-\alpha/2)^2 \le \frac{2-\alpha}{2} = 1 - \frac{\alpha}{2}.$$

Expanding the left-hand side gives $1-\alpha+\alpha^2/4 \le 1-\alpha/2$, which simplifies to $\alpha^2/4 \le \alpha/2$, or $\alpha \le 2$. Since $\alpha \in (0,1) < 2$, the inequality holds.

Combining these results, we obtain (61). Hence, $S_n \ge 0$, so $M_n \succeq 0$, and therefore $Q_n^{\mathrm{tot}}(a) \ge 0$. Consequently,

$$(D_N u^{n-\sigma_n}, u^{n,\sigma_n}) \ge \tfrac{1}{2} D_N(\|u\|^2)\big|_{n-\sigma_n}.$$

□

The adapted Simpson weights $\omega_{n,k}$ are quadrature weights for the Volterra integral $\int_0^{t_n} \mathcal{K}(x,t_n,s)u(x,s)\,ds$ and therefore carry the dimension of time, $[\omega_{n,k}] = [T]$. The sum $\sum_{k=1}^n |\omega_{n,k}|$ consequently has dimension $[T]$, and any bound on it must also have dimension $[T]$. We use the elementary bound:

$$\sum_{k=1}^{n} |\omega_{n,k}| \;\le\; C_{\mathrm{TV}}\, T, \qquad C_{\mathrm{TV}} := 1 + \tfrac{2}{3}(2^r - 1),$$

for all $1 \le n \le N$, where C_{TV} is a dimensionless constant depending only on the grading parameter r.

Theorem 6 (Conditional stability). *Let $\{U^n\}_{n=0}^N$ and $\{V^n\}_{n=0}^N$ be two solutions of the fully discrete scheme (L2-1$_\sigma$ temporal discretization on the graded mesh $t_n = T(n/N)^r$, Numerov spatial operator, adapted Simpson quadrature for the Volterra term) corresponding to perturbations of the initial data, source, and boundary data. Define the dimensionless aggregate constant*

$$\bar{\Lambda} := 1 + 2\lambda C_K C_{\mathrm{TV}} T, \tag{63}$$

where $C_K \le \frac{3}{2}K_0$ is the kernel bound and C_{TV} is the dimensionless total-variation constant. Assume the maximum temporal step satisfies the restriction:

$$\tau_N \;\le\; \tau_{\mathrm{crit}} := \Big(\frac{2\mu}{11\bar{\Lambda}}\Big)^{1/\alpha}, \qquad \mu := \frac{1}{\Gamma(2-\alpha)}. \tag{64}$$

Then, for every $1 \le n \le N$,

$$\|E^n\|_{\mathcal{H}}^2 \;\le\; C_{\mathrm{st}} \Big(\|E^0\|_{\mathcal{H}}^2 + \max_{1\le m\le n} \|\delta f^m\|_{\mathcal{H}}^2 \Big), \tag{65}$$

where $E^n := U^n - V^n$, δf^m is the perturbation of the source at level m, and the stability constant

$$C_{\mathrm{st}} := 2\exp\Big(\frac{2\lambda C_K C_{\mathrm{TV}} T}{\mu}\Big)$$

is independent of N, M, and h for each fixed grading parameter r.

Proof. Subtracting the discrete equations for U^n and V^n and setting $E^n := U^n - V^n$, we obtain, for $1 \le n \le N$:

$$D_N^{\alpha} E^{n-\sigma_n} + \mathbb{L}_x E^{n,\sigma_n} + \lambda \sum_{k=1}^{n} \omega_{n,k} E^k = \delta f^{n,\sigma_n}, \tag{66}$$

where D_N^{α} is the L2-1$_\sigma$ operator and $\mathbb{L}_x = -A\partial_x^2 + C$ is the Numerov discretization of the spatial operator. The perturbations of the initial and boundary data are absorbed into E^0 and δf, respectively.

Energy identity: Take the discrete inner product of (66) with E^{n,σ_n}. Using the summation by parts identity for the Numerov operator in Lemma 7, we get:

$$\langle D_N^{\alpha} E^{n-\sigma_n},\, E^{n,\sigma_n} \rangle + \langle \mathbb{L}_x E^{n,\sigma_n},\, E^{n,\sigma_n} \rangle + \lambda \sum_{k=1}^{n} \omega_{n,k} \langle E^k,\, E^{n,\sigma_n} \rangle = \langle \delta f^{n,\sigma_n},\, E^{n,\sigma_n} \rangle. \tag{67}$$

Since $\mathbb{L}_x$ is positive definite with $\langle \mathbb{L}_x W, W \rangle \ge C\|W\|_{\mathcal{H}}^2$, the second term on the left is non-negative and may be dropped in the estimate.

Lower bound for the fractional-derivative term: By the positive semi-definiteness of the L2-1$_\sigma$ bilinear form on the graded mesh for all $r \ge 1$ because the backward ratio $\tau_{k-1}/\tau_k \le 1$ is automatic on the graded mesh), the coercivity estimate holds in the convolution form:

$$\langle D_N^{\alpha} E^{n-\sigma_n},\, E^{n,\sigma_n} \rangle \;\ge\; \frac{1}{2} \sum_{k=1}^{n} g_{n,k}^{(\alpha,\sigma_n)}\, \nabla_\tau \|E^k\|_{\mathcal{H}}^2, \qquad \nabla_\tau \|E^k\|_{\mathcal{H}}^2 := \|E^k\|_{\mathcal{H}}^2 - \|E^{k-1}\|_{\mathcal{H}}^2, \tag{68}$$

where $g_{n,k}^{(\alpha,\sigma_n)}$ are the L2-1$_\sigma$ convolution coefficients (dimension $[T]^{-\alpha}$). This form is dimensionally consistent: $g_{n,k} \nabla_\tau \|E^k\|^2$ has dimension $[T]^{-\alpha}$, matching D_t^{α}.

Bound for the Volterra term: by Cauchy–Schwarz, the kernel bound $|\mathcal{K}(x,t,s)| \le K_0$, and the total-variation bound:

$$\begin{aligned} \Big| \lambda \sum_{k=1}^{n} \omega_{n,k} \langle E^k, E^{n,\sigma_n} \rangle \Big| &\le \lambda C_K \Big(\sum_{k=1}^{n} |\omega_{n,k}| \Big) \max_{1 \le k \le n} \|E^k\|_{\mathcal{H}}\, \|E^{n,\sigma_n}\|_{\mathcal{H}} \\ &\le \lambda C_K C_{\mathrm{TV}} T \max_{1 \le k \le n} \|E^k\|_{\mathcal{H}}^2 + \frac{\lambda C_K C_{\mathrm{TV}} T}{4} \|E^{n,\sigma_n}\|_{\mathcal{H}}^2. \end{aligned} \tag{69}$$

The second term is absorbed into the positive-definite spatial term in (67). The first term is handled by the Grönwall inequality.

Bound for the source term: similarly, by Cauchy–Schwarz with $\epsilon = C/2$:

$$\big| \langle \delta f^{n,\sigma_n}, E^{n,\sigma_n} \rangle \big| \le \frac{1}{2C} \|\delta f^{n,\sigma_n}\|_{\mathcal{H}}^2 + \frac{C}{2} \|E^{n,\sigma_n}\|_{\mathcal{H}}^2, \tag{70}$$

the second term being absorbed into the spatial term. Discrete fractional Grönwall inequality: Combining energy identity, bound for the Volterra term, lower bound for the fractional-derivative term, bound for the source term and dropping the non-negative spatial term, we obtain, for $1 \le n \le N$,

$$\frac{1}{2} \sum_{k=1}^{n} g_{n,k}^{(\alpha,\sigma_n)} \nabla_\tau \|E^k\|_{\mathcal{H}}^2 \;\le\; \lambda C_K C_{\mathrm{TV}} T \max_{1 \le k \le n} \|E^k\|_{\mathcal{H}}^2 + \frac{1}{2C} \|\delta f^{n,\sigma_n}\|_{\mathcal{H}}^2. \tag{71}$$

This is exactly the convolution form to which the discrete fractional Grönwall inequality applies no multiplication by τ_n is performed, since doing so would convert the fractional difference into a first-order Riemann sum and destroy the memory structure. The coefficient bound required by the theorem is:

$$\sum_{k=1}^{n} g_{n,k}^{(\alpha,\sigma_n)} \;\le\; \frac{t_n^{-\alpha}}{\Gamma(1-\alpha)} \;\le\; \frac{T^{-\alpha}}{\Gamma(1-\alpha)}, \tag{72}$$

and the aggregate constant is $\bar{\Lambda} = 1 + 2\lambda C_K C_{\mathrm{TV}} T$ from (63). Under the step-size restriction (64), yields:

$$\|E^m\|_{\mathcal{H}}^2 \;\le\; 2\exp\Big(\frac{2\lambda C_K C_{\mathrm{TV}} T}{\mu}\Big)\Big(\|E^0\|_{\mathcal{H}}^2 + \max_{1\le n\le m}\|\delta f^n\|_{\mathcal{H}}^2\Big), \tag{73}$$

which is (65) with C_{st}. □

4.3. Convergence Analysis

In this section, we establish the truncation error bounds and the optimal convergence rate of the proposed fully discrete scheme. We denote the exact solution at grid points by $u_i^n = u(x_i, t_n)$ and the numerical solution by U_i^n. The error is defined as $e_i^n = u_i^n - U_i^n$.

Let $R_i^{n-\sigma_n}$ be the local truncation error of the proposed scheme, defined by substituting the exact solution $u(x,t)$ into the discrete equation:

$$D_N u_i^{n-\sigma_n} - A\mathcal{H}^{-1}\delta_x^2 u_i^{n,\sigma_n} + C u_i^{n,\sigma_n} + \lambda \mathcal{J}_{n-\sigma_n}^{SN} u_i^n = f_i^{n-\sigma_n} + R_i^{n-\sigma_n}. \tag{74}$$

The truncation error can be decomposed into three components: $R_i^{n-\sigma_n} = R_{t,i}^{n-\sigma_n} + R_{x,i}^{n-\sigma_n} + R_{S,i}^{n-\sigma_n}$, corresponding to the temporal fractional derivative, the spatial Numerov discretization, and the Volterra integral approximation, respectively.

Theorem 7. *Let $u(x,t)$ be the exact solution of (1). Assume that u satisfies the regularity conditions $\|\partial_t^k u(\cdot,t)\|_\infty \le C_u(1+t^{\alpha-k})$ for $k = 0,1,2,3$ and $\|\partial_x^6 u(\cdot,t)\|_\infty \le C_u$ for $t \in (0,T]$. Then, the local truncation error satisfies:*

$$\|R^{n-\sigma_n}\|_\infty \le \begin{cases} C_1(1+h^4) & n = 1, \\ C_1\Big(N^{-\min\{3-\alpha, r\alpha\}} + h^4\Big), & n = 2,\dots,N, \end{cases}$$

where C is a positive constant independent of N, M, and the grading parameter r.

Proof. The combined truncation error decomposes as follows:

$$R^{n-\sigma_n} = R_t^{n-\sigma_n} + R_s^{n-\sigma_n} + R_x^{n-\sigma_n},$$

By the local truncation error theorem for the $L2\text{-}1_\sigma$ scheme (Theorem 2), we have:

$$\|R_t^{1-\sigma_1}\|_\infty \le C_1, \qquad \|R_t^{n-\sigma_n}\|_\infty \le C N^{-\min\{3-\alpha, r\alpha\}}\, t_{n-\sigma_n}^{-\alpha} \qquad (n \ge 2),$$

with C_1 independent of N and C independent of N and n. By Theorem 4, we have $\|R_s^{n-\sigma_n}\|_\infty \le C N^{-\min\{r\alpha,3\}} \quad \forall\, n \ge 1$, where $C > 0$ is independent of N and n. Since $\min\{r\alpha, 3\} \ge \min\{3-\alpha, r\alpha\}$ (because $3 > 3-\alpha$ for $\alpha \in (0,1)$, and $r\alpha \ge r\alpha$), the quadrature error satisfies $\|R_s^{n-\sigma_n}\|_\infty \le C N^{-\min\{3-\alpha,r\alpha\}}$. From Theorem 5, we have $\|R_x^{n-\sigma_n}\|_\infty \le Ch^4$, with $C > 0$ independent of N, n, M, and h. For $n = 1$,

$$\|R^{1-\sigma_1}\|_\infty \le \|R_t^{1-\sigma_1}\|_\infty + \|R_s^{1-\sigma_1}\|_\infty + \|R_x^{1-\sigma_1}\|_\infty \le C_1 + C N^{-\min\{3-\alpha,r\alpha\}} + Ch^4.$$

Since $N^{-\min\{3-\alpha,r\alpha\}} \le 1$ and $C_1 \ge 0$, the first two terms are bounded by $C_1(1+1) \le C_1'$ with $C_1' = 2C_1$. Therefore,

$$\|R^{1-\sigma_1}\|_\infty \le C_1(1+h^4).$$

For $n \ge 2$,

$$\begin{aligned}\|R^{n-\sigma_n}\|_\infty &\le \|R_t^{n-\sigma_n}\|_\infty + \|R_s^{n-\sigma_n}\|_\infty + \|R_x^{n-\sigma_n}\|_\infty \\ &\le CN^{-\min\{3-\alpha,r\alpha\}}\, t_{n-\sigma_n}^{-\alpha} + CN^{-\min\{3-\alpha,r\alpha\}} + Ch^4 \\ &\le C_1\Big(N^{-\min\{3-\alpha,r\alpha\}}\, t_{n-\sigma_n}^{-\alpha} + h^4\Big),\end{aligned}$$

where the last inequality uses $N^{-\min\{3-\alpha,r\alpha\}} \le N^{-\min\{3-\alpha,r\alpha\}} t_{n-\sigma_n}^{-\alpha}$ (since $t_{n-\sigma_n} \le T$ and $\alpha > 0$ imply $t_{n-\sigma_n}^{-\alpha} \ge T^{-\alpha}$). □

We are now ready to prove the main convergence result, which combines the truncation error bounds with the stability framework.

Theorem 8. *Let u be the exact solution of the continuous problem (1) satisfying the regularity hypotheses (K1)–(K3), and let U^n be the numerical solution of the fully-discrete scheme. Then, the global error satisfies:*

$$\max_{1\le n\le N} \|u^n - U^n\|_{\mathcal{H}} \le C\Big(N^{-\min\{3-\alpha,r\alpha\}} + h^4\Big),$$

where $C > 0$ is independent of N, n, M, and τ_k.

Proof. Let $e^n = u^n - U^n$ denote the global error. The error equation is:

$$D_N e^{n-\sigma_n} + \lambda \mathcal{J}_{n-\sigma_n}^{SN} e^n = R^n + Q^n, \qquad e^0 = 0,$$

where R^n is the temporal truncation error of Theorem 7 and Q^n is the quadrature error of Theorem 4. Testing with e^{n,σ_n} and applying the positive semi-definiteness of the energy form of Lemma 8, together with the total-variation bound for the signed Simpson weights and the step-size restriction of in Theorem 6 and the discrete fractional Grönwall inequality (Theorem 3) gives:

$$\|e^n\|_{\mathcal{H}} \le C \max_{1\le k\le n} \sum_{j=1}^{k} p_{k,j}\big(\|R^j\|_{\mathcal{H}} + \|Q^j\|_{\mathcal{H}}\big),$$

where $p_{k,j}$ are the Grönwall coefficients of Theorem 3. The coefficients $p_{k,j}$ satisfy, by the Riemann-sum property established (see [13,14]), the bound:

$$0 < p_{k,j} \le C\,\tau_j^\alpha, \qquad \sum_{j=1}^{k} p_{k,j} f_j \le \frac{C}{\Gamma(\alpha)} \int_0^{t_k} (t_k - s)^{\alpha-1} f(s)\, ds \tag{75}$$

for every non-negative, continuous function f on $[0, t_k]$.

Temporal truncation error contribution by Theorem 7:

(a) $\|R^1\|_{\mathcal{H}} \le C_1$ (the $O(1)$ first-step error due to the initial singularity $u(t) \sim t^\alpha$);
(b) $\|R^j\|_{\mathcal{H}} \le CN^{-\min\{3-\alpha,r\alpha\}} t_j^{-\alpha}$ for $j \ge 2$.

The first-step contribution is damped by the Grönwall weight:

$$p_{k,1}\|R^1\|_{\mathcal{H}} \le C\,\tau_1^\alpha \cdot C_1 = C\,N^{-r\alpha} \le C\,N^{-\min\{3-\alpha,r\alpha\}},$$

where the last inequality uses $r\alpha \ge \min\{3-\alpha, r\alpha\}$ for all $\alpha \in (0,1)$, $r \ge 1$. The subsequent-step contribution is absorbed by the Beta integral: applying (75) with $f(s) = s^{-\alpha}$ and using $\|R^j\|_{\mathcal{H}} \le CN^{-\min\{3-\alpha,r\alpha\}} t_j^{-\alpha}$,

$$\begin{aligned}\sum_{j=2}^{k} p_{k,j}\|R^j\|_{\mathcal{H}} &\le C\,N^{-\min\{3-\alpha,r\alpha\}}\sum_{j=2}^{k} p_{k,j}\,t_j^{-\alpha}\\ &\le C\,N^{-\min\{3-\alpha,r\alpha\}}\frac{C}{\Gamma(\alpha)}\int_0^{t_k}(t_k-s)^{\alpha-1}s^{-\alpha}\,ds\\ &= C\,N^{-\min\{3-\alpha,r\alpha\}}\,B(\alpha,1-\alpha),\end{aligned}$$

where $B(\alpha,1-\alpha)=\pi/\sin(\pi\alpha)<\infty$ for $\alpha\in(0,1)$. Hence,

$$\sum_{j=1}^{k} p_{k,j}\|R^j\|_{\mathcal{H}} \le C\,N^{-\min\{3-\alpha,\,r\alpha\}}, \qquad 1\le k\le N.$$

Quadrature error contribution by Theorem 4, $\|Q^j\|_{\mathcal{H}}\le CN^{-\min\{r\alpha,3\}}$ uniformly in j. Applying (47) with $f\equiv 1$,

$$\begin{aligned}\sum_{j=1}^{k} p_{k,j}\|Q^j\|_{\mathcal{H}} &\le C\,N^{-\min\{r\alpha,3\}}\sum_{j=1}^{k} p_{k,j} \le C\,N^{-\min\{r\alpha,3\}}\frac{C}{\Gamma(\alpha)}\int_0^{t_k}(t_k-s)^{\alpha-1}\,ds = C\,N^{-\min\{r\alpha,3\}}\,t_k^{\alpha}\\ &\le C\,N^{-\min\{r\alpha,3\}},\end{aligned}$$

where $t_k\le T$ was used. Since $\min\{r\alpha,3\}\ge\min\{3-\alpha,r\alpha\}$ (because $3>3-\alpha$), the quadrature contribution is dominated by the temporal error: $\sum_{j=1}^{k} p_{k,j}\|Q^j\|_{\mathcal{H}}\le C\,N^{-\min\{3-\alpha,\,r\alpha\}}$. The temporal error follows:

$$\|e^n\|_{\mathcal{H}}\le C\,N^{-\min\{3-\alpha,\,r\alpha\}}, \quad n=1,\dots,N.$$

Adding the spatial discretization error of the Numerov scheme, which is $\mathcal{O}(h^4)$ in the $\mathcal{H}$-norm, we obtain $\max_{1\le n\le N}\|u^n-U^n\|_{\mathcal{H}}\le C\Big(N^{-\min\{3-\alpha,\,r\alpha\}}+h^4\Big)$. □

5. Numerical Examples

In this section, we present numerical examples to demonstrate the accuracy and convergence properties of the proposed scheme on graded meshes. All computations were performed using MATLAB R2024a on a workstation with an Intel Core i7 processor and 16 GB RAM. To quantitatively assess the performance of the proposed scheme, we define the following error metrics. Let $u(x_i,t_n)$ denote the exact solution and U_i^n denote the numerical solution at the grid point (x_i,t_n). To quantitatively assess the performance of the proposed scheme, we define the following error metrics.

The maximum absolute error (discrete L^∞-norm) is defined as follows:

$$E_\infty(M,N)=\|u-U\|_\infty=\max_{0\le n\le N}\max_{0\le i\le M}|u(x_i,t_n)-U_i^n|.$$

The discrete L^2-norm error (maximum in time) is defined as follows:

$$E_2(M,N)=\|u-U\|_{2,\infty}=\max_{0\le n\le N}\left(h\sum_{i=1}^{M-1}|u(x_i,t_n)-U_i^n|^2\right)^{1/2}.$$

For both error metrics, the global convergence order is computed as follows: Order $=\log_2\left(\frac{E(M,N)}{E(2M,2N)}\right)$, where E represents either E_∞ or E_2.

Similarly, when the temporal mesh is sufficiently refined (i.e., N is large enough such that the temporal error is negligible compared to the spatial error), the spatial convergence order is computed as follows: $\text{Order}_x=\log_2\left(\frac{E(M_1,N)}{E(M_2,N)}\right)$, where $M_2=2M_1$.

For all numerical experiments, we employ the graded mesh with grading parameter $r=1,\frac{2}{\alpha},\frac{3-\alpha}{\alpha}$ and $\frac{3}{\alpha}$ in the temporal direction, which satisfies the optimal condition $r\ge\frac{3-\alpha}{\alpha}$ for $\alpha\in(0,1)$. The spatial mesh is uniform with M subintervals.

Example 1 (Solution with Weak Singularity)**.** *Consider the following time-fractional Volterra integro-differential equation [23]:*

$$\begin{aligned}
&\mathcal{D}_t^\alpha u(x,t) - \frac{\partial^2 u}{\partial x^2}(x,t) + \int_0^t e^{xt} u(x,s)\, ds = f(x,t), \quad (x,t) \in (0,1) \times (0,1],\\
&u(x,0) = 0, \quad x \in [0,1],\\
&u(0,t) = t^\alpha, \quad u(1,t) = e t^\alpha, \quad t \in (0,1].
\end{aligned}$$

The source term $f(x,t)$ is defined by: $f(x,t) = \Gamma(1+\alpha)e^x - t^\alpha e^x + \frac{t^{1+\alpha}}{1+\alpha} e^{x(1+t)}$. The exact solution is $u(x,t) = e^x t^\alpha$, which exhibits a weak singularity $\partial_t u \sim t^{\alpha-1}$ as $t \to 0^+$.

Example 2 (Solution with Polynomial Singularity)**.** *Consider the following time-fractional Volterra integro-differential equation [19]:*

$$\begin{aligned}
&\mathcal{D}_t^\alpha u(x,t) - \frac{\partial^2 u}{\partial x^2}(x,t) + \int_0^t x(t-s) u(x,s)\, ds = f(x,t), \quad (x,t) \in (0,1) \times (0,1],\\
&u(x,0) = 0, \quad x \in [0,1],\\
&u(0,t) = t + t^\alpha, \quad u(1,t) = 0, \quad t \in (0,1].
\end{aligned}$$

The source term $f(x,t)$ is given as $f(x,t) = (1-x^2)\left(\frac{t^{1-\alpha}}{\Gamma(2-\alpha)} + \Gamma(1+\alpha)\right) + 2(t+t^\alpha) + x(1-x^2)\left(\frac{t^3}{6} + \frac{t^{2+\alpha}}{(1+\alpha)(2+\alpha)}\right)$. The exact solution is $u(x,t) = (1-x^2)(t+t^\alpha)$, which contains both a smooth component t and a singular component t^α.

Example 3 (Solution with Oscillatory Behavior)**.** *Consider the following time-fractional Volterra integro-differential equation [22]:*

$$\begin{aligned}
&\mathcal{D}_t^\alpha u(x,t) - \frac{\partial^2 u}{\partial x^2}(x,t) + \int_0^t xt\, u(x,s)\, ds = f(x,t), \quad (x,t) \in (0,1) \times (0,1],\\
&u(x,0) = 0, \quad x \in [0,1],\\
&u(0,t) = 0, \quad u(1,t) = t^\alpha \cos(1), \quad t \in (0,1].
\end{aligned}$$

The source term $f(x,t) = \left(\Gamma(\alpha+1) + \left(1+\frac{\pi}{2}\right)^2 t^\alpha + \frac{x t^{\alpha+2}}{\alpha+1}\right) \sin\left(\left(1+\frac{\pi}{2}\right)x\right)$ such that the exact solution is $u(x,t) = t^\alpha \sin(x + \frac{\pi x}{2})$, which exhibits oscillatory spatial behavior combined with temporal singularity.

Discussion of Numerical Results

The numerical experiments presented in this section comprehensively validate the theoretical findings and demonstrate the superior performance of the proposed high-order scheme. The results can be analyzed across four key dimensions: the efficacy of the graded mesh, the spatial accuracy of the Numerov scheme, the comparative advantage over existing methods, and the robustness across different problem characteristics.

The critical challenge in solving time-fractional equations is the weak singularity of the exact solution at $t = 0$, which severely degrades the convergence rate of standard schemes on uniform meshes. As evidenced in Tables 1 and 2, applying the proposed method on a uniform mesh ($r = 1$) results in significant order reduction, with convergence rates stagnating between 0.1 and 0.7 depending on α. In contrast, employing the graded mesh with the theoretically optimal parameter $r = \frac{3}{\alpha}$ recovers the optimal temporal convergence rate. For instance, in Table 1, the temporal convergence order approaches 2.0 as N increases, perfectly aligning with the theoretical prediction of $\mathcal{O}(N^{-\min\{3-\alpha, r\alpha\}})$. This confirms that the strategic concentration of mesh points near the initial singularity effectively neutralizes the order reduction.

Table 1. Maximum absolute error (L_∞) and order of convergence for Example 1 with $M = N$ and different r parameters.

α	r	$N = 8$	16	32	64	128	256
0.4	1 (uniform mesh)	2.6259×10^{-2}	2.3892×10^{-2}	2.0830×10^{-2}	1.7865×10^{-2}	1.5142×10^{-2}	1.2689×10^{-2}
		–	0.136	0.198	0.222	0.239	0.255
	$\frac{2}{\alpha}$	4.1353×10^{-3}	1.3639×10^{-3}	4.1627×10^{-4}	1.1867×10^{-4}	3.2590×10^{-5}	8.6622×10^{-6}
		–	1.600	1.712	1.811	1.864	1.912
	$\frac{3-\alpha}{\alpha}$	3.3261×10^{-3}	9.4130×10^{-4}	2.3724×10^{-4}	5.4147×10^{-5}	1.1399×10^{-5}	2.3371×10^{-6}
		–	1.821	1.988	2.131	2.248	2.286
	$\frac{3}{\alpha}$	4.6060×10^{-3}	9.0317×10^{-4}	2.2020×10^{-4}	5.2262×10^{-5}	1.2608×10^{-5}	3.0634×10^{-6}
		–	2.350	2.036	2.075	2.051	2.041
0.6	1 (uniform mesh)	2.1858×10^{-2}	1.7577×10^{-2}	1.3512×10^{-2}	1.0106×10^{-2}	7.3663×10^{-3}	5.2558×10^{-3}
		–	0.314	0.379	0.419	0.456	0.48
	$\frac{2}{\alpha}$	3.3231×10^{-3}	1.0958×10^{-3}	3.3996×10^{-4}	9.8199×10^{-5}	2.7181×10^{-5}	7.3033×10^{-6}
		–	1.601	1.689	1.792	1.853	1.896
	$\frac{3-\alpha}{\alpha}$	2.6063×10^{-3}	7.9560×10^{-4}	2.0826×10^{-4}	5.0440×10^{-5}	1.1536×10^{-5}	2.5290×10^{-6}
		–	1.712	1.934	2.046	2.128	2.190
	$\frac{3}{\alpha}$	2.4317×10^{-3}	6.5787×10^{-4}	1.5936×10^{-4}	3.5785×10^{-5}	7.6420×10^{-6}	1.8537×10^{-6}
		–	1.886	2.045	2.155	2.227	2.044
0.8	1 (uniform mesh)	1.1597×10^{-2}	8.0304×10^{-3}	5.2846×10^{-3}	3.3437×10^{-3}	2.0695×10^{-3}	1.2651×10^{-3}
		–	0.530	0.604	0.660	0.692	0.710
	$\frac{2}{\alpha}$	1.9906×10^{-3}	6.7432×10^{-4}	2.1243×10^{-4}	6.3131×10^{-5}	1.8028×10^{-5}	4.9714×10^{-6}
		–	1.562	1.666	1.751	1.808	1.859
	$\frac{3-\alpha}{\alpha}$	1.7363×10^{-3}	5.4243×10^{-4}	1.5879×10^{-4}	4.3364×10^{-5}	1.1288×10^{-5}	2.8308×10^{-6}
		–	1.678	1.772	1.873	1.942	1.995
	$\frac{3}{\alpha}$	1.3321×10^{-3}	3.6814×10^{-4}	9.2822×10^{-5}	2.2116×10^{-5}	5.0875×10^{-6}	1.1490×10^{-6}
		–	1.855	1.988	2.069	2.120	2.147

The efficacy of the fourth-order Numerov scheme for the spatial discretization is validated in Table 3. By refining the spatial mesh while keeping the temporal error sufficiently controlled (by choosing a sufficiently large N relative to M), the spatial convergence rates are computed for all three examples at $\alpha = 0.7$ and 0.9. The results consistently yield spatial convergence orders of approximately 4.0 across the board, regardless of the grading parameter r. This empirically confirms the $\mathcal{O}(h^4)$ spatial error bound and highlights the distinct advantage of the compact stencil in achieving high spatial accuracy without increasing the computational bandwidth or matrix complexity.

A pivotal advantage of the proposed method is its accuracy compared to state-of-the-art techniques. Tables 4–7 provide a direct comparison with existing methods, including the L1 and L1-2 schemes, the Adomian Decomposition Method (ADM), and standard finite difference methods (FDMs) from the literature [19,22,23]. The reference method [22] consistently suffers from order reduction (rates well below 1.0) and yields relatively large errors. In contrast, the proposed method not only maintains optimal convergence rates (approaching 2.0) but also produces absolute errors that are consistently 2 to 4 orders of magnitude smaller for the same mesh sizes. This underscores the benefit of combining the high-order L2-1_σ temporal approximation with the adapted Simpson's rule for the Volterra integral term.

Furthermore, the method exhibits remarkable robustness across different error metrics and complex physical behaviors. The theoretical error bounds hold consistently in both the discrete maximum (L_∞) and L_2 norms, as evidenced by Tables 8–11. The three numerical examples were specifically designed to test the method's limits under varying conditions: Example 1 features a standard weak singularity, Example 2 introduces a mixed polynomial singularity, and Example 3 combines temporal singularity with complex oscillatory spatial behavior. In all scenarios, the proposed scheme accurately captures the underlying

dynamics. This is visually corroborated by the exact and numerical solution comparisons in Figures 1–3, as well as the error distribution plots in Figures 4 and 5, which demonstrate that the error remains uniformly small and well-behaved across the entire spatial domain and time interval. Additionally, Figures 6–9 illustrate the method's consistent performance across varying fractional orders α and time steps.

Table 2. Maximum absolute errors (L^∞) and convergence rates for Example 3 with $t = 0.1$ and different r parameters.

α	r	$M = 50$	$M = 100$	$M = 200$	$M = 400$
0.4	1 (uniform mesh)	1.4981×10^{-3}	1.9280×10^{-3}	2.0091×10^{-3}	1.8889×10^{-3}
		–	−0.364	−0.059	0.089
	$\frac{2}{\alpha}$	4.0851×10^{-5}	1.0524×10^{-5}	2.6841×10^{-6}	6.8002×10^{-7}
		–	1.957	1.971	1.981
	$\frac{3}{\alpha}$	8.8440×10^{-5}	2.2969×10^{-5}	5.8888×10^{-6}	1.6356×10^{-6}
		–	1.945	1.964	1.848
	$\frac{3-\alpha}{\alpha}$	6.7345×10^{-5}	1.7433×10^{-5}	4.4596×10^{-6}	1.1367×10^{-6}
		–	1.950	1.967	1.972
0.6	1 (uniform mesh)	1.4341×10^{-3}	1.0788×10^{-3}	7.7321×10^{-4}	5.3756×10^{-4}
		–	0.411	0.481	0.524
	$\frac{2}{\alpha}$	1.8622×10^{-5}	4.8433×10^{-6}	1.2266×10^{-6}	3.0785×10^{-7}
		–	1.943	1.981	1.994
	$\frac{3}{\alpha}$	2.8093×10^{-5}	7.3363×10^{-6}	1.8961×10^{-6}	4.8606×10^{-7}
		–	1.937	1.952	1.964
	$\frac{3-\alpha}{\alpha}$	1.8499×10^{-5}	4.8256×10^{-6}	1.2463×10^{-6}	3.1932×10^{-7}
		–	1.939	1.953	1.965

Table 3. Spatial maximum absolute errors and convergence rates of Examples 1–3 at $t = 0.1$ for $\alpha = 0.7, 0.9$ and $r = 2/\alpha$, $(3-\alpha)/\alpha$.

M	N	$\alpha = 0.7$				$\alpha = 0.9$			
		$r = \frac{2}{\alpha}$		$r = \frac{3-\alpha}{\alpha}$		$r = \frac{2}{\alpha}$		$r = \frac{3-\alpha}{\alpha}$	
		Error	**Rate**	**Error**	**Rate**	**Error**	**Rate**	**Error**	**Rate**
Example 1									
16	8	3.4863×10^{-4}	–	4.1951×10^{-4}	–	1.3500×10^{-4}	–	1.3710×10^{-4}	–
32	32	1.9081×10^{-5}	4.1915	2.2891×10^{-5}	4.1959	9.6258×10^{-6}	3.8099	9.4512×10^{-6}	3.8586
64	128	9.6658×10^{-7}	4.3031	1.1585×10^{-6}	4.3045	6.2713×10^{-7}	3.9401	5.9301×10^{-7}	3.9944
128	512	4.9184×10^{-8}	4.2966	5.7679×10^{-8}	4.3280	3.8980×10^{-8}	4.0080	3.5546×10^{-8}	4.0603
Example 2									
16	8	1.6998×10^{-5}	–	2.8244×10^{-5}	–	3.2414×10^{-5}	–	3.1607×10^{-5}	–
32	32	2.0570×10^{-6}	3.0468	3.1864×10^{-6}	3.1479	2.4977×10^{-6}	3.6980	2.3115×10^{-6}	3.7734
64	128	2.1793×10^{-7}	3.2386	3.1123×10^{-7}	3.3559	1.6662×10^{-7}	3.9059	1.4521×10^{-7}	3.9926
128	512	1.8375×10^{-8}	3.5680	2.5064×10^{-8}	3.6343	1.0313×10^{-8}	4.0140	8.4270×10^{-9}	4.1070
Example 3									
16	8	1.9325×10^{-4}	–	2.5549×10^{-4}	–	8.1245×10^{-6}	–	5.1823×10^{-6}	–
32	32	1.3993×10^{-5}	3.7877	1.8582×10^{-5}	3.7813	1.0338×10^{-6}	2.9744	6.8827×10^{-7}	2.9125
64	128	9.9513×10^{-7}	3.8137	1.3109×10^{-6}	3.8253	7.6760×10^{-8}	3.7514	4.3879×10^{-8}	3.9714
128	512	6.8020×10^{-8}	3.8709	8.8835×10^{-8}	3.8833	4.6892×10^{-9}	4.0329	2.0289×10^{-9}	4.4348

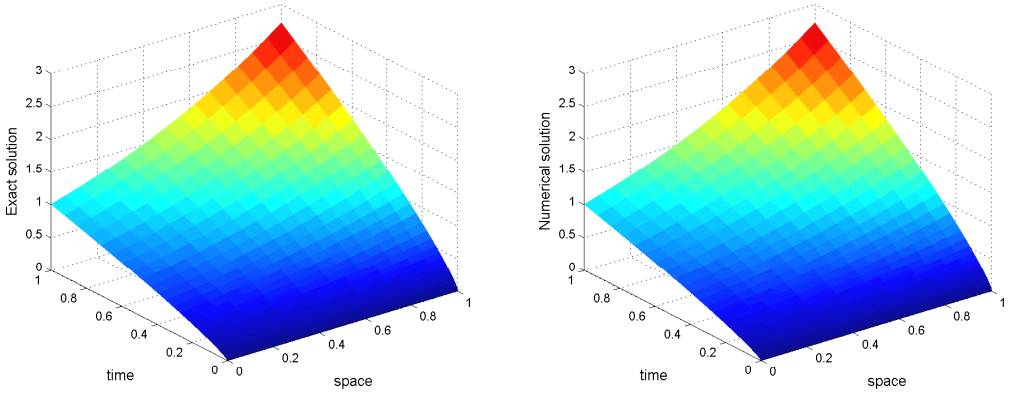

(**a**) Exact solution (**b**) Numerical solution

Figure 1. Comparison of exact and numerical solutions of Example 1 at $\alpha = 0.5, r = \frac{2}{\alpha}$ with $M = 16$ and $N = 32$.

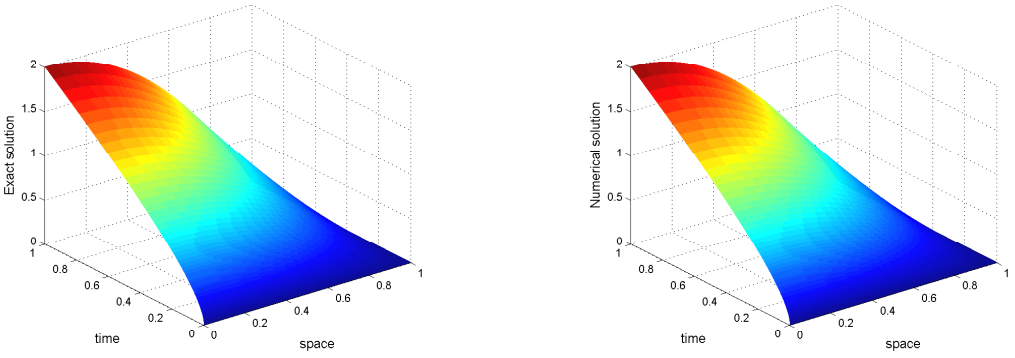

(**a**) Exact solution (**b**) Numerical solution

Figure 2. Comparison of exact and numerical solutions of Example 2 at $\alpha = 0.5$ with $M = N = 50$ and $r = \frac{2}{\alpha}$.

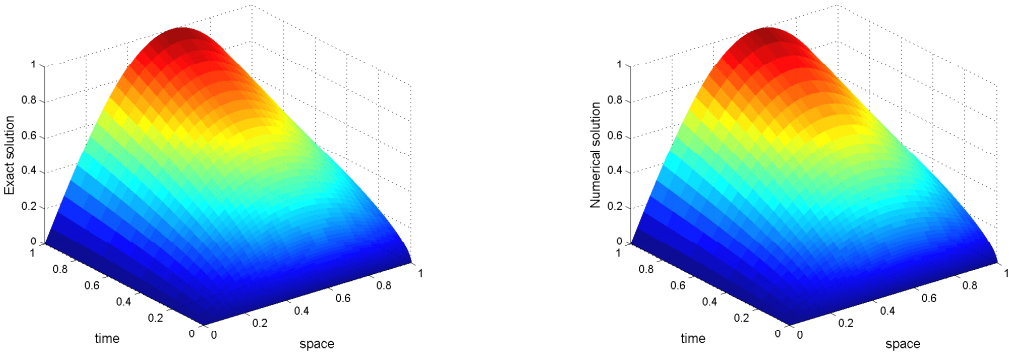

(**a**) Exact solution (**b**) Numerical solution

Figure 3. Comparison of exact and numerical solutions of Example 3 at $\alpha = 0.5$ with $M = 32$ and $N = 16$.

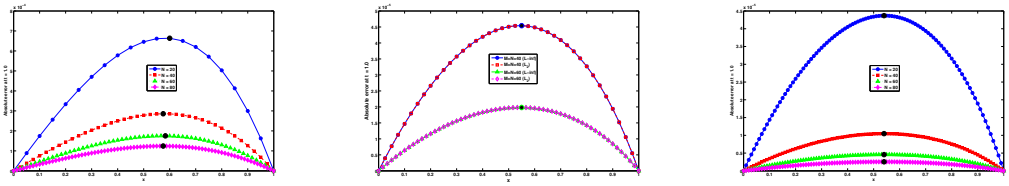

(**a**) $\alpha = 0.4, r = 1, M = N$ (**b**) $\alpha = 0.5, r = (3-\alpha)/\alpha, M = N$ (**c**) $\alpha = 0.85, r = 2/\alpha, M = 100$

Figure 4. Absolute error plot at $t = 1$ of Example 1.

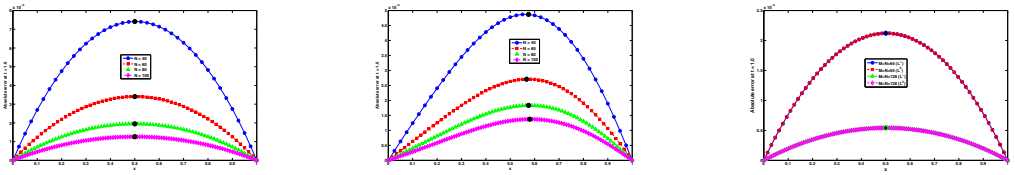

(**a**) $\alpha = 0.3, r = \frac{2}{\alpha}$ (**b**) $\alpha = 0.8, r = 1$ (**c**) $\alpha = 0.6, r = (3-\alpha)/\alpha$

Figure 5. Absolute error plot at $t = 1$ of Example 2 with $M = N$.

Table 4. Comparison of maximum absolute errors (L_∞) and L_2 errors and convergence orders for Example 1 with $N = 2M$ with $r = \frac{3-\alpha}{\alpha}$.

α	M = 32	64	128	256	512
Proposed method: L_∞					
0.5	5.1738×10^{-5}	1.1269×10^{-5}	2.3468×10^{-6}	4.7106×10^{-7}	1.0278×10^{-7}
	–	2.199	2.264	2.317	2.196
0.7	4.8539×10^{-5}	1.1783×10^{-5}	2.7478×10^{-6}	6.2036×10^{-7}	1.3653×10^{-7}
	–	2.042	2.100	2.147	2.184
0.9	3.0278×10^{-5}	8.5340×10^{-6}	2.3275×10^{-6}	6.1823×10^{-7}	1.6070×10^{-7}
	–	1.827	1.874	1.913	1.944
Proposed method: L_2					
0.5	2.2096×10^{-5}	5.2418×10^{-6}	1.2488×10^{-6}	2.9994×10^{-7}	7.2669×10^{-8}
	–	2.076	2.070	2.058	2.045
0.7	1.3128×10^{-5}	3.0653×10^{-6}	7.1326×10^{-7}	1.6658×10^{-7}	3.9196×10^{-8}
	–	2.099	2.104	2.098	2.087
0.9	7.0600×10^{-6}	1.8353×10^{-6}	4.6726×10^{-7}	1.1707×10^{-7}	2.8976×10^{-8}
	–	1.944	1.974	1.997	2.014
Ref. [22]: L_∞					
0.5	2.6378×10^{-2}	2.1991×10^{-2}	1.7784×10^{-2}	1.4003×10^{-2}	1.0788×10^{-2}
	–	0.262	0.306	0.345	0.376
0.7	1.3860×10^{-2}	9.7538×10^{-3}	6.6241×10^{-3}	4.4001×10^{-3}	2.8824×10^{-3}
	–	0.507	0.558	0.590	0.610
Ref. [23] (L1): L_∞					
0.5	7.9226×10^{-4}	2.9088×10^{-4}	1.0545×10^{-4}	3.7952×10^{-5}	1.3661×10^{-5}
	–	1.446	1.464	1.474	1.481
0.7	9.8393×10^{-4}	4.1017×10^{-4}	1.6874×10^{-4}	6.8987×10^{-5}	2.8216×10^{-5}
	–	1.262	1.281	1.290	1.295
Ref. [23] (L1-2): L_∞					
0.5	2.4791×10^{-3}	6.8745×10^{-4}	1.8251×10^{-4}	4.7220×10^{-5}	1.2098×10^{-5}
	–	1.850	1.913	1.951	1.972
0.7	8.4381×10^{-4}	2.3681×10^{-4}	6.3287×10^{-5}	1.6501×10^{-5}	4.2530×10^{-6}
	–	1.833	1.904	1.939	1.963

Table 5. Comparison of maximum absolute errors (L_∞) and convergence orders of Example 2 at $t = 0.5$ with $M = N$ for $r = (3-\alpha)/\alpha$, $r = 2/\alpha$, and $r = 3/\alpha$.

α	N	Proposed Method, $r = \frac{3-\alpha}{\alpha}$		Proposed Method, $r = \frac{2}{\alpha}$		Proposed Method, $r = \frac{3}{\alpha}$		Ref. [22]	
		Error E_∞	Order	Error E_∞	Order	Error E_∞	Order	Error E_∞	Order
0.4	64	3.0551×10^{-5}	—	1.8439×10^{-5}	—	4.0213×10^{-5}	—	7.7015×10^{-5}	—
	128	7.9088×10^{-6}	1.950	4.7512×10^{-6}	1.956	1.0442×10^{-5}	1.945	3.1966×10^{-5}	1.269
	256	2.0232×10^{-6}	1.967	1.2117×10^{-6}	1.971	2.6727×10^{-6}	1.966	1.3638×10^{-5}	1.229
	512	5.1883×10^{-7}	1.963	3.0699×10^{-7}	1.981	9.2989×10^{-7}	1.523	5.9723×10^{-6}	1.191
0.6	64	1.3133×10^{-5}	—	9.2622×10^{-6}	—	2.0139×10^{-5}	—	1.0674×10^{-4}	—
	128	3.3821×10^{-6}	1.957	2.3830×10^{-6}	1.959	5.1968×10^{-6}	1.954	4.5264×10^{-5}	1.238
	256	8.6430×10^{-7}	1.968	6.0859×10^{-7}	1.969	1.3299×10^{-6}	1.966	1.9694×10^{-5}	1.201
	512	2.1965×10^{-7}	1.976	1.5460×10^{-7}	1.977	3.3833×10^{-7}	1.975	8.7732×10^{-6}	1.167
0.8	64	3.8904×10^{-6}	—	3.2303×10^{-6}	—	7.0451×10^{-6}	—	1.4035×10^{-4}	—
	128	9.9892×10^{-7}	1.961	8.2941×10^{-7}	1.962	1.8083×10^{-6}	1.962	6.3712×10^{-5}	1.139
	256	2.5561×10^{-7}	1.966	2.1228×10^{-7}	1.966	4.6246×10^{-7}	1.967	2.9251×10^{-5}	1.123
	512	6.5207×10^{-8}	1.971	5.4172×10^{-8}	1.970	1.1791×10^{-7}	1.972	1.3547×10^{-5}	1.111

Table 6. Comparison of maximum absolute errors (L_∞) of Example 2 with $M = N = 10$ and $r = 1/\alpha$.

(x, t)	$\alpha = 0.5$			$\alpha = 0.7$		
	Proposed Method	ADM [22]	FDM [22]	Proposed Method	ADM [22]	FDM [22]
$(0.8, 0.2)$	3.2355×10^{-4}	2.1713×10^{-3}	3.0136×10^{-3}	1.0217×10^{-4}	4.0422×10^{-4}	3.1136×10^{-3}
$(0.6, 0.4)$	3.0554×10^{-4}	1.9929×10^{-2}	1.5344×10^{-3}	1.3260×10^{-4}	5.5585×10^{-3}	1.8397×10^{-3}
$(0.4, 0.6)$	2.5799×10^{-4}	5.8106×10^{-2}	7.4680×10^{-4}	1.1346×10^{-4}	2.0409×10^{-2}	9.4712×10^{-4}
$(0.2, 0.8)$	1.4404×10^{-4}	8.3181×10^{-2}	2.5420×10^{-4}	7.9007×10^{-5}	3.4305×10^{-2}	3.6554×10^{-4}

Table 7. Comparison of maximum absolute errors (L_∞) and convergence orders of Example 2 with $M = N$ for different α.

α	N	Proposed, $r = \frac{3-\alpha}{\alpha}$		Proposed, $r = \frac{2}{\alpha}$		Ref. [22]		Ref. [19]	
		Error	Order	Error	Order	Error	Order	Error	Order
0.4	64	4.4343×10^{-5}	—	4.9676×10^{-5}	—	1.3022×10^{-2}	—	4.9969×10^{-4}	—
	128	1.1100×10^{-5}	1.9981	1.3326×10^{-5}	1.8983	1.1640×10^{-2}	0.162	1.8612×10^{-4}	1.4248
	256	2.7748×10^{-6}	2.0002	3.4399×10^{-6}	1.9539	1.0214×10^{-2}	0.188	6.6651×10^{-5}	1.5160
	512	6.9242×10^{-7}	2.0027	8.7025×10^{-7}	1.9828	8.7980×10^{-3}	0.215	2.3306×10^{-5}	1.4815
0.6	64	2.1564×10^{-5}	—	4.1542×10^{-5}	—	8.8219×10^{-3}	—	8.6677×10^{-4}	—
	128	5.4460×10^{-6}	1.9854	1.1256×10^{-5}	1.8839	6.8197×10^{-3}	0.371	3.8105×10^{-4}	1.1857
	256	1.3740×10^{-6}	1.9868	2.9249×10^{-6}	1.9442	5.0877×10^{-3}	0.423	1.6002×10^{-4}	1.2517
	512	3.4630×10^{-7}	1.9884	7.4240×10^{-7}	1.9781	3.6865×10^{-3}	0.465	5.6240×10^{-5}	1.2944
0.8	64	1.8453×10^{-5}	—	2.6978×10^{-5}	—	3.5240×10^{-3}	—	1.1441×10^{-3}	—
	128	4.8219×10^{-6}	1.9361	7.6321×10^{-6}	1.8216	2.2877×10^{-3}	0.623	5.9561×10^{-4}	0.9417
	256	1.1989×10^{-6}	2.0079	2.0575×10^{-6}	1.8912	1.4296×10^{-3}	0.678	2.9922×10^{-4}	0.9932
	512	2.8758×10^{-7}	2.0597	5.3694×10^{-7}	1.9381	8.9469×10^{-4}	0.676	1.4623×10^{-4}	1.0330

Table 8. Maximum absolute (L_∞) and L_2 errors and convergence orders for the proposed method of Example 1 with $M = 256$ for $r = \frac{3-\alpha}{\alpha}$ and $r = \frac{2}{\alpha}$.

α	N	$r = \frac{3-\alpha}{\alpha}$				$r = \frac{2}{\alpha}$			
		L_∞		L_2		L_∞		L_2	
		Error	Order	Error	Order	Error	Order	Error	Order
0.4	32	2.3737×10^{-4}	—	1.1844×10^{-4}	—	4.1634×10^{-4}	—	8.1134×10^{-5}	—
	64	5.4154×10^{-5}	2.132	2.8697×10^{-5}	2.045	1.1867×10^{-4}	1.811	1.9228×10^{-5}	2.077
	128	1.1399×10^{-5}	2.248	6.9010×10^{-6}	2.056	3.2590×10^{-5}	1.864	4.5501×10^{-6}	2.079
	256	2.3371×10^{-6}	2.286	1.6620×10^{-6}	2.054	8.6622×10^{-6}	1.912	1.0846×10^{-6}	2.069
	512	5.8276×10^{-7}	2.004	3.9928×10^{-7}	2.057	2.2518×10^{-6}	1.944	2.6117×10^{-7}	2.054
0.5	32	2.2224×10^{-4}	—	9.2630×10^{-5}	—	3.8429×10^{-4}	—	7.1472×10^{-5}	—
	64	5.1738×10^{-5}	2.103	2.2095×10^{-5}	2.068	1.0963×10^{-4}	1.810	1.6698×10^{-5}	2.098
	128	1.1270×10^{-5}	2.199	5.2418×10^{-6}	2.076	3.0337×10^{-5}	1.854	3.8832×10^{-6}	2.104
	256	2.3468×10^{-6}	2.264	1.2488×10^{-6}	2.070	8.0749×10^{-6}	1.910	9.0958×10^{-7}	2.094
	512	4.7106×10^{-7}	2.317	2.9994×10^{-7}	2.058	2.1062×10^{-6}	1.939	2.1568×10^{-7}	2.076
0.6	32	2.0828×10^{-4}	—	7.1748×10^{-5}	—	3.4001×10^{-4}	—	6.3267×10^{-5}	—
	64	5.0452×10^{-5}	2.046	1.6935×10^{-5}	2.083	9.8227×10^{-5}	1.791	1.4789×10^{-5}	2.097
	128	1.1537×10^{-5}	2.129	3.9695×10^{-6}	2.093	2.7187×10^{-5}	1.853	3.4050×10^{-6}	2.119
	256	2.5290×10^{-6}	2.190	9.3372×10^{-7}	2.088	7.3033×10^{-6}	1.896	7.8327×10^{-7}	2.120
	512	5.3571×10^{-7}	2.239	2.2149×10^{-7}	2.076	1.9092×10^{-6}	1.936	1.8168×10^{-7}	2.108
0.9	32	1.0340×10^{-4}	—	2.6437×10^{-5}	—	1.2044×10^{-4}	—	2.8692×10^{-5}	—
	64	3.0308×10^{-5}	1.771	7.0599×10^{-6}	1.905	3.6839×10^{-5}	1.709	7.8858×10^{-6}	1.863
	128	8.5341×10^{-6}	1.828	1.8353×10^{-6}	1.944	1.0839×10^{-5}	1.765	2.1080×10^{-6}	1.903
	256	2.3275×10^{-6}	1.874	4.6726×10^{-7}	1.974	3.0894×10^{-6}	1.811	5.5108×10^{-7}	1.936
	512	6.1823×10^{-7}	1.913	1.1707×10^{-7}	1.997	8.5732×10^{-7}	1.849	1.4156×10^{-7}	1.961

Table 9. Comparison of maximum absolute errors (L_∞) and L_2 errors and convergence orders for the proposed method of Example 1 at fixed $T = 0.50$ with $r = 1/\alpha$ and $M = 2N$.

α	M = 16	32	64	128	256
Proposed method: L_∞					
0.20	8.7752×10^{-4}	1.5290×10^{-4}	3.3380×10^{-5}	7.7754×10^{-6}	1.8600×10^{-6}
	–	2.521	2.196	2.102	2.064
0.50	3.7251×10^{-4}	7.7485×10^{-5}	1.6547×10^{-5}	3.6566×10^{-6}	8.3494×10^{-7}
	–	2.265	2.227	2.178	2.131
0.80	1.0663×10^{-4}	2.4693×10^{-5}	5.4032×10^{-6}	1.0878×10^{-6}	1.8973×10^{-7}
	–	2.110	2.192	2.312	2.519
Proposed method: L_2					
0.20	6.4185×10^{-4}	1.1199×10^{-4}	2.4437×10^{-5}	5.6923×10^{-6}	1.3616×10^{-6}
	–	2.519	2.196	2.102	2.064
0.50	2.7293×10^{-4}	5.6785×10^{-5}	1.2124×10^{-5}	2.6802×10^{-6}	6.1228×10^{-7}
	–	2.265	2.228	2.177	2.130
0.80	7.7183×10^{-5}	1.7948×10^{-5}	3.9174×10^{-6}	7.7709×10^{-7}	1.2419×10^{-7}
	–	2.104	2.196	2.334	2.646

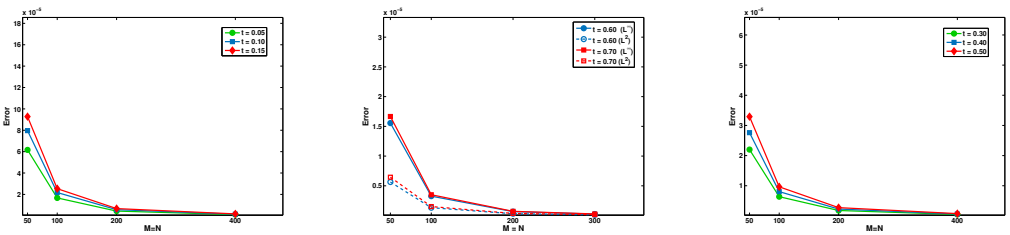

(**a**) $\alpha = 0.4$ (**b**) $\alpha = 0.4$ (**c**) $\alpha = 0.9$

Figure 6. Time-vary effect of Example 1 with $r = \frac{2}{\alpha}$ for different α values.

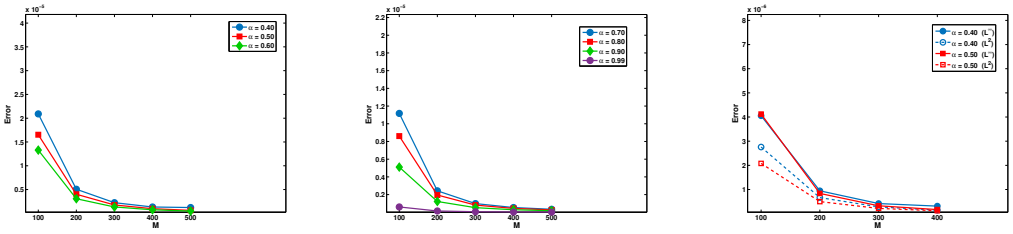

(**a**) $\alpha = 0.35, 0.45, 0.55, 0.65$ (**b**) $\alpha = 0.7, 0.8, 0.9, 0.99$ (**c**) $\alpha = 0.40, 0.50$

Figure 7. Fractional order effect of Example 1 with different α values with $N = M$ and $r = \frac{2}{\alpha}$.

Table 10. Maximum absolute (L_∞) and L_2 errors and convergence orders for the proposed method of Example 2 for $r = \frac{3-\alpha}{\alpha}$ and $r = \frac{2}{\alpha}$.

α	M	$r = \frac{3-\alpha}{\alpha}$				$r = \frac{2}{\alpha}$			
		L_∞		L_2		L_∞		L_2	
		Error	**Order**	**Error**	**Order**	**Error**	**Order**	**Error**	**Order**
0.5	64	3.1527×10^{-5}	—	1.8989×10^{-5}	—	4.6307×10^{-5}	—	1.3209×10^{-5}	—
	128	7.9387×10^{-6}	1.9896	4.8923×10^{-6}	1.9566	1.2442×10^{-5}	1.8961	3.4062×10^{-6}	1.9553
	256	1.9972×10^{-6}	1.9909	1.2515×10^{-6}	1.9669	3.2166×10^{-6}	1.9515	8.7218×10^{-7}	1.9654
	512	5.0233×10^{-7}	1.9912	3.1826×10^{-7}	1.9753	8.1432×10^{-7}	1.9819	2.2203×10^{-7}	1.9738
0.7	64	2.0539×10^{-5}	—	8.1294×10^{-6}	—	3.5162×10^{-5}	—	6.8662×10^{-6}	—
	128	5.0027×10^{-6}	2.0376	2.0782×10^{-6}	1.9678	9.7011×10^{-6}	1.8578	1.7460×10^{-6}	1.9755
	256	1.1543×10^{-6}	2.1157	5.2976×10^{-7}	1.9719	2.5510×10^{-6}	1.9271	4.4134×10^{-7}	1.9841
	512	2.5633×10^{-7}	2.1710	1.3475×10^{-7}	1.9751	6.5254×10^{-7}	1.9669	1.1135×10^{-7}	1.9868
0.9	64	1.2953×10^{-5}	—	2.6521×10^{-6}	—	1.5809×10^{-5}	—	2.8845×10^{-6}	—
	128	3.6748×10^{-6}	1.8175	6.9765×10^{-7}	1.9266	4.6580×10^{-6}	1.7630	7.8194×10^{-7}	1.8832
	256	9.9806×10^{-7}	1.8804	1.7973×10^{-7}	1.9566	1.3147×10^{-6}	1.8250	2.0679×10^{-7}	1.9189
	512	2.6275×10^{-7}	1.9254	4.5564×10^{-8}	1.9799	3.5948×10^{-7}	1.8707	5.3621×10^{-8}	1.9473

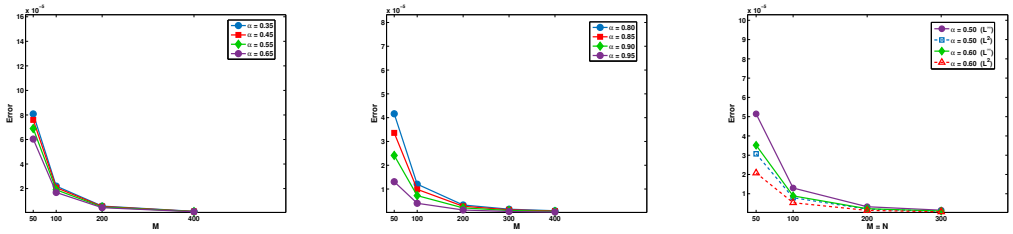

(**a**) $\alpha = 0.35, 0.45, 0.55, 0.65$ (**b**) $\alpha = 0.80, 0.85, 0.90, 0.95$ (**c**) $\alpha = 0.60, 0.70$

Figure 8. Fractional order effect of Example 2 with different α values with $N = M$ and $r = \frac{2}{\alpha}$.

Table 11. Maximum absolute (L_∞) and L_2 errors and convergence orders for Example 3 with $r = \frac{2}{\alpha}$.

M	$\alpha = 0.30$		$\alpha = 0.50$		$\alpha = 0.70$		$\alpha = 0.80$	
	L_∞	**Order**	L_∞	**Order**	L_∞	**Order**	L^∞	**Order**
Proposed method: L_∞								
50	1.4035×10^{-4}	—	9.0886×10^{-5}	—	5.7089×10^{-5}	—	4.3561×10^{-5}	—
100	3.5845×10^{-5}	1.969	2.3014×10^{-5}	1.982	1.5981×10^{-5}	1.837	1.2547×10^{-5}	1.796
200	9.0801×10^{-6}	1.981	5.8035×10^{-6}	1.988	4.2105×10^{-6}	1.924	3.4026×10^{-6}	1.883
400	2.6365×10^{-6}	1.784	1.4598×10^{-6}	1.991	1.0741×10^{-6}	1.971	8.8692×10^{-7}	1.940
Proposed method: L_2								
50	9.7087×10^{-5}	—	6.1071×10^{-5}	—	3.1048×10^{-5}	—	1.8969×10^{-5}	—
100	2.4945×10^{-5}	1.961	1.5588×10^{-5}	1.970	7.8929×10^{-6}	1.976	4.8165×10^{-6}	1.978
200	6.3408×10^{-6}	1.976	3.9545×10^{-6}	1.979	1.9998×10^{-6}	1.981	1.2178×10^{-6}	1.984
400	1.5863×10^{-6}	1.999	9.9895×10^{-7}	1.985	5.0545×10^{-7}	1.984	3.0695×10^{-7}	1.988

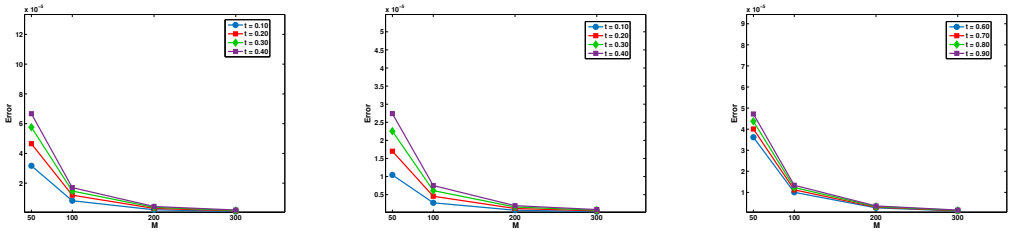

(**a**) $\alpha = 0.4$ (**b**) $\alpha = 0.75$ (**c**) $\alpha = 0.75$

Figure 9. Time-varying effect of Example 3 for different α values with $N = 2M$.

6. Conclusions

In this paper, we developed and analyzed a high-order numerical scheme for the solution of time-fractional partial Volterra integro-differential equations. The proposed method addresses the challenges associated with the weak singularity of the Caputo fractional derivative and the memory mechanism induced by the Volterra integral term. For the temporal discretization, the L2-1_σ-type fractional numerical differentiation formula on a graded mesh is employed to approximate the Caputo fractional derivative. The graded mesh concentrates grid points near the initial time $t = 0$, where the solution exhibits a weak singularity $\partial_t u \sim t^{\alpha-1}$. Simpson's 1/3 rule was adapted to the graded mesh framework for approximating the Volterra integral term, utilizing modified quadrature weights that account for the non-uniform step sizes while maintaining high-order accuracy. For the spatial discretization, the Numerov scheme was utilized, which achieves fourth-order accuracy, yielding higher computational efficiency compared to standard finite difference methods.

Using the discrete fractional Grönwall inequality on graded meshes, we proved that the proposed scheme is stable and achieves an optimal convergence rate of $\mathcal{O}(N^{-\min\{3-\alpha, r\alpha\}} + h^4)$, provided the mesh grading parameter satisfies $r \geq 1$. Three numerical examples are presented to demonstrate the accuracy and convergence properties of the scheme. The numerical results confirm the theoretical predictions and show that the scheme achieves smaller errors than existing methods in the literature. The proposed scheme on graded meshes provides a robust, accurate, and efficient framework for solving time-fractional Volterra integro-differential equations, with potential applications in viscoelasticity, anomalous diffusion, population dynamics, and other fields where dual-memory effects are present.

Several directions for future research emerge from this work. The proposed approach can be extended to two and three dimensional time-fractional Volterra integro-differential equations. The analysis can also be extended to nonlinear time-fractional Volterra integro-differential equations, where additional challenges arise from the nonlinear terms and the need for iterative solvers. Furthermore, the method can be generalized to problems with variable-order fractional derivatives, which are increasingly used in modeling complex systems with time-dependent memory effects.

Author Contributions: Conceptualization, A.T.C. and M.M.W.; methodology, A.T.C., K.S.M. and O.O.; software, A.T.C. and M.M.W.; validation, A.T.C., K.S.M. O.O. and M.M.W.; formal analysis, A.T.C. and K.S.M.; investigation, A.T.C. and M.M.W.; resources, K.S.M. and O.O.; data curation, M.M.W. and K.S.M.; writing—original draft preparation, A.T.C. and M.M.W.; writing—review and editing, M.M.W. and K.S.M.; visualization, A.T.C.; supervision, M.M.W.; project administration, K.S.M. and O.O.; funding acquisition, K.S.M. All authors have read and agreed to the published version of the manuscript.

Funding: This work was supported by the Deanship of Graduate Studies and Scientific Research at Qassim University (https://www.qu.edu.sa, (accessed on 19 November 2026)) for financial support (QU-APC-2026).

Data Availability Statement: All data generated or analyzed during this study are included in this article.

Acknowledgments: The researchers would like to thank the Deanship of Graduate Studies and Scientific Research at Qassim University (https://www.qu.edu.sa) for financial support (QU-APC-2026).

Conflicts of Interest: The authors declare no conflicts of interest.

References

1. Podlubny, I. *Fractional Differential Equations: An Introduction to Fractional Derivatives, Fractional Differential Equations, to Methods of Their Solution and Some of Their Applications*; Academic Press: San Diego, CA, USA, 1999; Volume 198.
2. Kilbas, A.A.; Srivastava, H.M.; Trujillo, J.J. *Theory and Applications of Fractional Differential Equations*; Elsevier: Amsterdam, The Netherlands, 2006; Volume 204.
3. Ayman-Mursaleen, M.; Haque, I.; Rao, N. A Study of King-Type Operators Connecting Wavelet and Quantum Calculus: Numerical and Graphical Analysis. *Mathematics* **2026**, *14*, 3627. https://doi.org/10.3390/math14193627.
4. Gurtin, M.E.; Pipkin, A. A general theory of heat conduction with finite wave speeds. *Arch. Ration. Mech. Anal.* **1968**, *31*, 113–126.
5. Brunner, H. *Collocation Methods for Volterra Integral and Related Functional Differential Equations*; Cambridge University Press: Cambridge, UK, 2004; Volume 15.
6. Singh, A.; Kumar, S. Error analysis of a high-order fully discrete method for two-dimensional time-fractional convection-diffusion equations exhibiting weak initial singularity. *Numer. Algorithms* **2025**, *99*, 251–284. https://doi.org/10.1007/s11075-024-01877-x.
7. Sun, Z.-z.; Wu, X. A fully discrete difference scheme for a diffusion-wave system. *Appl. Numer. Math.* **2006**, *56*, 193–209. https://doi.org/10.1016/j.apnum.2005.03.003.
8. Jin, B.; Lazarov, R.; Zhou, Z. An analysis of the L1 scheme for the subdiffusion equation with nonsmooth data. *IMA J. Numer. Anal.* **2016**, *36*, 197–221. https://doi.org/10.1093/imanum/dru063.
9. Stynes, M.; O'Riordan, E.; Gracia, J.L. Error Analysis of a Finite Difference Method on Graded Meshes for a Time-Fractional Diffusion Equation. *SIAM J. Numer. Anal.* **2017**, *55*, 1057–1079. https://doi.org/10.1137/16M1082329.
10. Hu, C.Y.; Lin, F.R. A New L2 Type Difference Scheme for the Time-Fractional Diffusion Equation. *Fractal Fract.* **2025**, *9*, 325. https://doi.org/10.3390/fractalfract9050325.
11. Kundaliya, P.J. α-Robust Error Analysis of $L2\text{-}1_\sigma$ Scheme on Graded Mesh for Time-fractional Nonlocal Diffusion Equation. *arXiv* **2023**, arXiv:2306.02576. https://doi.org/10.48550/arXiv.2306.02576.
12. Quan, C.; Wu, X. Global-in-time H^1-stability of $L2\text{-}1_\sigma$ method on general nonuniform meshes for subdiffusion equation. *arXiv* **2022**, arXiv:2208.01384. https://doi.org/10.48550/arXiv.2208.01384.
13. Huang, C.; Stynes, M. A Sharp α-Robust $L^\infty(H^1)$ Error Bound for a Time-Fractional Allen-Cahn Problem Discretised by the Alikhanov $L2-1_\sigma$ Scheme and a Standard FEM. *J. Sci. Comput.* **2022**, *91*, 43. https://doi.org/10.1007/s10915-022-01810-1.
14. Chen, H.; Stynes, M. Error Analysis of a Second-Order Method on Fitted Meshes for a Time-Fractional Diffusion Problem. *J. Sci. Comput.* **2019**, *79*, 624–647. https://doi.org/10.1007/s10915-018-0863-y.
15. Li, Q.; Xie, J.; Chen, S. A Fast $L2\text{-}1_\sigma$ Finite Element Method for Time Fractional Keller–Segel Equations with Weakly Singular Solutions. *Fractal Fract.* **2026**, *10*, 119. https://doi.org/10.3390/fractalfract10020119.
16. Liao, H.l.; McLean, W.; Zhang, J. A Discrete Grönwall Inequality with Applications to Numerical Schemes for Subdiffusion Problems. *SIAM J. Numer. Anal.* **2019**, *57*, 218–237. https://doi.org/10.1137/16M1175742.
17. Sun, Z.Z. Compact difference schemes for heat equation with Neumann boundary conditions. *Numer. Methods Partial Differ. Equ.* **2009**, *25*, 1320–1341. https://doi.org/10.1002/num.20402.
18. Du, R.; Cao, W.; Sun, Z. A compact difference scheme for the fractional diffusion-wave equation. *Appl. Math. Model.* **2010**, *34*, 2998–3007. https://doi.org/10.1016/j.apm.2010.01.008.
19. Maji, S.; Natesan, S. Analytical and numerical solution techniques for a class of time-fractional integro-partial differential equations. *Numer. Algorithms* **2023**, *94*, 229–256. https://doi.org/10.1007/s11075-023-01498-w.
20. Sabawi, Y.A.; Santra, S.; Das, P.; Mohammad, N.A. H^1 stability and convergence analysis of the L1/L1-2 Legendre spectral method for non-local weakly singular integro-PDEs. *Calcolo* **2025**, *62*, 42. https://doi.org/10.1007/s10092-025-00671-y.
21. Assanova, A.T.; Bakirova, E.A.; Iskakova, N.B.; Kadirbayeva, Z.M.; Kuanysh, S.K. Stability and convergence analysis of Fredholm-type parabolic integro-differential equations. *Math. Comput. Simul.* **2027**, *251*, 709–721. https://doi.org/10.1016/j.matcom.2026.08.027.

22. Santra, S.; Mohapatra, J. A novel finite difference technique with error estimate for time fractional partial integro-differential equation of Volterra type. *J. Comput. Appl. Math.* **2022**, *400*, 113746. https://doi.org/10.1016/j.cam.2021.113746.
23. Ghosh, B. Comparative Evaluation of Layer-Adaptive Schemes for Mildly Singular Time-Fractional Integro-Subdiffusion Equations. *Natl. Acad. Sci. Lett.* **2026**. https://doi.org/10.1007/s40009-026-02375-5.
24. Mohib, A.; Elbostani, S.; Rachid, A.; El Jid, R. Numerical approximation of a generalized time fractional partial integro-differential equation of Volterra type based on a meshless method. *Partial Differ. Equ. Appl. Math.* **2024**, *11*, 100791. https://doi.org/10.1016/j.padiff.2024.100791.
25. Wang, Y.; An, N.; Huang, C. Unconditional optimal error bounds of the fast nonuniform Alikhanov scheme for a nonlinear time-fractional biharmonic equation. *J. Appl. Math. Comput.* **2024**, *70*, 4053–4071. https://doi.org/10.1007/s12190-024-02120-5.

Disclaimer/Publisher's Note: The statements, opinions and data contained in all publications are solely those of the individual author(s) and contributor(s) and not of MDPI and/or the editor(s). MDPI and/or the editor(s) disclaim responsibility for any injury to people or property resulting from any ideas, methods, instructions or products referred to in the content.